A MATHEMATICAL MODEL FOR DYNAMIC SIMULATION OF APOPTOSIS PATHWAYS

Paolo Massari

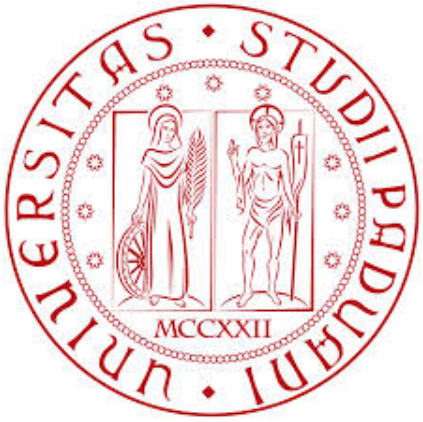

Department of Information Engineering

Bioengineering

University of Padova

April 2014

Advisor: **Gianna Maria Toffolo**
Coadvisor: **Barbara Di Camillo**

Anno Accademico: 2013-2014

Summary

Programmed cell death, termed apoptosis, plays a fundamental role in the development and homeostasis of multicellular organisms. Dysregulation of apoptosis can lead to numerous diseases, including autoimmune diseases, neurodegenerative diseases, and cancer. In mammalian cells apoptosis can be induced by intra- or extracellular stimuli. Extracellular stimuli comprise death ligands (like TRAIL or FAS/Apo-1/CD95) which can lead, through extrinsic pathway, to receptor-induced apoptosis. Intracellular signals, such as DNA damage, trigger the intrinsic pathway which results in release and activation, by mitochondria into cytosol, of proapoptotic factors. Apoptosis is promoted by a family of cysteine proteases, the caspases, which could lead to apoptotic phenotypes such as chromatin condensation, nuclear fragmentation, membrane blebbing, cell shrinkage, and formation of apoptotic bodies. A series of other non-apoptotic pathways occur when the cell is stymolated by death receptors. In particular nuclear factor kappa B is a protein complex that, when active, transfers into DNA generating transcriptional factors that could interact and inhibit caspase and mitochondrial apoptotic pathways. Creating models of apoptotic phenomenon is a key tool to understand the role of any singular molecule involved in this process. In particular, ordinar differential equations (ODEs) models allows to obtain quantitative concentrations of each molecule. There are a lot of ODEs models in literature, each of them dedicated to a different branch of apoptosis. The aim of this thesis is to perform a new ODE-based model (using BioNetGen language) by integrating those already existing. Therefore is possible to reproduce and simulate the complex signal of extrinsic apoptotic pathway and give new insights to cell death mechanism. In particular, were selected two models with similar cellular lines (HeLa cells). The first involves mitochondria reactions describing intrinsic apoptosis induced by TRAIL receptors. It represents cellular death like a biologic time switch, whose activation could be delayed by opportune inhibitors. The second delineates extrinsic apoptosis through NfkB pathway by stimolation of FAS receptors. The derived BioNetGen codes, for these two different approaches, was after imported in Matlab and integrated using non linear least square method (NNLSQ). The new model is conceived to join together mechanisms that leads to cellular death or survival. Controlling apoptosis inhibitor could delay caspase and mitochondrial events and, consequently, induce NfkB transcriptional factors activity, suppressing apoptosis in a definitive manner. To further study and validate it, sensitivity analysis and pattern classification were performed and underlining a good agreement with previous models. Since no complex algebric forms such as 'Hill functions' were used in the model, ultrasensitivity and other nonlinear behaviors arise from interactions among simple elementary reactions. In future perspectives, this model could be used for cross-talks investigation between different pathways and also for better description of NfkB influence in apoptosis propagation.

Contents

1 Introduction **1**

2 Apoptosis **4**

2.1 Key molecules on apoptosis pathway 4

2.1.1 Caspases as major effector molecules of apoptosis pathway 6

2.1.1.1 Caspase-8/10 activation at DISC 7

2.1.2 c-Flip proteins regulate caspase activation at the DISC 8

2.1.3 IAP family of proteins 9

2.1.3.1 XIAP and Smac/DIABLO 9

2.1.4 The Bcl-2 family 9

2.2 System biology of extrinsic apoptosis 10

2.2.1 Death receptor-induced apoptosis 10

2.3 System biology of intrinsic apoptosis 12

2.3.1 Mithocondrial apoptosis pathway 13

2.4 Nf-kB non-apoptotic pathway 14

2.4.1 CD95-Mediated NF-kB activation 14

2.4.2 TRAIL-Mediated NF-kB activation 14

3 Modelling biochemical systems **16**

3.1 introduction 16

3.2 Why modelling apoptosis? 16

3.3 Ultrasensitivity 17

3.3.1 Effect of feedbacks on ultrasensitive cascades 18

3.3.2 Bistability caused by positive feedback 19

3.4 Computational modeling techniques 19

3.4.1 ODE Models Describing Apoptosis Networks 21

3.4.1.1 Models of Extrinsic Apoptosis Pathway 21

3.4.1.2 Models of Intrinsic Apoptosis Pathway 22

3.4.1.3 Implicit Feedback Mechanism in Intrinsic Apoptosis . . . 22

3.4.1.4 Models with a switching / threshold mechanisms 23

3.4.1.5 Models with a timing switch 23

3.4.1.6 Nf-kB Models 24

3.5 Rule-based modeling 25

3.6 BioNetGen language 26

3.6.1 BioNetGen simulation tools 30

4 Mathematical model of apoptosis **32**
4.1 Introduction . . . 32
4.2 Albeck's model of intrinsic apoptosis with TRAIL . . . 32
4.2.1 Model description . . . 35
4.2.2 Model implementation using BioNetGen . . . 36
4.3 Neumann's model of extrinsic apoptosis with FAS/APO-1 . . . 40
4.3.1 Model description . . . 42
4.3.2 Model implementation using BioNetGen . . . 43
4.4 Model integration . . . 46
4.4.1 Robust parametric sensitivity analysis . . . 47
4.4.1.1 Neumann DISC sensitivity analysis . . . 49
4.4.1.2 Albeck DISC sensitivity analysis . . . 50
4.4.2 Merging using nonlinear least-squares method . . . 52
4.4.2.1 Parameters calibration . . . 54
4.4.2.2 Conclusion . . . 57

5 Model Analysis and validation **58**
5.1 Apoptosis model simulations: results and analysis . . . 59
5.1.1 Pattern classification . . . 59
5.1.1.1 Classification parameters . . . 60
5.1.1.2 Classification rules . . . 61
5.1.2 Classification analysis and discussion . . . 62
5.2 Model validation . . . 66
5.2.1 DISC formation, p43Flip and p43p41 activation . . . 66
5.2.2 mitochondrial amplification loop . . . 68
5.2.3 C3 - C6 feedback loop . . . 69
5.2.4 NfkB activation . . . 70
5.2.5 FAS pathway . . . 72
5.2.6 Sensitivity analysis . . . 72

6 Conclusions **76**
6.1 Future plans . . . 77

7 Appendix **78**

1 Introduction

Programmed cell death is a fascinating process common to all multicellular organisms. It results in the elimination of cells via a complex but a highly defined programme. Defects in the regulation of programmed cell death are associated with serious diseases such as cancer, autoimmunity, AIDS, and neurodegeneration. Apoptosis has been the best studied type of programmed cell death so far. Cells that undergo apoptosis are characterized by chromatin condensation, nuclear fragmentation, membrane blebbing, cell shrinkage, and formation of apoptotic bodies. The central role in apoptosis execution belongs to cysteine-specific aspartate proteases (caspases). Caspases are enzymes that orchestrate apoptosis via cleavage of cellular substrates.

There are two major pathways of apoptosis: intrinsic and extrinsic. The intrinsic pathway is triggered via chemotherapeutic drugs, irradiation, and growth factor withdrawal. These stimuli lead to mitochondrial outer membrane permeabilization (MOMP), which results in cytochrome-c release and caspase activation. In the extrinsic apoptotic pathway, the caspase cascade is triggered by signals emanating from the cell-surface death receptors (DR) triggered by death ligands (DL) (TNF, CD95L/FasL, TRAIL). The DR stimulation results in the formation of the death-inducing signaling complex (DISC) and subsequent caspase activation. DISC molecule, promotes caspase 8 and 10 activation and was inhibited by cellular FADD-like interleukin-1b-converting enzyme inhibitory proteins (c-Flips). Three splicing variants of c-Flips, c-Flip short (c-FlipS), c-Flip long (FlipL), and c-Flip Raji (FlipR) can heterodimerize with a monomer of procaspase-8 bound to a FADD molecule at the DISC and interfere with caspase-8 activation. c-Flips molecules promotes Nf-kB activation through the formation of p43Flip.

Despite the fact that signaling pathways of apoptosis have been described with an impressive level of detail, the understanding of apoptosis regulation in quantitative terms has been missing until recently. There were many unclear points: when does a cell decide that it has to die, what are the rate-limiting steps in apoptosis, is there a point of no return, how can cell death be accelerated or blocked, and many others. From another side the years of apoptosis research resulted in a profound understanding of how signaling in apoptosis occurs. All major apoptotic complexes have been identified from the DISC to the apoptosome, including the death receptors and adaptors and the most important enzymes and their inhibitors. Therefore, apoptosis was an ideal system to go into quantitative studies using the emerging field of systems biology.

On the modeling side there are a number of mathematical formalisms, e.g., Ordinary Differential Equations (ODEs), Boolean models, etc., that allow to address different

biological questions. Experimental work for systems biology of apoptosis involves the generation of quantitative data using different apoptotic assays. The development of this field in the recent years is fascinating. Studies of apoptosis using systems biology have provided novel insights into the quantitative regulation of cell death.

The aim of this thesis is to find new insights of the complex regulatory mechanism of apoptosis by implementing and simulation of a state-of-art model. Two models have been used from literature, each of them describing a different behavior of apoptotic pathway. The first model consider the pathway generated by TRAIL receptors and involves the mitochondrion. It conisder apoptosis like a biological switch that can be delayed by some molecules (called inhibitors of apoptosis). The second model evaluate two extrinsic pathways produced by FAS receptors: apoptosis and Nf-kB. The last could lead to the activation of trascriptional factors that act as inhibitors of both mitochondrial and apoptosi pathway. We will merge them togheter using sensitivty analysis and non-linear-least-square method. Then, we will study the new complete model using pattern classification, Hill equation and sensitivity analysis.

Structure of the thesis:

Chapter 2 starts with an overview of the biology of the different pathways involved in the apoptosis stimuli. We analyze both the extrinsic pathways (mediated by death receptors) and intrinsic pathways (mediated by mithocondrial and the formation of the apoptosome) and all the other major non-apoptotic pathways that occurs during the apoptotic stimuli.

Chapter 3 gives an overview of the main computational modeling techniques focusing on rule-based modeling approach and on BioNetGen language, the software implementing it. It also gives an insight of the most widespreads mathematical models used in apoptosis and cell death.

Chapter 4 starts illustrating two published models describing different apoptosis signalling branches to realize a final and more complete model. We analyze step by step their implementation using BioNetGen language. At last, we import the models in MatLab and we use sensitive analysis and the non linear square method for model integration and parameter adjustment.

In chapter 5 the new apoptosis model has been used to obtain predictions of the system. Simulated time series, describing concentrations of chemical species, has been considered to characterized the dynamic behavior of the system. Both sensitivity analysis and Hill equation have been used to further describe and validate the new model.

In chapter 6 we discuss the results and we introduce future plans. At last, chapter 7 shows model observables and BioNetGen source code.

Some chapters in section 2 and 3 are based on Inna Lavrik's [4] and Sangdun Choi's [11] books.

Suffix	Description
Apaf-1	Adaptor protein, apoptotic protease activating factor-1
Bcl-2	B-cell lymphoma protein 2
IAP	Inhibitor of Apoptosis
MOMP	Mitochondrial Outer Membrane Permeabilisation
BH	Bcl-2 homolgy
BIR	Baculoviral IAP Repeat
RING	Really Interesting New Gene
c-IAP1 and c-IAP2	Cellular inhibitor of apoptosis 1 and 2
XIAP	X-linked inhibitor of apoptosis protein
Smac	Second Mitochondria-derived Activator of Caspases
DIABLO	Direct IAP Binding Protein with Low PI
ODE	Ordinary Differential Equations
BAR	Bifunctional Apoptosis Regulator
NF-kB	Nuclear Factor-KappaB
IKK	IkB kinase
FRET	Foerster resonance energy transfer
TRAIL/Apo2L	Tumour Necrosis factor-Related Apoptosis-Inducing Ligand
TRAIL-R1	TRAIL receptor 1
CHX	Cycloheximide
ATP	Adenosine Triphosphate
CA	Cellular Automata
TNF	Tumor Necrosis Factor
TNFR1	Tumor Necrosis Factor Receptor 1
CD95L/FasL	death receptor
DISC	death-inducing signaling complex
DR	death receptor
DL	death ligand
BH3	Bcl2 Homology domain
C8/C8*	pro caspases 8 and the active form
FADD	Fas-Associated protein with Death Domain
CD95/Apo-1/FAS	First apoptosis signal ligand
c-FLIP	cellular FLICE inhibitory proteins

Table 1.1: Legend of molecules abbrevations

2 Apoptosis

Apoptosis or programmed cell death (PCD) is a genetically controlled process whereby cells die in response to environmental or developmental cues. The morphological characteristics of apoptosis include cytoplasmic blebbing, chromatin condensation and nucleosomal fragmentation. Dead cells are rapidly phagocytized to prevent damage to neighboring cells. Regulation of apoptosis is critical for normal development and tissue homeostasis and disruption of this process can have severe consequences. Too much cell death may produce neurodegenerative diseases and impaired development, while insufficient cell death can lead to increased susceptibility to cancer and sustained viral infection. Progress has been made in the past decade to identify many of the basic components that contribute to apoptosis, including transcriptional mediators, membranebound receptors (e.g. TNF-α receptor and Fas), Bcl-2 family members, kinases/ phosphatases, and cysteine proteases. We first illustrate (par. 2.1) different molecules involved in apoptosis pathway and then we focus on extrinsic (par. 2.2) intrinsic (par. 2.3) and non apoptotic pathways (par. 2.4). In particular we refer to pathway generated by TRAIL and FAS receptors. In table 1.1 we illustrate a legend of the common abbrevations used in this thesis.

2.1 Key molecules on apoptosis pathway

The importance of properly balanced cell survival and death in an organism is undeniable. Unscheduled survival and proliferation of cells beyond their natural life span can lead to the formation of tumours and cancer, while, at the other end of the spectrum, the premature death of differentiated cells such as neurons or cardiac muscle cells leads to irreversible, degenerative diseases. Given the complexity of the signaling involved, it is not surprising that a large variety of endogenous regulators of apoptotic signaling have been identified and investigated in mammalian cells. Of particular importance for the mitochondrial apoptosis pathway are the B-cell lymphoma protein 2 (Bcl-2) and inhibitor of apoptosis (IAP) protein families. On the other side, death receptor-induced apoptosis is regulated at several levels and involves numerous protein families. The interplay between the different levels of regulation provides a significant complexity, which can be understood better using systems biology. In the following sections, we will give a summary of the different protein families and their roles in intrinsic and extrinsic apoptosis. In fig. 2.1 it is represented a little part of the apoptotic pathway mediated by death receptor. In the red circles there are the molecules considered in this thesis.

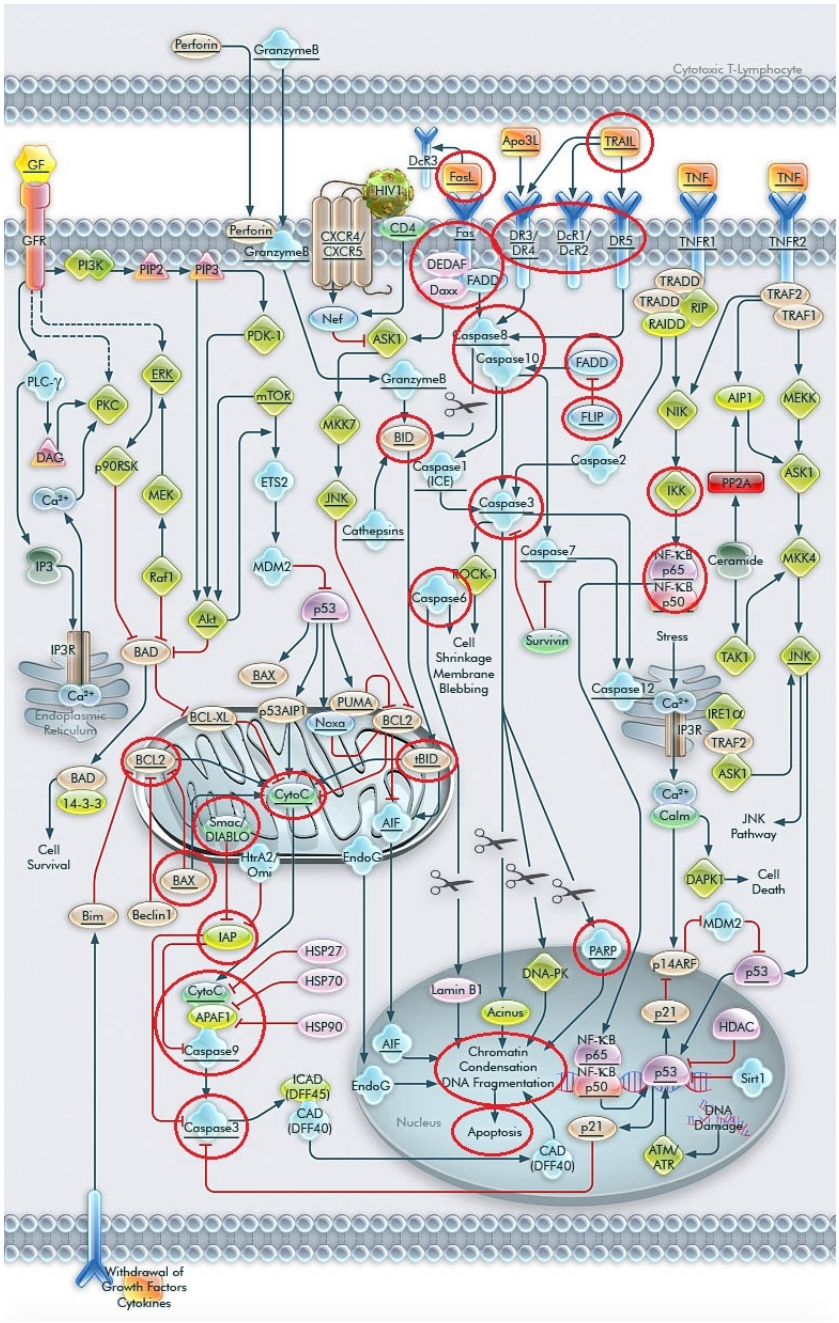

Figura 2.1: Cellular apoptosis pathway by death receptors. Red circles represent molecules and pathway evaluated in this study.

2.1.1 Caspases as major effector molecules of apoptosis pathway

Caspases are cysteine proteases and are the effector molecules of the apoptotic machinery. There are apoptotic, as well as inflammatory caspases. The apoptotic caspases are divided into initiator caspases, including caspase-2, -8, -9, and -10, and effector caspases, such as caspase-7 and -3. All caspases are present in the cell as inactive zymogens referred to as procaspases and are activated by internal cleavage. Initiator caspases act upstream of effector caspases and activate them through cleavage. Effector caspases then cleave a variety of cellular substrates, eventually resulting in cell death.

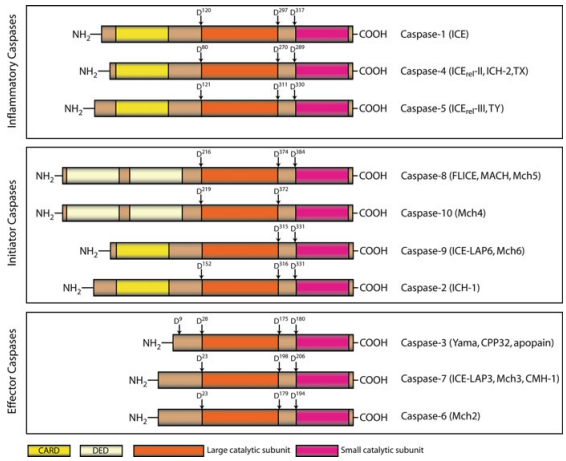

Figura 2.2: Structural organization of caspases. Caspases are generally divided into inflammatory and apoptotic caspases. Apoptotic caspases are further divided into initiator and effector caspases. Caspases possess a large (p20) and small (p10) subunit. Initiator caspases additionally have DEDs (procaspase-8/10) or CARD domains (procaspase-9) at their N-terminus [1]

All caspases share a common structure. Caspase monomers consist of a large (∼20 kDa) and small (∼10 kDa) subunit (Fig. 2.2). Initiator caspases additionally have specific recruitment domains at their N-terminus. Procaspase-8 and -10 have two tandem DED through which they interact with FADD at the DISC, procaspase-9 possesses a caspase-recruitment domain (CARD) which is required for recruitment to the apoptosome via interactions with Apaf-1. Active caspases are heterotetramers consisting of two large and two small subunits. Initiator caspases are present in the cytosol as monomers and are activated by dimerization or oligomerization at caspase-activating platforms and cleavage between the large and small subunits only stabilizes the dimer. It was shown that both dimerization and interdomain cleavage are required for full activation of caspase-8. Effector caspases on the contrary are present as inactive dimers and are readily activated by internal cleavage. This cleavage is performed by initiator caspases.

The conceptual difference between the two classes is that there is no proteolytic enzyme upstream of initiator caspases. Consequently, initiator caspases exhibit low zymogenicity, which is defined as the ratio of activity between the cleaved and the uncleaved form. While initiator caspases have highest ratios of 10 (caspase-9) or 100 (caspase-8), the ratio for caspase-3 is more than 10,000.

2.1.1.1 Caspase-8/10 activation at DISC

Two isoforms of procaspase-8 procaspase-8a (p55) and -8b (p53) are recruited to the DISC. After binding to the DISC, procaspase-8a/b (p55/p53) undergoes processing, thus generating active caspase-8 (Fig. 2.3). This processing has been suggested to occur via dimerization of two procaspase-8 monomers followed by a conformational change, leading to autoactivation of procaspase-8 homodimers. Procaspase-8a/b (p55/p53) processing at the DISC also results in the generation of the N-terminal cleavage products p43/p41, the prodomains p26/p24, as well as the C-terminal cleavage products p30, p18, and p10. Active caspase-8 heterotetramers (p10/p18) generated at the DISC initiate the execution of apoptotis. Recently, it has been reported that the cleavage products p30 and p43/p41 also possess catalytic activity leading to apoptosis initiation. Hence, procaspase-8 processing at the DISC initiates apoptosis through the generation of several catalytically active cleavage products.

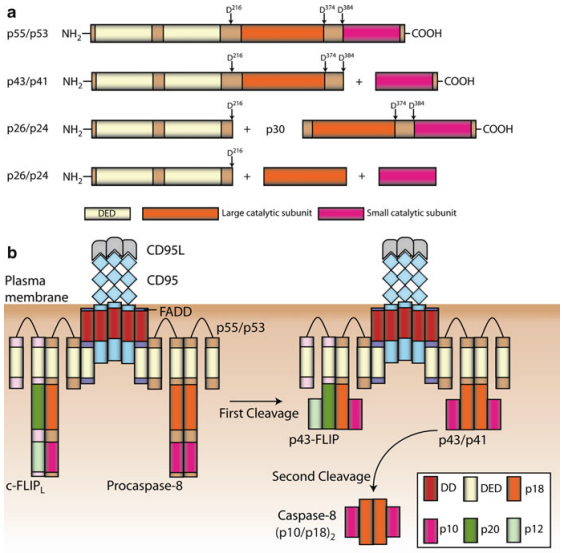

Figura 2.3: Caspase-8 cleavage products and processing at the DISC. (a) Procaspase-8 can be cleaved between the large and small subunit or between the prodomain and the large catalytic subunit, resulting in numerous different cleavage products. (b) Procaspase-8 homodimers at the DISC can be processed to the active caspase-8 heterotetramers (p10/p18) via the intermediate p43/p41. The procaspase-8/c-FLIPL heterodimer can only be processed to the intermediate p43-FLIP

Three isoforms of caspase-10 namely procaspase-10a, procaspase-10c, and procaspase-10d were reported to be bound to the DISC. Procaspase-10 is also activated at the DISC via generation of homodimers, leading to the formation of an active heterotetramer. However, whether caspase-10 cantrigger cell death in the absence of caspase-8 in response to CD95 stimulation is controversial.

The pathways generating apoptosis are usually divided into two principal categories: extrinsic and intrinsic. The first are generated by an external stimulus (e. g. through receptors) while the second are produced by reactions that occur inside the cell. Other pathways occur when cell undergo apoptosis and some of them promote cell survival. They are usually called non-apoptotic or survival pathways.

2.1.2 c-Flip proteins regulate caspase activation at the DISC

Three c-FLIP isoforms and two cleavage products have been characterized so far (Fig. 2.4). Three isoforms include one long, c-FLIPL, and two short variants, c-FLIPS and c-FLIPR. All three c-FLIP isoforms possess two tandem DED domains at their N-terminus. c-FLIPL additionally contains catalytically inactive caspase-like domains (p20 and p12).

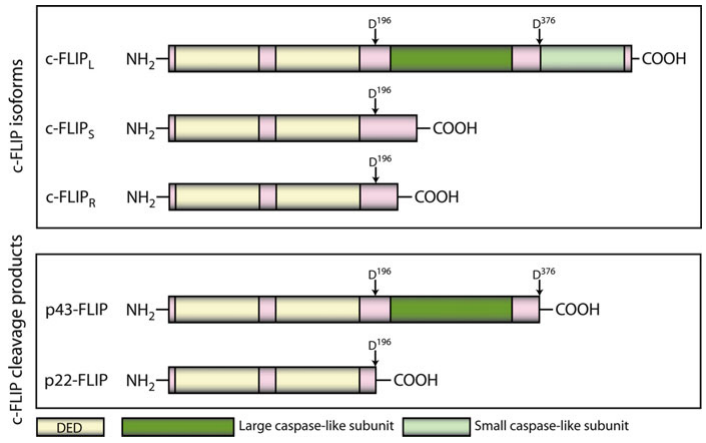

Figura 2.4: c-FLIP isoforms and cleavage products. Three isoforms of c-FLIP proteins exist, one long (c-FLIPL) and two short variants (c-FLIPS and c-FLIPR). All isoforms contain two tandem DEDs which are required for DISC recruitment. c-FLIPL additionally has a large and small caspase-like subunit, which are catalytically inactive. C-FLIPL can be cleaved by caspase-8 at different positions generating the N-terminal fragment p43-FLIP or N-terminal fragment p22-FLIP [1]

The two short isoforms, c-FLIPS and c-FLIPR, block DR-induced apoptosis by inhibition of procaspase-8 activation at the DISC. This has been suggested to occur through the formation of catalytically inactive procaspase-8/c-FLIPR/S heterodimers. c-FLIPL can play both a pro- and an antiapoptotic role. It can act as an antiapoptotic molecule, functioning in a way analogous to c-FLIPS when it is present at high concentrations

at the DISC. c-FLIPL can act proapoptotic when expressed at lower concentrations, in combination with strong receptor stimulation or in the presence of high amounts of either of the short c-FLIP isoforms c-FLIPS or c-FLIPR. Under these conditions c-FLIPL facilitates the activation of procaspase-8 at the DISC. This occurs via the formation of catalytically active procaspase-8/c-FLIPL heterodimers in which the procaspase- 8 active loop is stabilized by c-FLIPL, thereby increasing the catalytic activity of procaspase-8.

2.1.3 IAP family of proteins

The Inhibitors of Apoptosis (IAP) proteins directly inhibit caspases. They all share a conserved sequence motif of 70–80 amino acids, the baculoviral IAP repeat (BIR) domain, which is arranged around a coordinated zinc atom, of which each family member can possess up to three copies. There are six human IAPs,which include XIAP, c- IAP1, c-IAP2, NAIP, Bruce, and survivin. Numerous mammalian IAPs, as well as IAPs in flies and viruses, possess a C-terminal RING domain, however, the requirement of this domain for apoptosis suppression remains unclear. There are reports that both domains are required for their antiapoptotic function in insects, however, c-IAP1, c-IAP2, and XIAP in humans could still inhibit apoptosiswhen lacking the RINGdomain. XIAP directly inhibits active caspase-3. During the intrinsic apoptosis, mitochondrion is activated and opens its pores (MOMP). After MOMP Smac is released from the mitochondria into the cytosol and relieves XIAP-mediated inhibition. This causes a delay between receptor-mediated initiator phase and final commitment to cell death in type II cells [2]. XIAP also contains a RING domain with E3 ubiquitin ligase activity, which promotes caspase-3 degradation by the proteasome ([2, 5]).

2.1.3.1 XIAP and Smac/DIABLO

Among the IAPs, XIAP is the most potent inhibitor of cell death, capable of blocking both the intrinsic and extrinsic pathways of apoptosis through inhibition of the initiator caspase-9 and effector caspases-3 and -7. In addition to its caspase inhibition abilities, XIAP also has a RING motif which functions as an E3 ubiquitin protein ligase to catalyse the ubiquitination of itself as well as substrate proteins. Caspase inhibition by XIAP may be counteracted by the release of Second Mitochondria-derived Activator of Caspases/ Direct IAP Binding Protein with Low PI (Smac/DIABLO) or the serine protease Omi/HtrA2, both of which are released by mitochondria into the cytosol during apoptosis.

2.1.4 The Bcl-2 family

The Bcl-2 family of proteins are probably the best described endogenous modulators of the mitochondrial pathway of apoptosis, and regulate apoptosis by either promoting or preventing mitochondrial outer membrane permeabilisation (MOMP). Pro- and anti-apoptotic family members can heterodimerise and neutralise each other's function. The Bcl-2 family proteins can be divided into three subfamilies. The first subfamily comprises the anti-apoptotic proteins (Bcl-2, Bcl-xL, Bcl-w, Mcl-l, Al and Boo) which are

potent inhibitors of the apoptotic programme and antagonise pore formation at the mitochondrial outer membrane. These proteins are structurally characterised by four Bcl-2 homolgy (BH) domains. The remaining two subgroups, the Bax/Bak family and the BH3-only protein family, are pro-apoptotic and required for the initiation of apoptosis. The multi-domain, pro-apoptotic proteins, Bax and Bak (and potentially a third protein, Bok), bear three BH domains, and oligomerise and facilitate pore formation in the outer mitochondrial membrane. The BH3-only proteins promote apoptosis by not only selectively binding to the anti-apoptotic Bcl-2 family members, but also by directly inducing the activation and oligomerisation of the Bax and Bak proteins. Activation of Bax and Bak is essential for the activation of the mitochondrial apoptosis pathway. It should also be noted that there is crosstalk between the mitochondrial and death receptor apoptosis pathways. This crosstalk is carried out by caspase-8- mediated cleavage of the BH3-only protein family member, Bid.

2.2 System biology of extrinsic apoptosis

The extrinsic signaling pathway leading to apoptosis involves transmembrane death receptors that are members of the tumor necrosis factor (TNF) receptor gene superfamily. Members of this receptor family bind to extrinsic ligands and transduce intracellular signals that ultimately result in the destruction of the cell. The signal transduction of the extrinsic pathway involves several caspases which are proteases with specific cellular targets. Once activated, the caspases affect several cellular functions as part of a process that results in the death of the cells. The focus of this chapter is on understanding the signaling complexity of the extrinsic apoptotic pathway using systems biology. We summarize the main signaling paradigms and the major features of the extrinsic pathway.

2.2.1 Death receptor-induced apoptosis

Death receptors (DR) belong to the tumor necrosis factor (TNF) family of proteins and are characterized by extracellular cysteine rich domains (CRD) and an intracellular ∼80 amino acid long motif, the death domain (DD). The best characterized DRs are CD95 (also named Fas/APO-1), TNFR1, TRAIL receptor 1 (TRAIL-R1), and TRAIL-R2. Death ligands (DL) are assumed to be homotrimeric and exist in a membrane-bound or a soluble form.

CD95/Apo-1/FAS

The CD95-induced apoptotic pathway is one of the best-studied signaling pathways. The natural ligand of CD95, CD95L, is expressed on a variety of cells, such as cytotoxic T cells, as a type II membrane protein[1]. Stimulation of CD95 with its ligand or with agonistic anti-CD95 antibodies, such as anti-APO-1, triggers the oligomerization of CD95. This leads to the recruitment of Fas-associated death domain (FADD) through DD interactions, as well as procaspase-8, procaspase-10 (par. 2.1.1), and cellular FLICE

[1]Type II membrane proteins are trans membrane proteins that have their amino terminus on the cytoplasmic side of the cell and the carboxy terminus on the exterior.

inhibitory proteins (c-FLIPs) via N-terminal death effector domains (DED) (par. 2.1.2), and formation of the death-inducing signaling complex (DISC). In the DISC procaspase-8/10 are activated by dimerization and internal cleavage, which is regulated by c-FLIP proteins. Recent structural analyses challenge the concept of a trimeric ligand binding to a trimeric receptor. Triggering of CD95 has also been reported to induce nonapoptotic pathways, such as NF-kB, AKT, and ERK [3]. However, the detailed mechanisms of the induction of CD95-mediated nonapoptotic pathways are not elucidated yet. Activated caspase-8 is released from the DISC and activates effector caspases-3 and -7, which cleave a variety of substrates, and are responsible of the fragmentation of chromosomes.

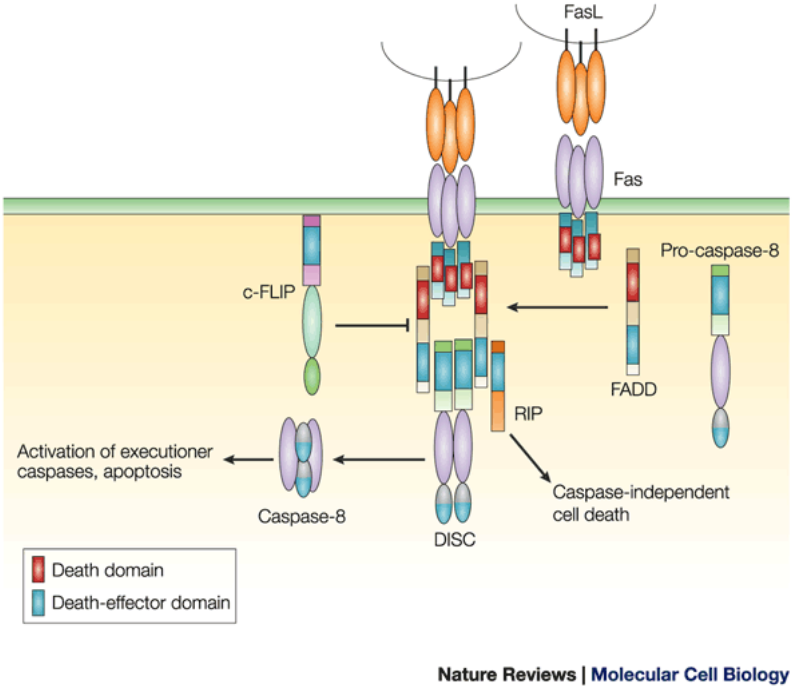

Figura 2.5: Fas ligand and receptor

Additionally, caspase-8 cleaves Bcl-2 protein Bid (par. 2.1.4). The C-terminal part, tBid, then translocates to the mitochondria resulting in mitochondrial outer membrane permeabilization (MOMP) and the release of proapoptotic factors into the cytosol, such as cytochrome c, Apaf-1, or endonuclease G. This results in the formation of another complex, the apoptosome, including cytochrome c, Apaf-1, ATP and procaspase-9, and activation of procaspase-9 in this complex. Caspase-9 also cleaves and activates caspase-3. In CD95-induced apoptosis two different cell types are distinguished: Type I and Type II. Type I cells are characterized by high amounts of CD95 DISC, which results in very efficient procaspase-8 activation, leading to massive activation of caspase-3 and

cell death. Type II cells, on the other side, are characterized by lower amounts of CD95 DISC formation, that results in less active procaspase-8 and require signal amplification through tBid-mediated mitochondrial permeabilization.

TRAIL

TRAIL (TNF-Related Apoptosis-Inducing Ligand) is a protein consisting of 281 amino acids. It is also called Apo2L. Five proteins, TRAILR1 (DR4), TRAILR2 (DR5/ TRICK2 or KILLER), TRAILR3 (DcR1/ TRID or LIT), TRAILR4 (DcR2 or TRUNDD), and Opg (Osteoprotegerin), have been identified as TRAIL receptors (Ref.1). Both TRAILR1 and TRAILR2 contain the functional DD (Death Domain), capable of inducing apoptosis. The other three receptors DcR1, DcR2 and Opg serve as "decoy" receptors. These three receptors can bind to TRAIL, but cannot induce apoptosis. DcR1 is a glycosylphosphatidylinositol-anchored cell surface protein, which contains the TRAIL-binding region as well as a region that anchors the receptor to the membrane. But unlike the other receptors, DcR1 lacks an intracellular tail needed to spark the death pathway. DcR2 is also able to bind TRAIL but contains a truncated DD that does not signal apoptosis induction but can activate NF-KappaB (Nuclear Factor-KappaB). Finally, Opg, slightly weaker receptor for TRAIL also binds to OpgL (Osteoprotegrin Ligand/Receptor), activator for NF-KappaB ligand (RANKL/Receptor Activator of NF-KappaB Ligand), inhibits osteoclastogenesis, and increases bone density. A cell expressing more decoy receptors is more likely to survive upon binding of the death ligands. TRAIL has been demonstrated to kill a wide variety of tumor cells with minimal effects on normal cells. This is because TRAIL's death receptors (TRAILR1 and TRAILR2) are mainly expressed in transformed cells while its decoy receptors are expressed in normal cells. Binding of TRAIL to DR4 and DR5 leads to the recruitment of an adaptor protein FADD (Fas-Associated Death Domain), which functions as a molecular bridge to Caspase8. Caspase8 then oligomerizes and is activated via autocatalysis. Activated Caspase8 stimulates apoptosis via two parallel cascades: it directly cleaves and activates Caspase3, and it cleaves BID (BH3 Interacting Death Domain) (par. 2.1.4). tBID (Truncated BID) translocates to mitochondria, inducing CytoC (Cytochrome-C) release, which sequentially activates Caspases9 and 3. BAX (BCL-2 Associated X-Protein) deficiency has no effect on TRAIL-induced Caspase8 activation and subsequent cleavage of BID; however, it results in an incomplete Caspase3 processing due to inhibition by XIAP (Inhibitor of Apoptosis, X-Linked). Release of SMAC/DIABLO from mitochondria through TRAIL-Caspase8-tBID-BAX cascade is required to remove the inhibitory effect of XIAP and allow apoptosis to proceed. BAX-dependent release of SMAC, not CytoC from mitochondria, mediates the contribution of mitochondrial pathway to TRAIL through death receptor-mediated apoptosis. Caspase3 directly cleaves downstream substrates e.g. PARP (Poly ADP Ribose Polymerase).

2.3 System biology of intrinsic apoptosis

For intrinsic apoptosis we usually mean the mitochondrial apoptosis pathway. Mitochondria have multiple functions. Apart from their role in the regulation of cellular bioen-

ergetics, redox homeostasis and signal transduction, mitochondria are able to initiate apoptosis. The Bcl-2 family proteins are the key regulators of the mitochondria-initiated caspase activation pathway. Activation of caspases is considered one of the most important regulatory steps for apoptosis. Caspase cascades can be initiated or amplified by the release of cytochrome-c from the mitochondria. On release into the cytosol, cytochrome-c binds to Apaf-1. Apaf-1 oligomerises and engages the initiator caspase, pro-caspase-9, which in turn activates downstream caspases-3 and -7. Furthermore, the release of Smac from mitochondria assists the amplification of the caspase cascade by abrogating the function of caspase inhibitors such as XIAP. Moreover, mitochondria are involved in caspase independent cell death with the release of factors including apoptosis-inducing factor. There have been considerable developments in recent years in further understanding the complex signaling networks and cellular decision making during mitochondria-initiated apoptosis through the use of systems biology. In this chapter, we examine the modeling approaches that are currently employed to further our understanding of the mitochondrial pathway of apoptosis.

2.3.1 Mithocondrial apoptosis pathway

In mammalian cells there are at least three main pathways which lead to caspase activation, the intrinsic or mitochondrial pathway, the extrinsic or death receptor pathway and the cytotoxic T-lymphocytes (CTL)/natural killer (NK)-derived granzyme B-dependent pathway. There is a certain amount of crosstalk between the pathways and all may ultimately result in the apoptotic death of the cell. The intrinsic pathway of apoptosis can be initiated by various forms of stress such as DNA damage, trophic factor withdrawal, nutrient deprivation, heat shock and oxidative stress. Apoptotic signaling in this pathway results in an increase in the permeability of the mitochondrial outer membrane and the subsequent release of several proteins from the inter-membrane space of the mitochondria into the cytoplasm, resulting in the activation of both initiator and effector caspases. Central to this pathway is the release of cytochrome c from the mitochondria. Normally cytochrome-c resides in the inter-membrane space of the mitochondria, where it functions by transporting electrons between protein complexes of the respiratory chain during oxidative phosphorylation. On release of cytochrome-c into the cytosol, it binds to and activates the adaptor protein, apoptotic protease activating factor-1 (Apaf-1). Oligomerisation of Apaf-1 results in the recruitment of the initiator caspase pro-caspase-9 and the formation of the apoptosome. Once activated, the mature caspase-9 remains part of the apoptosome complex, with Apaf-1 functioning as an allosteric regulator of caspase-9 activity, allowing it to cleave and activate downstream effector caspases such as pro-caspase-3 and pro-caspase-7. The executioner caspases-3 and -7 exist within the cytosol as inactive dimers. When activated, these caspases cleave and activate further downstream caspases such as caspases-2 and -6. Caspase-3 is also involved in a feedback amplification loop to further activate caspase-9.

2.4 Nf-kB non-apoptotic pathway

The eukaryotic transcription factor NF-kB was originally discovered transcribing the immunoglobulin kappa light chain gene in B cells. NF-kB can be activated following a variety of stimuli, including bacterial lipopolysaccharide (LPS), T cell receptor (TCR) signaling, different cytokines, such as TNFa, interleukin 1 (IL-1) and IL-2, viral infections, UV and X-ray radiation, nitric oxide, and also CD95. The NF-kB transcription family comprises multiple members, including RelA (p65), NF-kB1 (p50, p105), NF-kB2 (p52, p100), c-Rel, and RelB. All NF-kB proteins share a conserved N-terminal 300-amino acid motif, the Rel homology domain (RHD), which contains a dimerization, nuclear localization as well as DNA-binding domain. NF-kB proteins form homo- or heterodimers with each other, except for RelB. The most prominent dimer which is commonly referred to as NF-kB is the heterodimer of p65 with either p50 or p52. Importantly, only c-Rel, RelA, and RelB possess a transactivation domain and thus act as transcriptional activators, while other NF-kB proteins act as transcriptional repressors. In the absence of activating stimuli NF-kB dimers are inhibited by IkB (inhibitor of NF-kB) proteins via ankyrin-repeat motifs and masking their nuclear localization signal. IkB proteins are phosphorylated by IkB kinases (IKKs) and subsequently degraded by the proteasome. The IKK complex, consisting of IKKa, IKKb, and NEMO (IKKg) regulates NF-kB activation following various stimuli and lack of either IKK complex component blocks NF-kB activation.

2.4.1 CD95-Mediated NF-kB activation

Accumulating evidence suggests that stimulation of CD95 can also induce nonapoptotic pathways, such as tumor growth and invasion, as well as proliferation and programmed necrosis, termed necroptosis. CD95-mediated nonapoptotic signaling occurs via induction of NF-kB, Akt and mitogen-activated protein kinases (MAPK) pathways. These, however, are not well understood, but have been reported to require caspase-8 activity [3]. C-FLIP proteins play a very important role in the regulation of caspase-8 activation [6, 7] as well as induction of nonapoptotic pathways. It could be shown that the cleavage product of c-FLIPL p43-FLIP directly interacts with the IKK complex, leading to the activation of NF-kB [3]. Other prominent players in nonapoptotic pathways are receptor-interacting protein 1 (RIP1) and RIP3 which are important for CD95-induced necroptosis, as well as activation of NF-kB.

2.4.2 TRAIL-Mediated NF-kB activation

Upon binding to TRAILR1, TRAILR2, or TRAILR4, TRAIL can also activate the transcriptional factor NF-kB and JNK (c-Jun N-terminal Kinase). Recently, it was suggested that TRAF2 (TNF Receptor-Associated Factor-2), an important effector of TNF (Tumor Necrosis Factor) signaling, was involved in both NF-kB and JNK activation induced by overexpression of TRAIL receptors. Inactive NF-kB is located in the cytoplasm because its interaction with the inhibitory proteins, IkBs, masks its nuclear translocation

signal. When IKK is activated, it phosphorylates IkBs. Then the phosphorylated IkBs will be polyubiquitinated and rapidly degraded by the proteasome. The degradation of IkBs leads to the release of NF-kB and allows NF-kB to translocate into the nucleus and to activate its target genes, some of which are the crucial mediators of the NF-kB antiapoptotic function.

3 Modelling biochemical systems

3.1 introduction

Signal transduction inside cells is carried out by network of interacting signal mediators and is often a very complex process. Complexity derives not only from the enormous amount of different molecules involved in the process but also from the presence of numerous feedbacks and feedforward loops, both negative or positive, concerning the pathway itself, and ample crosstalks involving distinct pathways. This high degree of complexity issues new challenges in understanding how cellular signaling works in detail and thus new and more powerful tools have to be introduced beyond the simple reasoning on experimental data. Apoptosis signaling pathway represents a typical example of complex network due to the numerous molecules constituting it and the several types of interactions between these elements. Hence, in order to analyse in detail the dynamics which characterizes this network it is necessary to make use of mathematical tools able to model the system comprising the majority of its biochemical reactions. The resulting model can be used to make predictions of signaling pathway in physiological state to gain new knowledge about the process or may be used to test the system varying some quantities and parameters which describe the model to obtain information about network malfunctioning and mimicking pathological condictions. The most common approach makes use of a system of ordinary differential equations (ODEs) to model the kinetics of the molecules populating the system. This method works well in case of simple networks comprising just few molecules. When the system under investigation is particularly large and involves a great amount of interactions between molecules, the ODEs approach is no more efficient from both implementational and computational point of view. For this reason the rule-based modeling approach has been introduced providing an easy way to implement the system and new simulation tools.

3.2 Why modelling apoptosis?

Apoptosis is a phenomenologically easily observable process. However, understanding its mechanistic basis is challenging owing to complex interactions of a large number of signaling proteins and emergent behavior at the systems level. After applying a sufficiently strong death-inducing stimulus to a population of cells, irreversible signaling events are initiated leading to the characteristic appearance of an apoptotic cell: membrane blebbing proceeds, the cell shrinks, and organelles disintegrate. Apoptosis occurs for extrinsic stimuli on a timescale of hours and for intrinsic stimuli of days, and is accessible to several experimental techniques allowing for the acquisition of quantitative data.

The wide range of available experimental techniques and the detailed knowledge about molecular events render apoptosis a system suitable for modeling analyses. Apoptosis induced by death ligands is one of the few cell fate decisions known to proceed by purely post-transcriptional mechanisms, thus further simplifying the formulation of mathematical models. Even though individual steps of the apoptotic signal transduction cascades are well understood, we lack insights into the system properties and the dynamics of the death decision. Questions to be addressed in apoptosis by systems biology approaches include:

1. How do cells ensure that apoptosis robustly occurs in all-or-none manner? What is the "point-of-no-return" representing irreversibility in apoptosis? Which signaling motifs are responsible for such digital and history-dependent behavior? As detailed below, mechanisms proposed using kinetic modeling include bistability due to positive feedback and sigmoidal responses arising from competitive inhibition.

2. How is specificity in the apoptosis vs. survival responses ensured? A topic of particular interest for apoptosis modeling is that apoptotic stimuli trigger survival or death signaling depending on initial conditions and the stimulus strength. Modeling can be employed to identify critical nodes of signaling crosstalk that tip the balance between cell death and survival. Furthermore, the interlocked regulation of cell cycle is a topic followed by modelers.

3. What are the principles underlying cell-to-cell variability in the apoptosis response of a cell population? Why do cell types differ in their sensitivity to death-inducing stimuli? Currently, several therapeutic applications are tested to stimulate apoptosis in cancer cells, to decelerate tumor growth, or to prevent cells, preferentially neurons or cardiomyocytes, from undergoing programmed cell death. Modeling approaches could help to plan therapies and to predict the outcome on a population of cells. Particularly by distinguishing cell death kinetics and the behavioral heterogeneity of different cell types, and predicting drug sensitization by cotreatments, modeling could be a valuable tool.

To answer these questions, we first give an overview of the basics of mathematical formalisms in system biology (par. 3.3 and 3.4). At last we review successful application of ODE apoptosis models created to characterize apoptosis pathway (par. 3.4.1).

3.3 Ultrasensitivity

In molecular biology, ultrasensitivity describes an output response that is more sensitive to stimulus change than the hyperbolic Michaelis-Menten response[1] [22]. Ultrasensitivity

[1] In biochemistry, Michaelis–Menten kinetics is one of best-known models of enzyme kinetics. The model takes the form of an equation describing the rate of enzymatic reactions, by relating reaction rate v to $[S]$, the concentration of a substrate S. Its formula is given by: $v = \frac{V_{max}[S]}{K_m+[S]}$. V_{max}represents the maximum rate achieved by the system. The Michaelis constant $K_m$is the substrate concentration ati which the reaction rate is half of V_{max}.

can help to filter out noise or can delay responses. Mechanisms that lead to ultrasensitive stimulus-response curves include cooperativity, multisite phosphorylation, feed-forward loops, and enzymes operating under saturation. The latter mechanism has been termed zero-order ultrasensitivity because a necessary condition is that the opposing enzymes of a covalent modification cycle display zero-order kinetics. Molecular binding is an interaction between molecules that results in a stable association between those molecules. Cooperative binding occurs if the number of binding sites of a macromolecule, that are occupied by a specific type of ligand, is a non-linear function of this ligand's concentration. This can be due, for instance, to an affinity for the ligand that depends on the amount of ligand bound.

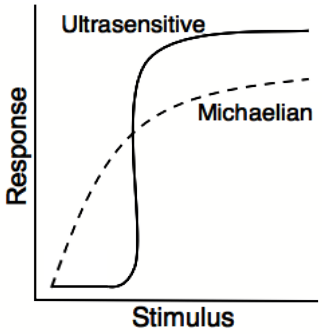

Figure 3.1: Ultrasensitive versus Michaelian curve response [22]

Oscillations can be observed if an ultrasensitive cascade possesses a negative feedback. Bistability (hysteresis) can occur if such an ultrasensitive cascade is equipped with a positive feedback. Ultrasensitive responses are usually represented by sigmoidal graphs.

3.3.1 Effect of feedbacks on ultrasensitive cascades

The dynamic behavior of signal transduction cascades is strongly controlled by feedback loops. These feedbacks act on all levels of signal transduction. Feedbacks arise from autocrine induction of hormones, from the transcriptional regulation of cascade intermediates, from their covalent modification or from receptor internalization. Positive feedback is a process in which the effects of a small disturbance on a system include an increase in the magnitude of the perturbation. That is, A produces more of B which in turn produces more of A. Mathematically, positive feedback is defined as a positive loop gain around a feedback loop. That is, positive feedback is in phase with the input, in the sense that it adds to make the input larger. Positive feedback tends to cause system instability. When the loop gain is positive and above 1, there will typically be exponential growth, increasing oscillations or divergences from equilibrium. System parameters will typically accelerate towards extreme values, which may damage or destroy the system, or

may end with the system latched into a new stable state. Positive feedback may be controlled by signals in the system being filtered, damped, or limited, or it can be cancelled or reduced by adding negative feedback. In the following sections, the consequences of such feedback loops on the dynamics are briefly reviewed.

3.3.2 Bistability caused by positive feedback

Many theoretical and experimental investigations have shown that a positive (or double negative) feedback loop in gene regulatory circuits is a structural condition that allows for bistability. A bistable system is a system that exhibits two stable steady states, separated by an unstable state. Often the coexistence of the steady states is a function of a stimulus; therefore, the system can be switched from one state to another at so-called saddle-node bifurcations. There is now ample evidence that bistability is important in biological signal processing, in the cell cycle, in apoptosis, and in the yeast Gal/Glc network. A prerequisite for observing bistability is that either the cascade or the feedback loop is ultrasensitive. Bistability provides the means for a biological signaling system to suppress noise, to memorize the signaling history, or to perform all-or-none decisions. It is a mechanism to establish checkpoints, i.e. a threshold, which a stimulus has to exceed before the system is committed into a new state, e.g. cell cycle phase.

3.4 Computational modeling techniques

Analyzing the cell on a systems view can be done by top-down and bottom-up approaches. Detailed mechanistic mathematical models constructed from the molecular characteristics of individual proteins ("bottom-up models") have only been developed for metabolic and signaling networks. In contrast, transcriptional regulatory networks, and the link between signaling networks and ultimate cellular decisions are best tackled by statistical methods which integrate huge amounts of data but are mostly phenomenological ("top-down modeling"). Top-down approaches examine the cell on a global level, treating individual regulatory modules as black boxes that are not analyzed mechanistically but only characterized with respect to input–output behavior. Thus, top-down methods typically do not require much prior knowledge about the system, so that many signaling and/or metabolic pathways can be studied at once. Most top-down approaches are solely data-driven and rely on high throughput screens of cellular behavior (gene expression profiling, proteomics, siRNA screening, sequencing, and affinity assays). Typically, the ultimate goal of top-down approaches is to identify biologically relevant patterns and correlations to the data (e.g., disease marker gene identification) or to predict new molecular interactions (e.g., reverse engineering algorithms). Bottom-up approaches focus on well-characterized parts of the biochemical regulatory network, and are typically based on the assumption that the properties of these subnetworks (or "modules") can be studied in isolation. Based on prior knowledge and on time-resolved experimental data, mechanistic mathematical models describing the interactions of individual proteins in the module are constructed (e.g., by using sets of coupled differential equations). The goal of bottom-up modeling is to identify physiologically relevant systems-level properties emerging from

complex interactions within the network (e.g., feedback). Apoptosis-inducing signaling cascades, especially those induced by death ligands, were mainly studied using bottom-up modeling approaches, since (1) the molecular events are well characterized; (2) transcriptional events can be neglected; (3) the ultimate death decision often closely correlates with all-or-none activation of effector caspases, implying that statistical methods are not required to link signaling to cellular phenotypes.

However, bottom-up approaches to apoptosis are diverse and the methodology of choice depends on the complexity of the signaling network under study, the available experimental data, and the question to be addressed by modeling. Boolean approaches are typically employed to qualitatively analyze the (quasi-)static behavior of large apoptosis-survival crosstalk networks which comprise many molecular species. Ordinary differential equation (ODE) models allow for the quantitative description of network dynamics but typically require knowledge about many kinetic parameters which either limits the network size and/or requires huge amounts of experimental data. Standard ordinary differential equations (ODE) modeling may even not be sufficient if spatiotemporally resolved single-cell data is available

(1) spatial gradients within the cell can be modeled using subcellular compartment ODE models or partial differential equations (PDEs);

(2) cell-to-cell variability may arise due to stochastic dynamics of the apoptotic signaling cascade ("intrinsic noise") or due to cell-to-cell variability in the expression of pathway components ("extrinsic noise").

While ODE models with randomly sampled initial protein concentrations can be employed to simulate extrinsic noise, stochastic simulation algorithms are required to understand intrinsic noise. In the following, we will give an overview of principal differences between boolean and quantitaive ODE models.

Boolean models:
Simulations of largescale networks is therefore often performed using boolean or logic modeling, a qualitative approach that is based on network topology, but does not take into account quantitative features of individual reactions. Instead protein activities are represented by nodes which can either be on or off (activity 0 or 1), depending on the activities of upstream input nodes. Logic rules are applied at each iteration: For example, in a so-called AND-gate, the node Z will be activated if and only if both input nodes X and Y are active. In contrast, an OR-gate simply requires either X or Y to be active. Thus, boolean rules can be used to qualitatively represent real biochemical mechanisms such as functional redundancy (OR-gate) or coincidence detection (AND-gate), the latter, arising from sequential processing by two distinct enzymes. Since logical rules are applied iteratively, the approach can be used to study temporal phenomena such as adaptation. Moreover, boolean networks can exhibit nonlinear dynamic phenomena such as oscillations, and stable vs. unstable attractors.

Quantitative models:
Boolean models are inherently limited in their capability of quantitatively describing the temporal dynamics of biochemical networks. In the context of perturbation analysis,

boolean approaches are restricted to the simulation of complete elimination of network nodes and/or reactions; thus, gradual phenomena such as dosage compensation cannot be studied. Moreover, the qualitative effects of perturbations as revealed by boolean modeling are often intuitively clear. Thus, in many cases, nontrivial and experimentally testable predictions require quantitative modeling approaches such as ODE and PDE modeling, as well as stochastic simulations. ODE approaches assume that large numbers of signaling molecules are present within the cell, so that random fluctuations in reaction events can be neglected by averaging over the whole molecule population. Moreover, in ODE modeling it is assumed that the cell represents a well-stirred reactor, implying that diffusion effects do not matter. In apoptosis networks, these assumptions are likely to be fulfilled, as caspase and their regulators are typically expressed at the number of several hundred thousand molecules per cell. Furthermore, the time scale of apoptosis induction (hours) is slow relative to the time scale of protein diffusion within a cell (milliseconds to seconds); therefore, spatial gradients of apoptosis signaling molecules are unlikely to play a decisive role in apoptosis initiation.

3.4.1 ODE Models Describing Apoptosis Networks

In this section, we will review some models of apoptosis found in literature. The first mechanistic apoptosis model of coupled differential equations, presented by Fussenegger et. al. [12], described sequential activation of caspase-8, caspase-9, and caspase-3 by intrinsic or extrinsic stimuli. The model encountered for a positive feedback from caspase-3 promoting the release of cytochrome c from mitochondria and thus promoting the additional activation of caspase-9 in apoptosomes. As this model was not trained against quantitative data, it provided only predictions on activated fractions of initiator and executioner caspases dependent on initial concentrations of apoptosis promoting or inhibiting proteins. A lot of progress has been made since this first apoptosis model, and different aspects have been studied in detail. In the following, we will review a piece of the current literature on ODE-based apoptosis modeling.

3.4.1.1 Models of Extrinsic Apoptosis Pathway

Understanding bistability in the process of apoptosis initiation was the focus of the study of Eissing et. al. [13]. Their model described the bistability in extrinsic apoptosis within the context of caspase-mediated positive feedback. Caspase-8 activated by receptor-induced apoptosis in type I cells activates caspase-3, while caspase-3 promotes positive feedback by caspase-8 activation. A stability analysis of this minimal model showed that bistability and therefore a stable live steady state were only possible parameter values far off the experimentally measured kinetic parameters. By extending the model topology, the authors concluded that bistable caspase activation within the physiologically reasonable parameter range required the consideration of inhibitors of activated caspase-8. It was found that BAR molecule palys an important role in establish bistability. The important antiapoptotic role of the protein BAR was investigated also in the study of Pace et. al. [14].

3.4.1.2 Models of Intrinsic Apoptosis Pathway

The theoretical study by Bagci at. al. [15] addressed origins of bistability on the level of MOMP and apoptosome formation. Two positive feedback mechanisms contribute to bistability: first, caspase-3 cleaves and inactivates the MOMP inhibitor Bcl-2, and thereby amplifies its own production. A second feedback arises from the cleavage of the MOMP inducer Bid by caspase-3; thus Bid cleavage, initially triggered by caspase-8, can be enhanced by caspase-3. Their mass-action model describes oligomerization of Apaf-1 bound to cytochrome c to the heptameric complexes of apoptosomes. As this cooperative oligomerization process leads to higher-order terms in the corresponding rate equation, the positive feedback interactions can result in bistable regimes corresponding to either survival or apoptosis. In the model of Bagci at. al. [15], bifurcation points in the caspase-3 activity were investigated, that are dependent on the production or degradation of Bax and their relation to inhibitory Bcl-2 proteins. Above a certain threshold for the degradation rate of Bax or below a certain threshold for the Bax production rate, the bistable behavior is changed into a monostable survival state.

3.4.1.3 Implicit Feedback Mechanism in Intrinsic Apoptosis

In the modeling studies summarized so far, the positive feedback mechanisms known from the biomedical literature and their contribution to bistability were analyzed. Additionally, mathematical modeling could provide valuable insights into non-obvious, hidden feedback loops that arise from the topology of the apoptosis network. This phenomenon has been referred to as implicit positive feedback regulation. The interplay of caspase-3, caspase-9, and inhibitors of apoptosis (IAPs) in the mitochondrial proapoptotic pathway was investigated in a model by Legewie at. al. [16]: cytochrome c released from mitochondria, triggers activation of caspase-9, which in turn cleaves procaspase-3 into active caspase-3. Both caspase-3 and caspase-9 are inhibited by XIAPs to prevent autoreactive activation. Interestingly, an implicit positive feedback loop arises from the dual inhibition of both caspases by XIAPs: once active caspase-3 is generated, it can bind to XIAPs, thus sequestering XIAPs away from caspase-9. This sequestration effect enhances caspase-9 activation, resulting in autoamplification of caspase-3 cleavage. In the model by Legewie et al., the dependency of the concentration of active caspase-3 as the response to an Apaf-1 concentration shows different characteristics of either monostable, bistable reversible, or bistable irreversible behavior. The authors concluded that implicit positive feedback alone brings a very small range of bistability; however, implicit feedback synergizes with other feedback mechanisms to establish a broad bistable range and irreversibility in the life–death decision. The studies of Chen et. al. [17] combined ODE, stochastic and cellular automaton modeling to further understand signaling processes that potentially lead to MOMP. In these studies interactions between pore-forming effectors (Bax, Bak), activators and enablers (tBid and several others), and inhibitors (Bcl-2 amongst others) that lead to or prevent mitochondria outer membrane permeabilization are analyzed. After translocation to mitochondria, inactive Bax and Bak are catalyzed to their active form by an activator. Subsequently, activated Bax and Bak lead

to membrane pore formation and cell death. In the study of Cui et. al. [18], models involved in the bistability of MOMP were further developed. Questions on the possible model topology led to hierarchical considerations in Chen's[17] and Cui's [18] studies: do activators and enablers indirectly induce apoptosis by sequestering Bcl-2 away from Bax, or are activators directly proapoptotic by catalyzing the reaction of Bax to its active form that can cause pore formation and cytochrome c release? This question led to an indirect model recapturing the inhibition of Bcl-2 by activators and topologies describing direct Bax activation. Inhibitors as Bcl-2 in the indirect topology interfere by inhibiting Bax and thereby preventing its oligomerization at the pores. In direct topologies they inhibit activators from catalyzing Bax activation. Direct topologies were favored in this study, as they involve two possible feedback mechanisms that could contribute to a bistability in Bax activation.

3.4.1.4 Models with a switching / threshold mechanisms

The critical roles of c-FLIPL and c-FLIPS, which potentially act as stoichiometric inhibitors in the DISC, were investigated in a model of Bentele et. al [19]. The dependence of the ligand concentration threshold on the concentrations of both splicing variants of c-FLIP was characterized, and it was concluded that c-FLIPs establish a stoichiometric switch. A large-scale model comprising DISC assembly, caspase activation, MOMP, interference from caspase inhibitors, and degradation processes was derived. By a global sensitivity analysis, clusters of modeled signaling proteins with high mutual sensitivities of protein concentrations were defined, which lead to functional subsystems. By disregarding parameters that had low sensitivities to parameters in one cluster, the dimensionality of the parameter estimation problem could be decreased. It could be shown that the threshold ligand concentration was highly sensitive to the c-FLIP concentration which is consistent with a stoichiometric switch mechanism. It could be shown that the concentration of c-FLIP at the time of ligand addition is central to apoptosis timing. Another monostable model of the apoptosis threshold was introduced in the theoretical study of Stucki and Simon [20]. However, these authors did not focus on the mechanism of ultrasensitivity, but represented all-or-none caspase-3 activation phenomenologically using a Heaviside function[2] in the caspase-3 production term. The major focus of the study was to analyze how the caspase-3 activation threshold could be modulated by the caspase-3 inhibitory XIAPs, the XIAP antagonist Smac, and Smac-binding antiapoptotic proteins such as survivin. The potentially limiting role of caspase-3 degradation was addressed, and it was concluded that XIAPs efficiently suppress apoptosis by triggering the degradation of caspase-3 in a nonlinear manner.

3.4.1.5 Models with a timing switch

Steady states, bistable switches, and ultrasensitivity govern long-term decision making within biochemical signaling networks. However, in the context of apoptosis, it is also

[2]The Heaviside step function, or the unit step function, usually denoted by H (but sometimes u or ϑ), is a discontinuous function whose value is zero for negative argument and one for positive argument.

important that the time course of effector caspase activation is abrupt. Such temporal switching ensures complete and coherent initiation of cellular demise. A recent study concluded that the apoptosis timing in single cells consists of a variable lag time followed by the sudden switch-like effector caspase activation (Albeck et. al. [5]). While the lag time varies within the range of one to several hours, dependent on the stimulus strength, the sudden switching time was shown to be relatively invariant around 30 min. This robustness of sudden switching can be interpreted as necessary to prevent from states of partial destruction that could cause genomic instability. The lag time is lengthened by proteins upstream of activated Bax, as c-FLIP, BAR, or cytosolic Bcl-2, and shortened by TRAIL receptors, caspase-8, Bid, and Bax. Moreover, the robustness of the switching time is determined on the level of Bax–Bcl-2 interaction leading to mitochondria pore formation. Thus, most modeling studies characterizing the temporal dynamics of apoptosis initiation in type II cells employing the mitochondrial pathway focused on regulation at caspase-8 or Bcl-2 level. In a combined experimental and theoretical study, Rehm et. al. [21] analyzed the kinetics of temporally switch-like effector caspase activation downstream of mitochondria. In particular, they focused on the control of effector caspase activation by XIAP. Their model described apoptosis signaling following MOMP induced by the drug staurosporine. In their model, Smac and cytochrome c released from mitochondria served as stimuli. Subsequent events in the model include apoptosome formation, caspase-9 as well as caspase-3 activation and caspase inhibition by XIAP. Specifically, their model predict that a reduction of XIAP levels would not affect apoptosis timing, while an XIAP overexpression would significantly delay effector caspase activation.

3.4.1.6 Nf-kB Models

To understand the double-edged role of CD95 (APO-1/Fas) activation in apoptosis as well as in NF-êB activation, models describing the role of c-FLIP on both cell fates were established (Fricker [7]; Neumann [3]). A focus of the models is the balance between caspase activation and inhibitory processes at the DISC. Cleavage of procaspase-8 homodimers bound to FADD can result in two forms that possess catalytic activity: an intermediate form p43 that remains bound to the DISC as a homodimer, and the completely processed form p18 that dissociates from the DISC as p182–p102 heterotetramers. Three splicing variants of the cellular FADD-like interleukin-1b-converting enzyme inhibitory protein (c-FLIP), c-FLIP short (c-FLIPS), c-FLIP long (FLIPL), and c-FLIP Raji (FLIPR) can heterodimerize with a monomer of procaspase-8 bound to a FADD molecule at the DISC and interfere with caspase-8 activation. The two variants c-FLIPS and c-FLIPR block procaspase-8 autoprocessing in a heterodimer and therefore inhibit propagation of the apoptosis signal. In contrast, c-FLIPL can facilitate procaspase-8 cleavage to p43 but not to p18. While the two forms c-FLIPS and c-FLIPR clearly inhibit signal propagation, it was not obvious if c-FLIPL promotes or also inhibits apoptosis. To resolve this question, a study of Fricker [7] on the signaling function of c-FLIPL combined experiments and modeling, and showed an ambiguous function of the protein as dependent on the stimulus strength. Their model considered the formation of homodimers of procaspase-8 or heterodimers of procaspase-8 and c-FLIP variants at the DISC and either termination

of further reactions or processing to caspase-8 or p43-FLIPL by other active homo- or heterodimers.

3.5 Rule-based modeling

We mentioned the importance to catch every site-specific detail of protein-protein interactions in order to achieve the complete comprehension of how a signaling pathways works. In addiction to difficulties arising from incomplete experimental data, another impediment is present due to the intrinsic complexity in describing every interaction occurring in the network. Signaling proteins contain multiple functional components and several sites of post-translational modification. As result, interactions among signaling proteins may generate a myriad of protein complexes and post-translational modification states. For instance, a protein containing n phosphorylation sites can be found in up to 2n distinct states. This feature has been called combinatorial complexity and has been recognized as a significant challenge to our understanding about cellular regulation. In conventional model specification using a set of ODEs, each chemical species that potentially populates the system and each reaction that can occur must be explicitly specified and this may generate a combinatorial number of coupled differential equations making model implementation tedious, prone to errors or even impossible. Since the same molecule found in a different state represents a different chemical species, to describe completely each molecule as many of differential equations as the number of its dinstict states are necassary (without considering any kind of interaction with other molecules). Taking the example above, a protein containing n phosphorylation sites is described by 2n differential equations. Moreover, the amount of differential equations increases rapidly when molecules with more than one site bind together forming in a complex which can be found in a myriad of different possible states. The most common solution adopted to overcome this limitation entails the simplification of the model. Proteins with multiple phosphorylation sites are represented with a single phosphorylation site which reassumes the properties of all sites, termed virtual phosphorylation site. The same procedure is adopted when a complex sequential multi-step process is taking place by substituting it with a single step. Obviously these simplifications conflicts with the knowledge of cellular biochemistry and there is no proof that these assumptions could not afflict model predictions in some way. In order to deal with the issue of combinatorial complexity, a new useful tool has been introduced with the purpose to specify all the reactions arising from molecular interactions in a more efficient and compact way. Rule-based modeling approach is based on the key assumption that the characteristics of molecular interactions depend on local properties of the protein involved and this modularity mostly determines the network dynamics. According to this assumption, structure of a reaction occurring in the network can easily be defined by means of a rule. A rule represents a class of reactions involving reactants with common components and component properties. The important simplification of the rule-based modeling approach is that all the reactions within a class are assigned the same rate law. In conclusion, both rule-based model and ODEs model provide a representation of chemical kinetics but they are different in the

model specification procedure. While in ODEs model the modeler must state explicitly which chemical species populate the system and how these are connected and influence each other, in a rule-based model, the modeler must state only the interactions occurring in the system and their contextual dependencies. Rule-based modeling approach is implemented by means of two major languages, termed Kappa and BioNetGen. Due to its facility of use we chose BioNetGen language to implement our models but the differences compared with Kappa language are neglegible.

3.6 BioNetGen language

BioNetGen [4] is a set of software tools for rule-based modeling and is a mnemonic for "Biological Network Generator". The software not only generates reaction networks starting from reaction rules, but also simulates such networks using a variety of methods. In order to understand how this software practically implements a biological system using rule-based modeling, we report a simple example taken from that will clear the basic concepts lying beneath this approach.

Bionetgen language encoding example: Fig. 3.2 depicts the implementation of a simple network in all its essential parts. Molecules are implemented as structured objects that can be constituted by different components. These components represent functional elements of proteins and may have associated states representing covalent modifications or conformations (e.g. phosphorylated/ unsphosphorylated state, active/inactive state etc.). The expression reported in Fig.3.2(A) indicates the definition of two molecules types. A(a) represents the presence of molecules type A having only the componet a. B(b1,b2∼U∼P) represents molecules type B having two components, b1 and b2. In particular, the expression b2∼U∼P indicates that component b2 may be found in two possible states, ∼U and ∼P, which can be used to indicates respectively the unphophorylated and the phosphorylated states. Components of distinct molecules can link together forming a bond, thereby building complexes of assembled molecules. Patterns can be used to select particular molecular attributes. In particular, the pattern B(b1) shown in Fig. 3.2(B) selects molecules B having the binding site b1 completely free despite of the phosphorylation and binding status of b2 component. Rules are needed to specify the biochemical transformations that can potentially take place in the system. The term "transformation" is used instead of "reaction" to indicate that the same reaction rule is applied to a selected set of reactant species and not necessarily to only one chemical species. This approach is worthy if, as already said, the chemical reactions mainly depend on the local properties of protein components. Modularity feature implies that the same reaction rule can be used to describe the transformation of different chemical species sharing common components and component properties. This selection method of the chemical species permits to write many complicated chemical reactions in a set of few rules making more compact and efficient the implementation of the model. In rules, the "pattern matching" is accomplished specifying two essential parts:

- the protein components directly modified by the transformation (reaction center)

and

- the components and components states needed for the selection of chemical species (reaction context).

In Fig. 3.2(C) are reported 3 different rules and their reaction centers are underlined. Rule 1 A(a) + B(b1) <-> A(a!1).B(b1!1) kp1,km1 represents a common reaction of binding and unbinding between molecules A and B. Bond formation involves the components a of molecule A and component b1 of molecules B. Since nothing is specifyed about component b2, the reaction between the two molecules takes place indipendently from the phosphorylation state of b2.

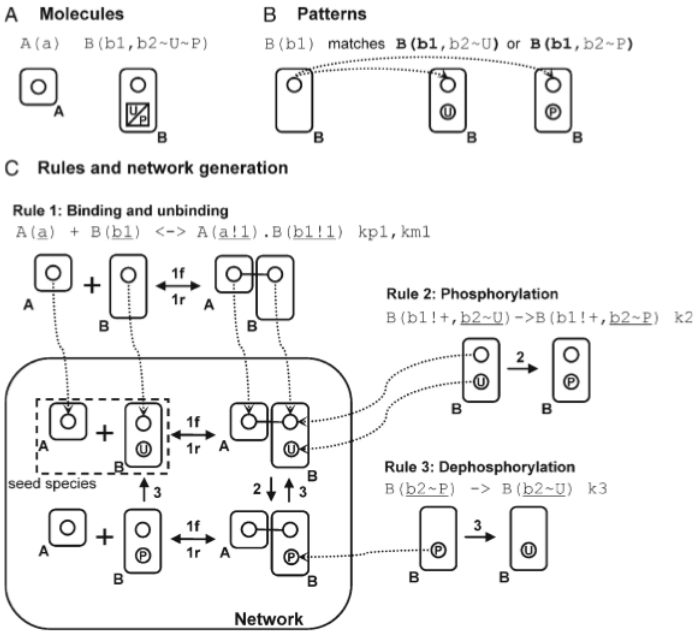

Figure 3.2: BioNetGen language encoding example. Figure taken from [4]

Since this reaction is reversible (<->) its kinetics is described by means of two parameters, kp1 and km1, which respectively determine the speed of the forward and backward reactions. Rule 2 B(b1!+,b2∼U) -> B(b1!+,b2∼P) k2 describes a typical phosphorylation event. Component b2 of molecule B changes its state from ∼U to ∼P according to kinetics parameter k2. The expression b1!+ specifies that the reaction takes place only if site b1 is bound to another molecule. Finally, rule 3 B(b2∼P) -> B(b2∼U) k3 describes a desphosphorylation event. Component b2 of molecules B changes its state from ∼P to ∼U according to rate k3. Since nothing is specifyed about b1, the reaction takes place indipendently from presence of bond in component b1. Starting from the seed species

the rules are applied generating other new species and thus new reactions. The process continue iteratively until no new reactions are found or some other stopping criteria are satisfied creating the complete network model. Fig. 3.2(C) depicts this phase starting from the seed species A(a) and B(b1,b2∼U) up to the creation of a complete network containing all the possible species which may populate the system according to rules 1, 2 and 3. This simple but explicative example depicts some of the typical events occurring in a biological pathway. Phosphorylation and dephosphorylation of a molecular site and binding and unbinding of two proteins are fundamental events taking place in a signaling pathway and governing its dynamics. However, this set of few rules can be extended using more molecules with different components and components properties opening the door to implementation of very complex systems.

A BioNetGen input file is mainly constituted by six sections including all the information about the biological system and they are briefly presented here:

- (parameters) Define the parameters that govern the dynamics of the system such as rate constants, the values for initial concentrations of chemical species, compartment volumes and physical constants used in unit conversions. The synthax of a line in the parameters block is

[index] parameter [=] value

  where square brackets indicate optional elements, parameter is a string consisting of only alphanumeric characters plus the underscore character and containing at least one nonnumeric character. value may be either a number in integer, decimal or exponential notation or a formula involving numbers and other parameters in C-style math synthax;

- (molecule types) Define molecules, including components and allowed component states. As already said, molecules are structured objects composed of components able of binding to each other. Components typically represent physical part of proteins such as domains and motives and may also be associated with a list of state labels, which represent states or properties of the components. Examples of component states modeled using state labels may concern conformation (e. g. open or closed), phosphorylation status and location (e. g. extracellular space, membrane, cytoplasm). The synthax of a line in the molecule types block is

[index] moleculeTypes

  where moleculeTypes has the synthax for a BioNetGen species;

- (seed species) Define the initial state of system such as initial chemical species to which rules are applied. The synthax of a line in the seed species block is

[index] species [initialPopulation]

where species has the synthax for a BioNetGen species described above and initialPopulation is a number or formula that specifies the amount of the species present at the start of the first simulation (default is zero);

- (observables) Define model outputs, which are functions of the population levels of multiple chemical species sharing a set of properties. The synthax of a line in the observables block is

```
[index] [observableType] observableName pattern1[ ,pattern2]
```

where observable Type is either Molecules or Species (default is Molecules), observable Name is a valid name for a BioNetGen observable, and each pattern is a valid BioNetGen pattern;

- (functions) Define the functions describing the kinetic rate constants which cannot be described by a simple constant value but which show a kind of dependencies from concentrations of some chemical species present in the system. The synthax of a line in the functions block is

```
f() = formula
```

where f() is the name of the function and formula is an mathematical expression involving the concentration of one or more chemical species which have to be necessarily listed in the observables block;

- (reaction rules) Define rules describing which chemical species are involved in a transformation and which are the consequences of this transformation. Each rule is similar to a standard chemical reaction notation having four basic elements: reactant patterns, an arrow, product patterns and a rate law specification. The synthax of a line in the reaction rules block is

```
[index] rPattern1 [+rPattern2] ... arrow pPattern1 [+ pPattern2] ...
rateLaw1[,rateLaw2] [command1] ...
```

where each Pattern is a valid BioNetGen pattern, arrow is one of "->" or "<->", each rateLaw is a parameter or a rate law function. Rules may transform a selected set of reactant species by adding or deleting molecules or bonds and by changing component state labels. An example for each case is reported below

```
begin reaction rules
 #Add a bond
 A(a) + B(b) -> A(a!1).B(b!1) k_a
 #Delete a bond
 A(a!1).B(b!1) -> A(a) + B(b) k_d
 #Change a component state label
 A(Y~P) -> A(Y~U) km3
 #Add a molecule
 I() -> I() + A(a,Y~U) ksynth
 #Delete a molecule
 A() -> Trash() kdeg
end reaction rules
```

- actions) Perform two basic types of actions, generate the chemical reaction network implied by the model specification and simulate this network using different methods. An example of actions commonly used are reported below

```
#actions
generate_network({overwrite=>1});
#kinetics
writeSBML({});
simulate_ode({t_end=>120,n_steps=>120});
resetConcentrations();
simulate_ssa({suffix=>ssa,t_end=>120,n_steps=>120});
```

- generate_network command directs BioNetGen to generate a network of species and reactions through iterative application of the rules starting from the set of seed species. This behaviour can be overridden setting the option overwrite=>1. writeSBML indicates that the network is written to an SBML file. simulate_ode command initiates a simulation of the dynamics implementing and numerically solving a set of ODEs. t_end and n_steps specify respectively the end time for the simulation and the number of steps at which the results are written to the output files. reset Concentrations command restores the concentrations to the initial values. simulate_ssa command initiates a stochastic simulation. suffix=>ssa command appends "_ssa" to the basename for output files of the simulation.

All the information about BioNetGen software and syntax are fully described in [4].

3.6.1 BioNetGen simulation tools

It is worthy to clear some aspects concerning the simulation tools offered by BioNetGen software. One possible method (the one presented above) entails the iterative application of rules to the set of defined seed species in order to generate a network before the

simulation starts. Subsequently, the simulation may be carried out either by numerically solving ODEs or by implementing a stochastic simulation algorithm (SSA). SSA implies a kinetic Monte Carlo simulation using the Gillespie algorithm [9] and produces stochastic trajectories representing the concentrations of observables species. Alternatively, the rules may be applied during the simulation as the set of populated species grows using a procedure that has been called "on-the-fly" network generation and simulation. As a first step only the reactions involving seed species are initially generated. Then, BioNetGen detects when a reaction event occurs that populates one or more species to which rules have not been previously applied and automatically expands the network through rule application. This method is useful when a network is potentially unrestricted such as in polimerization processes which allows aggregates formation of any size. For this reason to generate a complete network before prediction starts may be dangerous unless some stopping criteria are specified. An example of this simulation method is reported below

```
#simulation on-the-fly
generate_network({overwrite=>1,max_iter=>1});
simulate_ssa({t_end=>50,n_steps=>20});
```

where max_iter set to 1 indicates that only the reactions involving seed species are initially generated. For all the mentioned methods the simulation cost scales with the network size, hence simulation of large-scale reaction networks may become impractical. In particular, the CPU time required for model simulation increases exponentially as the number of network reactions grows. In order to overcome this computational limit, networkfree methods have been introduced such as NFsim. NFsim [10] guarantees a constant cost of simulation per reaction event and thereby implies a linear increase of the CPU time with the number of reaction events in the system. NFsim generalized the rule-based version of Gillespie's stochastic simulation algorithm (SSA) and guarantees very similar results compared with SSA but with a outstanding saving in time. An example of NFsim is reported below

```
#network-free simulation
simulate_nf({suffix=>nf,complex=>1,t_end=>50,n_steps=>20})
```

.

4 Mathematical model of apoptosis

4.1 Introduction

In this section we implement a model of the apoptosis pathway. As seen in the previous section (3.4.1) there are a lot of models in literature, each of them describing a different behavior of the pathway. We decided to focus only on two models that describe with high accuracy two different and important extrinsic apoptosis pathways: Albeck's and Neumann's model. The first evaluates the molecular reactions generated by stimolation of TRAIL receptors related to mitochondrion, while the second generates a series of reactions by CD95 (FAS) receptors and takes into account both caspase (apoptotic) and Nf-kB (non apoptotic) pathways.

At first, we have realized the models separately and verified the match between results obtained and those showed in literature. Subsequently, we have integrated them creating a single complete model including as many elements as possible of the apoptosis signaling pathway. The rule-based modeling approach has been prefered in order to overcome combinatorial complexity that often limits the implementation of large models. BioNetGen language, as said in the previous section, is a software that allows to follow this new modeling approach and to encode the model by means of a simple set of rules. Models taken from literature were originally implemented using sets of ordinary differential equations (ODEs) and thus they needed to be translated using the rule-based modeling approach. In the following chapters there will be decribed in details Albeck's [2, 5] and Neumann's [3] model of extrinsic and intrisinc apoptosis pathway.

4.2 Albeck's model of intrinsic apoptosis with TRAIL

Albeck's model [2, 5], already introduced in section 3.4.1.5 describes the pathway generated by the exposure of TRAIL ligand. They supposed that apoptotic events occurs like a biological switch. To understand how this extrinsic apoptosis switch functions in quantitative terms, they constructed a mathematical model based on a mass-action representation of known reaction pathways. The model was trained against experimental data obtained by live-cell imaging, flow cytometry, and immunoblotting of cells perturbed by protein depletion and overexpression. The trained model accurately reproduces the behavior of normal and perturbed cells exposed to TRAIL, giving the possibility of study switching mechanisms in detail. In thier studies, Albeck et al. examine the relative dynamics of initiator and effector caspase activation and MOMP using four experimental tools:

1. live-cell reporters specific to initiator and effector caspases;

2. a biologically inert reporter of MOMP;
3. flow cytometry and immunoblot analysis of endogenous substrates;
4. perturbation of specific proteins using RNAi, protein over-expression and small molecule drugs.

To monitor caspase behavior in single living cells, they constructed three fluorescent protein (FP) fusions (Fig. 4.1 A, B). The first, effector caspase reporter protein (EC-RP), monitors caspase-3 activity (and, to a lesser extent, caspase-7 activity) and is composed of a Forster Resonance Energy Transfer (FRET) donor-acceptor pair (CFP and YFP) connected via a flexible linker that contains the caspase cleavage sequence DEVDR (Fig. 4.1 B). When the linker is cleaved, energy transfer is lost and CFP signal increases. This event can be monitored by live-cell microscopy. Initiator caspase reporter protein (IC-RP) carries tandem copies of IETD in its linker, a sequence that is efficiently cleaved by caspase-8, but poorly by caspases-3,7. IETD constitutes the site in procaspase-3 for initiator caspase cleavage, and IC-RP cleavage is therefore a good readout of procaspase-3 activation.

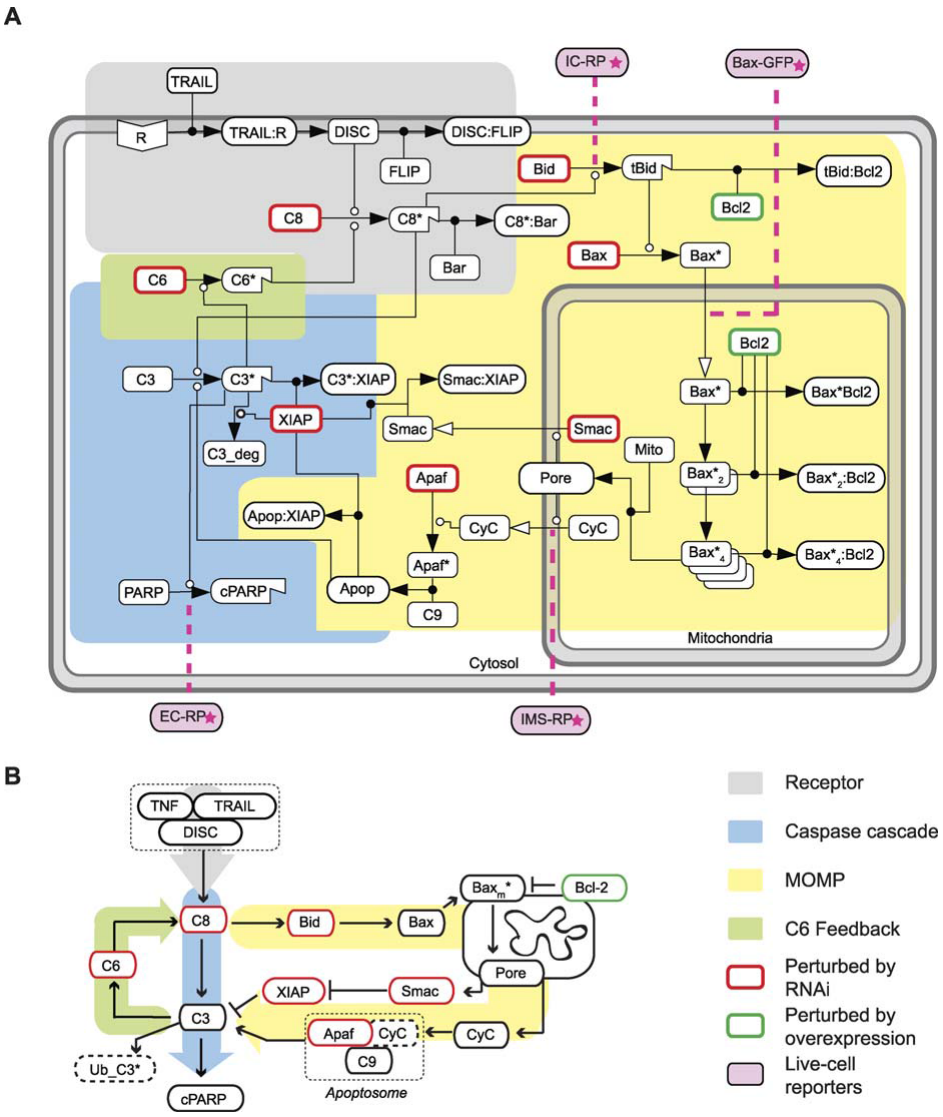

Figure 4.1: Process diagram of the death receptor network modeled by Albeck et al. (A) The major features of the network are highlighted by color: gray, receptor module; blue, direct caspase cascade; green, positive feedback loop; yellow, mitochondrial feed-forward loop. (B) A condensed alternate representation of the network.

Finally, a reporter for MOMP that localizes to the inter-membrane space (IMSRP) was created by fusing RFP to the mitochondrial import sequence of Smac (residues 1- 59). FP fusions to full-length cytochrome c and Smac have been described by other authors, but IMSRP differs from these fusions in lacking an IAP-binding motif, and it is therefore

biochemically inactive. To validate the properties of EC-RP, IC-RP, and IMS-RP in vivo, HeLa cells stably expressing the reporter proteins were treated with TRAIL and cycloheximide (CHX) and fluorescence signals monitored every 3 min over an 8-12 hr period.

When Albeck et al. try to implement the model, three simplifications were made to reduce the number of species and free parameters. The first concerns the details of DISC and apoptosome assembly, both of which involve multiple copies of several protein species, that are replaced by simplified ''lumped parameter'' representations. The second is refered to the omission of all mechanism involved in protein synthesis by performing the experiments in the presence of cycloheximide (which is commonly used to sensitize cells to the action of TNF, but which, in thier works, also simplifies modeling by eliminating source terms). As third semplification, proteins with similar biochemical activities were represented by single species: C8 and caspase-10 (C10) by C8 alone; C3 and C7 by C3 alone; and Bcl-2-like family of proteins by three prototypical examples: Bid, a pro-apoptotic ''activator,'' Bcl-2, an apoptosis inhibitor, and Bax, a pore-forming protein. The last parameters discussed are still a matter of dispute about the precise mechanism by which Bcl-2-like proteins regulate MOMP; so, they decided to implement the simplest form of ''direct activation'' of Bax molecules by t-Bid formation (see par. 2.1.4).

Mathematical model of proteins was constructed using elementary reactions, represented by ODEs. All biochemical transformations were represented as unimolecular or bimolecular reactions. Transport between cellular compartments is also modeled as an elementary unimolecular reaction while the assembly of multiprotein complexes is modeled as a series of bimolecular reactions. Because no complex algebric forms, such as Hill functions, are used in Albeck's model, ultrasensitivity and other nonlinear behaviors arise from interactions among simple elementary reactions rather than the proprieties of higher-order equations.

The final model contains 58 species corresponding to 18 gene products having nonzero initial conditions and 40 additional species representing complexed, cleaved, or differentially localized forms of the initial species, which interact via 28 reactions described by 70 nonzero rate constants (including forward, reverse, and kcat rates for each reaction).

4.2.1 Model description

The dynamics of extrinsic apoptosis made by Albeck can be summarized in a three cooperating but asynchronous processes: direct cleavage of effector caspases by initiators, cytosolic translocation of pro-apoptotic mitochondrial proteins, and feedback from effector to initiator caspases. Activation of initiator and effector caspases is a defining characteristic of apoptosis. Effector caspases cleave essential cellular substrates and directly dismantle cells, while initiator caspases have a more limited range of substrates and act primarily to regulate effector caspases. The precise all-or-none control of caspase activation is critically important for control of cell fate: effector caspases must not turn on prematurely, but once active they must fully cleave their substrates and provoke cell death.

The chain of events that initiates extrinsic cell death begins with ligand-induced assem-

bly of death-inducing signaling complexes (DISCs) on TNF, Fas, or TRAIL receptors. The initiator caspases-8 and -10 are activated by enforced dimerization at DISCs, after which they cleave effector pro-caspases. The activation of procaspase-3 by proteolysis is mediated exclusively by initiator caspases. Subsequent to cleavage by initiators, effector caspases are regulated by trans-acting factors such as Xlinked inhibitor of apoptosis protein (XIAP), which blocks the proteolytic activity of caspase-3 by binding tightly to its active site. XIAP may also encode an E3 ubiquitin ligase that promotes caspase-3 ubiquitination and its subsequent proteasome mediated degradation.

In most cells (those with type-II regulation), XIAP-mediated inhibition of caspase-3 is relieved by a pathway that involves mitochondrial outer membrane permeabilization (MOMP). MOMP is regulated by the Bcl-2 family of proteins, which function either as proapoptotic (e.g. Bid or Bax) or anti-apoptotic (e.g. Bcl-2) factors. Initiator caspases directly cleave Bid, which then activates Bax by altering its conformation. Activated Bax translocates to the mitochondria, forming pores that allow Smac/Diablo and cytochrome c to translocate from their normal locations in the mitochondrial inter-membrane space to the cytosol. Smac binds tightly to XIAP, blocking XIAP's caspase-3-inhibitory activity, while cytochrome c binds Apaf-1 and caspase-9 to form the apoptosome. Finally, in at least some cells, active caspase-3 cleaves procaspase-6, which then generates additional caspase-8 in a feedback loop. In the described model is possible to recognise mainly four interacting cell death subcircuits (fig. 4.1) :

1. a lumped-parameter representation of receptor binding by TNF or TRAIL and the subsequent activation of pro-C8 by receptor-bound death-inducing signaling complexes (DISC) to form C8* (fig. 4.1, gray);

2. an enzyme cascade in which C8* directly cleaves C3 to form active C3*, which can cleave effector caspase substrates (a process represented in our model by cleavage of PARP to form cPARP) but not when bound to XIAP (X-linked IAP fig. 4.1, blue);

3. a mitochondrial feed-forward pathway in which C8* cleaves Bid (into tBid) to activate Bax (to Bax*) and promote formation of pores in the mitochondrial membrane through which CyC and Smac translocate into the cytosol following MOMP; cytosolic CyC then binds Apaf-1 and C9 to form the apoptosome (which also cleaves pro-C3), and Smac neutralizes XIAP, thereby de-inhibiting C3* (fig. 4.1, yellow);

4. a positive feedback loop in which pro-caspase-6 (pro-C6) is cleaved by C3* to form C6*, which then activates additional pro-C8 (fig. 4.1, green).

4.2.2 Model implementation using BioNetGen

In this paragraph is desctibed the model implementation using BioNetGen language, on the base of what already explained on section 3.6. First, we defined initial parameters and kinetics of the reactions from Albeck's work. We wrote them in the 'begin parametes' section.

```
pC8_init 2e4 # pro cas 8
Bar_init 1e3 # Bifunctional apoptosis regulator
....
k1 4e-7*60
k_1 1e-3 *60
kc1 1e-5*60
...
```

After that, we defined different configurations of the initial species in the dedicated section "begin molecule types" in the command line. In the example below, procaspase 3 has a binding site named B and can reach active (a), inactive (i) or ubiquinated (u) states while Bax molecule has 4 binding sites and 3 different states: inactive (i), active(a) and inside the mitochondrial (m). In this command section it is possible to define both chemical and spatial different conformations.

```
C3(B,S~a~i~u)
Bax(B1,B2,B3,B4,S~i~a~m)
```

In the "begin species" section we initialized the species with the same starting values of Albeck's paper. We used the labels wrote in the "begin parametes" section. We have to set an initial concentration only on a single state of the molecule (e.g. we have to define two initial concentrations of caspase 8 because it can be in two different states: active and inactive). In this case we defined only procaspase 8 concentration and the active form value was setted automatically to 0.

```
C8(B,S~i) pC8_init
```

In the "begin observables" section we decided which concentrations examine during the analysis, following its evolution with a graph. We showed different molecules combination by usings flags according to chapter 3.6. In the following example the label "DISC_Flip" is referred to the concentration of DISC molecule linked to Flip molecule in the binding site "Bs".

```
Molecules DISC_Flip flip(Bs!1).DISC(Bs!1)
```

In the last section ("begin reaction rules") we have described the reactions present in the system, representing the dynamic of the interactions between different molecules. Now, we define new different molecules and complexes generated by molecule binding. This is the case, for example, of active C8 generation by binding of DISC with proC8 through an unidirectional reaction, regulated by $kc3$ kinetic (defined before in the "begin parameters" section).

active C8 by C6 loop

C3(B,S~i) indicates the inactive form of caspase 3 (procaspase 3). In the first reaction (7) procaspase 3 binds to active caspase 8 C8(B,S~a) producing the new molecule C3(B!1,S~i).C8(B!1,S~a). Double arrows indicate that reaction is under equilibrium, so it can be reversible. In reaction (8), C3(B!1,S~i).C8(B!1,S~a) gives active caspase 3 and active C8. Considering both (7) and (8) reactions, that have in common

C3(B!1,S~i).C8(B!1,S~a), is interesting observing that the only species that changes its physical state is caspase 3 that turns from inactive to active form. The same mechanism occurs considering the combination of (9) and (10) reactions: procaspase 6 (C6(B,S~i)) binded to active C3, promotes active caspase 6 (C6(B,S~a)) formation. In turn reactions (11) and (12), as final step, form active caspase 8 (C8(B,S~a)) from pro caspase 8 and active caspase 6. Summarizing, active C8 generates a positive feedback loop through a series of reactions ending with formation of other active C8.

```
7 C3(B,S~i) + C8(B,S~a) <-> C3(B!1,S~i).C8(B!1,S~a) k5, k_5
8 C3(B!1,S~i).C8(B!1,S~a) -> C3(B,S~a) + C8(B,S~a) kc5
9 C6(B,S~i) + C3(B,S~a) <-> C6(B!1,S~i).C3(B!1,S~a) k6, k_6
10 C6(B!1,S~i).C3(B!1,S~a) -> C6(B,S~a) + C3(B,S~a) kc6
11 C8(B,S~i) + C6(B,S~a) <-> C8(B!1,S~i).C6(B!1,S~a) k7, k_7
12 C8(B!1,S~i).C6(B!1,S~a) -> C8(B,S~a) + C6(B,S~a) kc7
```

mythocondrial amplification loop

Mitochondrial amplification loop starts with t-Bid molecule. The latter is generated by active C8 that binds to Bid (Bid(B,S~i)) molecule (17) and cleaves it (Bid(B,S~t)) (18). The mechanism behind Bax and mitochondrial activation is still unknown. Albeck et al. supposed direct molecule activation through t-Bid.

```
17 Bid(B,S~i) + C8(B,S~a) <-> Bid(B!1,S~i).C8(B!1,S~a) k10, k_10
18 Bid(B!1,S~i).C8(B!1,S~a) -> Bid(B,S~t) + C8(B,S~a) kc10
```

Truncated Bid (Bid(B,S~t)) binds to Bax inactive form (20) (Bax(B1,B2,B3,B4,S~i)), present in the citosol, and makes it active (21) (Bax(B1,B2,B3,B4,S~a)). In the next step (22) Bax translocates reversibly into the mitochondrion (Bax(B1,B2,B3,B4,S~m)). At first Bax oligemerizes (24) with another molecule of Bax (Bax2) to finally form (26) a complex composed by 4 molecules (Bax4). Bax, Bax2, Bax4 can be inhibited by mitochondrial Bcl2 molecule (23, 25, 27) (Bcl2(B,S~m)), a stronger apoptotic suppressor. When four molecules of Bax bind together they start to open mythocondrial pores (28, 29) that becomes active Mit(B,S~a). Reactions (30 ,31, 34) and (32, 33, 40) represent cytosolic release of apoptotic factors like cytocrome-c (cytC(B,P~c)) and SMAC (SMAC(B,P~c)). They change from an inactive state (cytC(B,P~m), SMAC(B,P~m)), inside the mitochondrion, to an active state (cytC(B,P~a), SMAC(B,P~a)) and translocate into the citosol.

```
20 Bax(B1,B2,B3,B4,S~i) + Bid(B,S~t) <-> Bax(B1!1,B2,B3,B4,S~i).Bid(B!1,S~t)
k12, k_12
21 Bax(B1!1,B2,B3,B4,S~i).Bid(B!1,S~t) -> Bax(B1,B2,B3,B4,S~a) + Bid(B,S~t) kc12
22 Bax(B1,B2,B3,B4,S~a) <-> Bax(B1,B2,B3,B4,S~m) k13, k_13
23 Bax(B1,B2,B3,B4,S~m) + Bcl2(B,S~m) <->
Bcl2(B!1,S~m).Bax(B1!1,B2,B3,B4,S~m) k14, k_14
24 Bax(B1,B2,B3,B4,S~m) + Bax(B1,B2,B3,B4,S~m) <-> Bax2(B) k15, k_15 # Bax2
+ Bcl2 <–> MBax2:Bcl2
25 Bax2(B)+ Bcl2(B,S~m)<-> Bax2(B!1).Bcl2(B!1,S~m) k16, k_16 # Bax2 + Bax2
<–> Bax2:Bax2 == Bax4
26 Bax2(B) + Bax2(B) <-> Bax4(B) k17, k_17 # Bax4 + Bcl2 <–> MBax4:Bcl2
27 Bax4(B) + Bcl2(B,S~m) <-> Bax4(B!1).Bcl2(B!1,S~m) k18, k_18 # Bax4 + Mit0
<–> Bax4:Mito
28 Bax4(B) + Mit(B,S~i) <-> Bax4(B!1).Mit(B!1,S~i) k19, k_19 # Bax4:Mito –>
AMito
29 Bax4(B!1).Mit(B!1,S~i) -> Mit(B,S~a) kc19 # AMit0 + mCtoC <–> AMito:mCytoC
30 Mit(B,S~a) + cytC(B,P~m) <-> Mit(B!1,S~a).cytC(B!1,P~m) k20, k_20 #
AMito:mCytoC –> AMito + ACytoC
31 Mit(B!1,S~a).cytC(B!1,P~m) -> Mit(B,S~a) + cytC(B,P~a) kc20 # AMit0 + mS-
Mac <–> AMito:mSmac
32 Mit(B,S~a) + SMAC(B,P~m) <-> Mit(B!1,S~a).SMAC(B!1,P~m) k21, k_21 #
AMito:mSmac –> AMito + ASMACC
33 Mit(B!1,S~a).SMAC(B!1,P~m) -> Mit(B,S~a) + SMAC(B,P~a) kc21 # ACytoC
<–> cCytoC
34 cytC(B,P~a) <-> cytC(B,P~c) k22, k_22 # Apaf + cCytoC <–> Apaf:cCytoC
40 SMAC(B,P~a) <-> SMAC(B,P~c) k26, k_26
```

Once released, cytocrome-c binds (35, 36) to inactive Apaf complex (Apaf(B,S~i)) activating it (Apaf(B,S~a)). Procaspase 9 (C9(B,S~i)) iteracts with Apaf to form Apoptosome (Apop(B)) (37). Albeck et al. semplificates Apoptosome formation by considering only a single Apaf molecule instead of seven. At last, Apoptosome (38, 39) binds procaspasi 3 (Apop(B!1).C3(B!1,S~i)) and promotes its activation (C3(B,S~a)). The new active caspase 3 enhances, like a positive feedback loop, those just formed by active C8 direct cleavage (8).

```
35 cytC(B,P~c) + Apaf(B,S~i) <-> cytC(B!1,P~c).Apaf(B!1,S~i) k23, k_23 #
Apaf:cCytoC –> Apaf* + cCytoC
36 cytC(B!1,P~c).Apaf(B!1,S~i) -> cytC(B,P~c) + Apaf(B,S~a) kc23
37 Apaf(B,S~a) + C9(B,S~i) <-> Apop(B) k24, k_24 # Apaf*+ Procasp9 <->
Apoptosome
38 Apop(B) + C3(B,S~i) <-> Apop(B!1).C3(B!1,S~i) k25, k_25 # Apop +
pCasp3 <–> Apop:cCasp3 –> Apop + Casp3
39 Apop(B!1).C3(B!1,S~i) -> Apop(B) + C3(B,S~a) kc25
```

Parp degradation and apoptosis

At last active C3 (C3(B,S~a)) binds PARP substrate (15) (C3(B!1,S~a).PARP(B!1,S~a)) and starts to degradate it (16) (PARP(B,S~d)). When active C3 pass a certain threshold, apoptosis occurs in a irreversible manner.

```
15 C3(B,S~a) + PARP(B,S~a) <-> C3(B!1,S~a).PARP(B!1,S~a) k9, k_9
16 C3(B!1,S~a).PARP(B!1,S~a) -> C3(B,S~a) + PARP(B,S~d) kc9
```

4.3 Neumann's model of extrinsic apoptosis with FAS/APO-1

Neumann's model, already introduced in section 3.4.1.6, explores the dilemma in cellular signaling that triggering of CD95 (Fas/APO-1) in some situations results in cell death and in others leads to the activation of NF-kB. They established an integrated kinetic mathematical model for CD95-mediated apoptotic and NF-kB signaling.

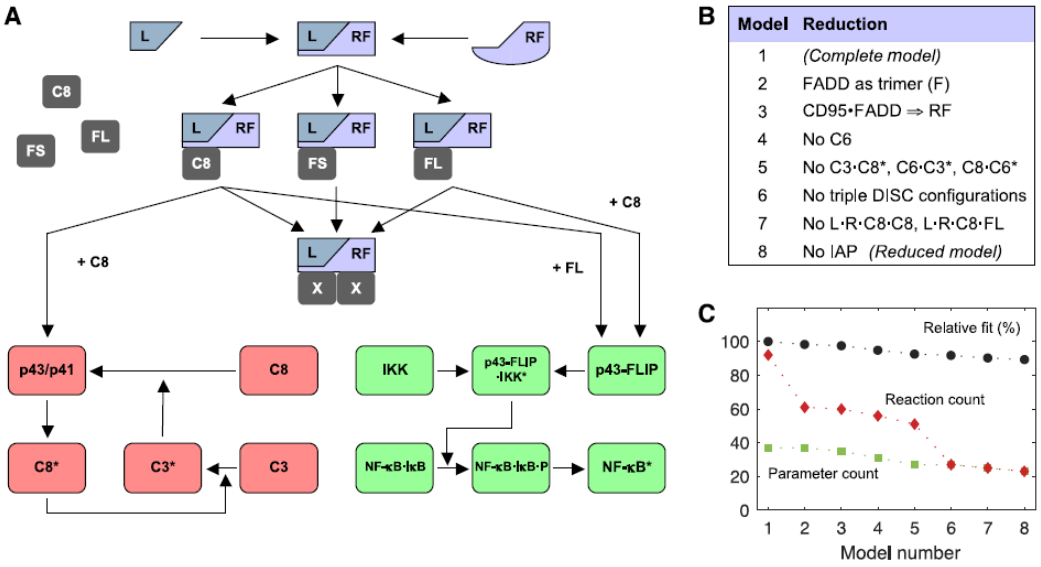

Figure 4.2: Reduced model is sufficient to explain dynamics of life/death signaling. (A) Reduced model of CD95-mediated caspase and NF-kB activation. CD95 receptor and FADD are merged into one entity named RF. (B) The table lists the consecutive reduction steps performed from models 1 to 8. (C) Model comparison using the relative goodness of fit, expressed in % of the values associated with model 1, are labelled with black circles. Red diamonds indicate the number of reactions of each model and squares show the corresponding number of parameters.

They perform a model reduction resulted in a surprisingly simple model well approximating experimentally observed dynamics. The model postulates a new link between c-FLIPL cleavage in the death-inducing signaling complex (DISC) and the NF-kB pathway.They validated experimentally that CD95 stimulation resulted in an interaction of p43-FLIP with the IKK complex followed by its activation. Furthermore, they showed that the apoptotic and NF-kB pathways diverge already at the DISC. Model and ex-

perimental analysis of DISC formation showed that a subtle balance of c-FLIPL and procaspase-8 determines life/death decisions in a nonlinear manner. Cell death can occur in two different ways in type I and type II cells. Type I cells are characterized by high levels of CD95 DISC formation and increased amounts of active caspase-8, leading to the direct activation of downstream effector caspases-3 and -7 and subsequent apoptosis. Type II cells are characterized by lower levels of CD95 DISC formation, and caspase-3 activation requires additional amplification through the release of pro-apoptotic factors from mitochondria triggered by the caspase-8-mediated cleavage of the Bcl-2 family protein Bid. Recently, experiments have demonstrated that CD95L is not only a potent apoptosis inducer but can also activate multiple nonapoptotic pathways, in particular induction of transcription factor NF-kB.

The NF-kB family regulates the expression of genes crucial for innate and adaptive immune responses, cell growth and apoptosis. In most cells, the NF-kB dimer is sequestered in the cytosol by inhibitors of the kB protein (IkB), and its nuclear translocation can be induced by a wide variety of stimuli through activation of the IkB kinase (IKK) complex. The IKK complex consists of two catalytic subunits, IKKa and IKKb, and a regulatory subunit IKKg/NEMO. On activation of the IKK complex, IkB is phosphorylated and degraded in an ubiquitin-dependent manner. The NF-kB dimers can then translocate into the nucleus to induce transcription of target genes. However, the exact molecular mechanism of NF-kB activation through CD95 remains unclear. DED-containing proteins, such as procaspase-8 and c-FLIP have a prominent role in NF-kB activation. c-FLIP N-terminal cleavage products p43-FLIP and p22-FLIP strongly induce NF-kB. p43-FLIP is generated by procaspase-8 at the DISC on CD95 stimulation. It has been shown to interact with components of the TNFR-mediated NF-kB activation pathway, TNFRassociated factor 1 (TRAF1), TRAF2 and receptor-interacting protein (RIP), which together promote NF-kB activation. Interestingly, it has been shown that c-FLIPL/S/R form heterodimers with procaspase-8, resulting in the generation of the cleavage fragment p22-FLIP. This protein mediates NF-kB activation by binding directly to the IKK complex. p22-FLIP differs from p43-FLIP in that it is generated in nonapoptotic cells without DR stimulation. Thus, various molecules of the CD95 signaling machinery, such as procaspase-8 and c-FLIP have a complex role in CD95-mediated apoptosis and NF-kB pathways. These findings motivated their systems biology approach and prompted them to determine whether CD95- mediated signaling should be considered as a dynamic system resulting in life/death decisions. It has been shown repeatedly that decision making is often a process brought about by a reaction system rather than by the influence of a single molecule. Neumann propose an integrated quantitative model supported by experimental data for CD95-mediated apoptosis and NF-kB activation. A direct interaction between p43-FLIP and the IKK complex is postulated by the model and validated experimentally. The model also predicts a divergence of the two pathways at the DISC and that the cellular decision depends on the balance between the levels of c-FLIPL and caspase-8. Experimental modulations of DISC protein amounts are all consistent with the model predictions.

For the model validation Neumann used HeLa, HeLa-CD95, HeLa-CD95–p65–mCherry and HeLa-CD95–c-FLIPL cells. A total of 10^7 cells were either treated with indicated

amounts of anti- CD95 antibody for indicated periods of time at 37°C. They investigated CD95 signaling by western blot analysis of HeLa cells stably overexpressing CD95–GFP (HeLa-CD95) and treated the cells with agonistic anti-CD95 antibodies at three concentrations: 1500, 500 and 250 ng/ml. The simultaneous induction of apoptosis and NF-kB activation and their different dynamics led them to investigate the divergence point of the two pathways.

To reduce the large number of free parameters, they simplified the reactions to be irreversible with the exception of a reversible enzymatic scheme used for caspase activation. The model contains unknown reaction constants and concentrations that they estimated from their data by least-squares optimization.

4.3.1 Model description

The CD95 protein (APO-1/Fas) is a member of the death receptor (DR) family, a subfamily of the tumor necrosis factor receptor (TNF-R) superfamily. Cross linking of CD95 with its natural ligand, CD95L, or with agonistic anti-CD95 antibodies induces apoptosis in sensitive cells. The signal transduction of CD95 starts with the formation of the death-inducing signaling complex (DISC) detectable within seconds after receptor stimulation. The DISC consists of CD95, the adaptor molecule FADD, procaspase-8a/b, procaspase-10 and c-FLIPL/S/R. Procaspase-8 is converted at the DISC, through a series of autoproteolytic cleavage steps, into p43/p41 and p18, which leads to the activation of effector caspase-3. Procaspase-3 was also cleaved to the active subunit p17 showing the induction of the apoptotic pathway. In parallel, they observed the phosphorylation of IkBa followed by its degradation. Stimulation of CD95 caused apoptosis at all antibody concentrations. The quantified blots demonstrate that apoptotic and NF-kB pathways were activated on a similar time scale. They hypothesized that p43-FLIP is the missing link between the DISC and the IKK complex. The kinetics of phosphorylated IkBa indicate a temporal correlation between CD95 stimulation and IKK activity. The simplest scheme to explain this phenomenon would be through p43-FLIP generation at the DISC and subsequent interaction with the IKK complex.

Neumann model assumes a trimerized ligand (L) that binds to a trimerized CD95 receptor (R) that can recruit three copies of FADD (F) leading to the DISC formation. Subsequently, DEDcontaining proteins, such as procaspase-8 (C8), c-FLIPL (FL) and c-FLIPS (FS) can bind to FADD. The order of protein binding gives rise to a combinatorial variety of intermediates.

Assembled DISCs can be categorized into three groups: the first group contains at least two copies of procaspase-8 and is further processed by p43/p41 into active protease subunits, p18 and p10, forming an active caspase-8 heterotetramer (C8*). This apoptotic branch of the model also includes procaspase-3 and procaspase-6 (C3 and C6), their active forms (C3* and C6*), the inhibitor IAP and a feedback loop from caspase-6 to caspase-8. The second group of DISCs features at least one copy of procaspase-8 and one copy of c-FLIPL giving rise to p43-FLIP. The model postulates that p43-FLIP interacts with the IKK complex leading to phosphorylation of IkB (NF-kB IkB P), which entails its degradation and the translocation of p65 to the nucleus (NF-kB*). For simplicity, they

assume that the entire pool of IkB is bound to NF-kB.

In the third group of DISCs, they considered all remaining configurations. They do not participate in further signaling and are merged in a terminal state (L R F F F X X X). The key features of the model are its partitioning into DISC formation, apoptotic and NF-kB signaling, and the confinement of all interactions between the two pathways to the DISC. As expected from the model structure, c-FLIPS inhibited both pathways, although p43-FLIP generation was inhibited at a lower threshold than p43/p41 generation. Low and high levels of c-FLIPL both inhibited p43-FLIP generation, giving rise to a bell-shaped activation profile. In this model, the gene transcription induced by NF-kB was neglected. It shows that the activity of effector caspases is not required for reproducing the dynamics of CD95-mediated NF-kB activation. The model was tested on wild type HeLa cells and they found taht the increased receptor number in HeLa-CD95 cells resulted in the amplification of both CD95-mediated apoptosis and NF-kB signaling. Furthermore, they observed that the amount of CD95 receptors determines the death rate, in contrast to the apoptotic threshold concentration that remained constant (30-100ng/ml of anti-CD95 antibodies). An intresting dynamic behavior is that the peak of phosphorylated IkB-a was reached within 1h and was rather invariant to the stimulus intensity; on the contrary, the dynamics of caspase-8 and caspase-3 activation showed a marked delay with decreasing stimulus strength.

4.3.2 Model implementation using BioNetGen

Following chapter 4.2.2 we started with the "begin parameters" section by defining concentration of species and kinetics of the model. We also define the three anti-CD95 doses that was used to valuate the model. We labelled them L01, L02 and L03: from the greatest to the smallest.

```
L01 1.1322e2
L02 3.7740e1
L03 1.887e1
pC3_init 1.4434
```

We wrote differrent molecule conformations in the "begin molecules types" section. Then, we set the initial concentrations of the species in the "begin molecules species" section according to the labels defined before in the "begin parameters" section. For example: NfkB is naturally present in the cytosol as a complex, binded with IkB kinase, so, we define initial concentration of the complex (NfkB(B!1,S∼i).IkB(B1!1,B2)) with "NF_kB_IkB_init" value.

```
NfkB(B!1,S∼i).IkB(B1!1,B2) NF_kB_IkB_init
IKK(B,S∼i) iIKK_init
```

DISC formation

DISC, represented by (L(Rb!1).Rf(B1!1,B2,B3)) molecule, could bind three different molecules: procaspase 8 (C8(B,S∼i)), cFLIP-L (FL(Bs)) and cFLIP-S (FS(Bs)). In reaction (2), DISC binds C8 forming L(Rb!1).Rf(B1!1,B2!2,B3).C8(B!2,S∼i) complex ,

in reaction (3) binds c-FlipL forming L(Rb!1).Rf(B1!1,B2!2,B3).FL(Bs!2) complex and in reaction (4) binds c-FlipS forming L(Rb!1).Rf(B1!1,B2!2,B3).FS(Bs!2) complex. As DISC has two binding sites and could bind three different molecules, a different combination of nine complexes can be found.

```
# DISC-C8 formation
2 L(Rb!1).Rf(B1!1,B2,B3) + C8(B,S~i) -> L(Rb!1).Rf(B1!1,B2!2,B3).C8(B!2,S~i)
k2
# DISC-FL formation
3 L(Rb!1).Rf(B1!1,B2,B3) + FL(Bs) -> L(Rb!1).Rf(B1!1,B2!2,B3).FL(Bs!2) k3
# DISC-FS formation
4 L(Rb!1).Rf(B1!1,B2,B3) + FS(Bs) -> L(Rb!1).Rf(B1!1,B2!2,B3).FS(Bs!2) k4
```

DISC that binds just one molecule of FS (5, 6, 7, 9, 10) or, two molecules of cFlipL (8) (L(Rb!1).Rf(B1!1,B2!2,B3!3).FL(Bs!2).FL(Bs!3)), don't generate any pathway. For this reason, these ones, are considered inhibitors of DISC formation.

```
# DISC-C8-FS formation - NO signalling
5 L(Rb!1).Rf(B1!1,B2!2,B3).C8(B!2,S~i) + FS(Bs) ->
L(Rb!1).Rf(B1!1,B2!2,B3!3).C8(B!2,S~i).FS(Bs!3) k7
# DISC-FS-FS formation - NO signalling
6 L(Rb!1).Rf(B1!1,B2!2,B3).FS(Bs!2) + FS(Bs) ->
L(Rb!1).Rf(B1!1,B2!2,B3!3).FS(Bs!2).FS(Bs!3) k7
# DISC-FS-C8 formation - NO signalling
7 L(Rb!1).Rf(B1!1,B2!2,B3).FS(Bs!2) + C8(B,S~i) ->
L(Rb!1).Rf(B1!1,B2!2,B3!3).C8(B!2,S~i).FS(Bs!3) k5
# DISC-FL-FL formation - NO signalling
8 L(Rb!1).Rf(B1!1,B2!2,B3).FL(Bs!2) + FL(Bs) ->
L(Rb!1).Rf(B1!1,B2!2,B3!3).FL(Bs!2).FL(Bs!3) k6
# DISC-FS-FL formation - NO signalling
9 L(Rb!1).Rf(B1!1,B2!2,B3).FS(Bs!2) + FL(Bs) ->
L(Rb!1).Rf(B1!1,B2!2,B3!3).FS(Bs!2).FL(Bs!3) k6
# DISC-FL-FS formation - NO signalling
10 L(Rb!1).Rf(B1!1,B2!2,B3).FL(Bs!2) + FS(Bs) ->
L(Rb!1).Rf(B1!1,B2!2,B3!3).FS(Bs!2).FL(Bs!3) k7
```

A combination of DISC, FL and C8 (18, 19) molecules, form p43-flip (p43FLIP(B)) that promotes Nf-kB pathway. DISC that links two molecules of procaspase 8 (11) (L(Rb!1).Rf(B1!1,B2!2,B3).C8(B!2,S~i) + C8(B,S~i)) generates two molecules of p43p41 (p43p41(B) + p43p41(B)) that iniziate caspases apoptotic pathway.

```
# DISC-C8 + C8 generate p43p41
11 L(Rb!1).Rf(B1!1,B2!2,B3).C8(B!2,S~i) + C8(B,S~i) -> p43p41(B) +
p43p41(B) k5
# DISC-FL-C8 generate p43FLiP
18 L(Rb!1).Rf(B1!1,B2!2,B3).FL(Bs!2) + C8(B,S~i) -> p43FLIP(B) k5
# DISC-C8-FL generate p43FLiP
19 L(Rb!1).Rf(B1!1,B2!2,B3).C8(B!2,S~i) + FL(Bs) -> p43FLIP(B) k6
```

Caspase 3 amplification loop

Two molecules of p43p41, combined together (13), form one molecule of active caspase 8 (C8(B,S~a)) that promotes (15) activation of caspase 3 (C3(B,S~a)). At last (17), active caspases 3 iteracts with procaspase 8 and form new p43p41 molecules (p43p41(B)). This mechanism is used (11) to create new active caspase 8 and represents a positive feedback amplification loop. Reactions (14) and (16) represent natural cellular degradation of active caspase 8 and 3 respectively (-> Trash()).

```
# 2 p43p41 forms active caspase 8
13 p43p41(B) + p43p41(B) -> C8(B,S~a) 2*k8
# degradation of active C8
14 C8(B,S~a) -> Trash() k11
15 C3(B,S~i) + C8(B,S~a) -> C3(B,S~a) + C8(B,S~a) k9
16 C3(B,S~a) -> Trash() k12
17 C8(B,S~i) + C3(B,S~a) -> p43p41(B) + C3(B,S~a) k10
```

Nf-kB pathway

Once that p43Flip was activated at DISC, it leads to the activation (20) of the cytoplasmatic IKK molecule (p43FLIP(B!1).IKK(B!1,S~a)). This one iteracts (22) with NfkB, that is linked to IkB (NfkB(B!1,S~i).IkB(B1!1,B2)), and phosforilate it (NfkB(B!1,S~i).IkB(B1!1,B2!2).P(B!2)). At last, the phosforilated complex (23) becomes active NfkB (NfkB(B,S~a)) and translocates into the nucleus. Some degradation reactions ((21) and (24)) was also introduced.

```
20 p43FLIP(B) + IKK(B,S~i) -> p43FLIP(B!1).IKK(B!1,S~a) k13
21 p43FLIP(B!1).IKK(B!1,S~a) ->Trash() k16
# NfkB phosforilation
22 NfkB(B!1,S~i).IkB(B1!1,B2) + p43FLIP(B!1).IKK(B!1,S~a) ->
NfkB(B!1,S~i).IkB(B1!1,B2!2).P(B!2) + p43FLIP(B!1).IKK(B!1,S~a) k14
23 NfkB(B!1,S~i).IkB(B1!1,B2!2).P(B!2) -> NfkB(B,S~a) k15
# degradation of NfkB
24 NfkB(B,S~a) -> Trash() k17
```

4.4 Model integration

When we analized system biology pathways (par. 2.2.1) we found that both Trail and Fas upregulates DISC formation and Nf-kB formation in a different manner [8]. Therefore, we aim to create a new model of type II cells[1] that takes into account both mytochondrial activation and Nf-kB generation from DISC. Nf-kB activation induces transcriptional factors (Flip,Bid,..) which may inhibit DISC formation and mitochondrial release of apoptotic factors. This mechanism could be a way to ensure cell survival. Neumann's model is based on type I cells, that are caracterized by high level of DISC formation; instead, those considered by Albeck, is based on type I cells and need mytochondrial amplification to ensure cell death.

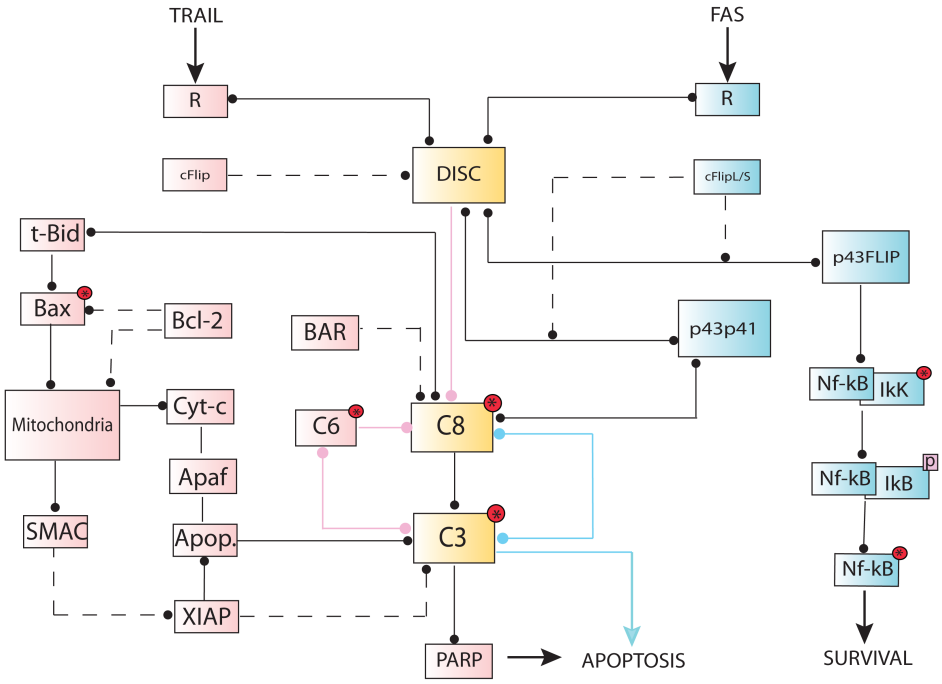

Figure 4.3: It represent a schematic of the overlapping parts of Neumann's and Albeck's model. In the middle (yellow rectangles) there are molecules present in both models. Pink connections mean that the pathway belong to Albeck while blue connections belong to Neumann.

These two models also contain several overlapping parts (fig. 4.3). They both modeled DISC formation and C8 feedback loop but in a different way. Neumann et. al. consider trimerization at the DISC (section 4.3.1) that may binds different combination of three molecules: procaspase 8, c-FLIPL and c-FLIPS; while Albeck et. al. (section 4.2.1)

[1] Type II cells has been defined to be mitochondrial-dependent, they need release of mitochondrial factors to enhance and definitively lead cell to apoptosis.

modeled DISC like a dimer that may binds only two molecules: procaspase8 and FLIP (he also simplified both the two isoforms of Flip in one entity). Neumann et. al. semplified C8 feedback loop (C8->C8*->C3*->C6*->C8*) by deleting the contribute of procaspase 6, while Albeck et. al. considered the entire loop reaction.

The new model will consider activation of Nf-kB and mitochondrial pathway by both Trail and Fas receptors. We started by adding at Albeck's model, two Neumann's reactions: DISC complex formation and Nf-kB pathway. We kept the original mitochondrial and C6 amplification loop. Before integrating the two models, we performed calibration of the systems. We made a time conversion from seconds to minutes in Albeck's model and we coverted concentration from nM to number of molecules/cell in Neumann's model (see 4.4.2.1).

As will be defined in the following, As previous seen, we have performed sensitivity analysis of both the models at DISC in order to find parameters that are important for the dynamic of the systems. Then, we used a nonlinear least-squares method performed in MatLab for model merging and calibration. We used, like objective function, the difference between Albeck's active C8 time concentration and that predicted by our new model. To import the model from BioNetGen to MatLab we used the BioNetGen command:

```
writeMfile();
```

Which generate a 'xxx.m' file, where 'xxx' is the same name of the BioNetGen file. Inside there will be a function structured like this:

```
function [err, timepoints, species_out, observables_out] = apoptosis_albeck(
timepoints, species_init, parameters)
```

We can now simulate our model by controlling a lot of parameters. We can modify the time samples by altering the column vector named *timepoints*, we can change species initial values in the raw vector called $species - init$ and change parameter values by adjusting the raw vector called *parameters*. The latter input vector (*parameters*) was very advantageous because permits to perform sensitivity analysis that need parameter perturbation (see below). As outputs, the function returns four different vectors: *err* that is 0 if the integrator exits without errors, *timepoints* that return a row vector of timepoints defined inside of the function and generated before in BioNetGen (see 3.6.1), $species - out$: an array with population trajectories of the species and $observable - out$ that contains only observable trajectories defined in the "begin observable" section of BioNetGen. $Observable - out$ trajectories are a subset of $species - out$ trajectories. To summarize, by calling this function you can simulate any concentration of the species and change any initial value parameters in order to make some useful analysis like sensitivity analysis or parameter calibrations.

4.4.1 Robust parametric sensitivity analysis

Parametric sensitivity analysis (PSA) has become one of the most useful tools in computational systems biology, in which the sensitivity coefficients are used to study

the parametric dependence of biological models. As many of these models describe dynamical behaviour of biological systems, PSA has subsequently been used to elucidate important cellular processes that regulate this dynamics. This algorithm permits to understand what are the key molecules and the core reactions of the system. These informations may be used to make model adjustement or modification. A little variation of sensitive parameters may cause a big perturbation of the dynamic of the entire system. In the case of programmed cell death, ligand concentration needs to exceed a certain threshold to induce a complete apoptosis. Sensitivity analysis provides a useful tool to investigate how this threshold and thus cellular susceptibility to apoptosis could be modulated pharmacologically. Moreover, sensitivity analysis has been applied to identify reactions determining whether a cell dies by type I or type II cell death, and to reduce model complexity. We use it mainly to find modificable parameters in order to perform model integration. A standard PSA consider the contrubute of a little (local) variation of a parameter dp_j compared to the difference between the old and the new outputs obtained by parameter variation: dx_i. To normalize this comparison we divide them by their original values. Therefore, the relative sensitivity of a variable x_i at time t (in min) with respect to a parameter p_j is given by:

$$s_{ij}(t) = \frac{p_j}{x_i} \cdot \frac{dx_i}{dp_j} \tag{4.1}$$

The digital version of 4.1 is:

$$s_{ij}(t) = \frac{p_j}{x_i} \cdot \frac{\triangle x_i}{\triangle p_j} = \frac{p_j}{x_i} \cdot \frac{x_i - xold_i}{p_j - pold_j} \tag{4.2}$$

To implement 4.2 equation, we have first to decide the increment $\triangle p_j$ for each parameter (e. g. 10% of the original value). Then we use it to calculate the new output i at time$t$: x_i. If we select a positive increment, we will ignore the possible contribute that negative increment may have in our system dynamics. Therefore, we considered not only a small positive increase of a single parameter, but a uniform distribution of negative and positive variation of the same parameter at a fixed percentage: $p_j(k)$. For example, we can select a series of N=50 variations distribuited between -10% and +10% of a single parameter p_j. Once selected, the percentage increment and the length of the serie (N), we evaluate each new parameter with 4.2 formula. Hence, we obtain N of the s_{ij} coefficent for each parameter. To find the total sensitive coefficent, we perform the mean:

$$\bar{s_{ij}}(t) = \frac{1}{N} \cdot \sum_{N} |s_{ij}(t, p_j(k))| \tag{4.3}$$

We summed absolute values to rule out that positive and negative sensitivities cancel each other. Finally we calculate the time-averaged sensitivities according to:

$$S_{ij} = \int \bar{s_{ij}}(t) \cdot dt \tag{4.4}$$

Equation 4.4 was evaluated in MatLab with digital trapezoid method. This different way to perform sensitivity analisis using 4.3 ,that considered local surrounding of each parameter, make standard parametric sensitivity analisis more roboust. All of the sensitivity coefficents S_{ij} can be plotted in a 3D-bar diagram having $p_j$parameters instead of axis x , each x_i observables instead of axis y and S_{ij} values instead of axis z. In this thesis another bar diagram (2D) was made by meaning all the sensitivity coefficents S_{ij} across the different observables:

$$S_j = \frac{1}{M} \cdot \sum_i S_{ij} \tag{4.5}$$

In this way we obtain an overall single sensitivity index for each parameter calculated only in a range of observables. The sensitive algorithm code performed in MatLab is present in Appendix section.

4.4.1.1 Neumann DISC sensitivity analysis

In Neumann's work [3] they have just performed a sensitivity analysis to further confirm the importance of DISC protein levels in the dynamics of apoptosis. They found that the initial concentrations of DISC proteins especially of c-FLIP isoforms were the most sensitive parameters, summing up to 63% of the total sensitivities.

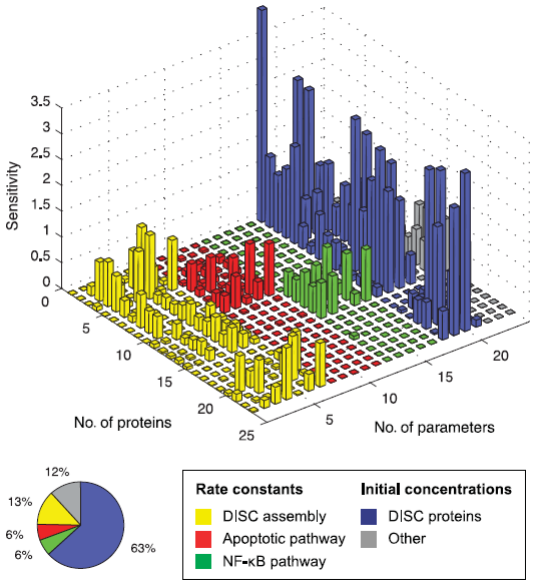

Figure 4.4: Sensitivity analysis. Absolute values of relative sensitivities were averaged over a time interval of 360 min. The pie chart shows the contribution of different parameter categories to the total sensitivity. No of parameters indicate different parameters in the model while no.proteins indicate the different observables of the system.

The remaining 20 parameters contributed only to 37% of total sensitivities. This result explains how relatively small changes in the abundance of DISC proteins might lead to drastic changes in downstream signaling as already observed for the amount of CD95. The decrease in procaspase-8 level resulted in a significantly lower amount of p43-FLIP after CD95 stimulation. Subsequently, it led to the abolishment of CD95-mediated phosphorylation of IkB. Furthermore, the amount of active caspase-8, p18, was decreased, hence leading to reduced apoptosis. Therefore, by perturbing the ratio of procaspase-8 to c-FLIPL at the DISC, they have influenced the induction of apoptosis and NF-kB activation.

4.4.1.2 Albeck DISC sensitivity analysis

Albeck et. al. did not perform a sensitivity analysis of his model. Therefore, we did it by using methods explained in previous chapter. We obtained a 2D bar diagram using, like observables, the concentrations involved in DISC formation: TRAIL-receptor, DISC reclutation, Bar, Flip, procaspase 8 and its active form. We used only observables that represent a key mechanism in apoptosis propagation and cell death. Apoptosis is a cascade of reactions that leads to substrate degradation so, some chemical reactions are a consequence of more important upstream reactions. For this reason, it is not good to select them in sensitivity analysis. E.g: Bax activation, Smac release and all mitochondrial reactions are all regulated by a more important upstream reaction: Bid molecule truncated by active C8. By considering only tBid concentration we take into account almost all the reactions involved in mitochondrial propagation.If you perform a parametric sensitivity analysis considering, like observables, all the concentration of the species, you will obtain sensitivity coefficents that are insubstantialy. There will be coefficents, like Bid or procaspase 8 initial concentration, that will outnumber all the other parameters for the fact that they regulate a large series of reactions. For these reasons, we selected active C8 activity concentration to perform sensitivity analysis because it regulates multiple processes: from mythocondrial activation loop to C6 activation loop, from C3 activation to cell death. As seen in the figure 4.5, we found intresting results. TRAIL concentration ($L50$ in figure) and kinetic, that activate DISC complex ($kc1$), are sensitive factors. They regulate both DISC concentration and C8 activity in a direct manner. Affinity of pro caspase 8 to the DISC ($k3$) and initial concentration of the species present in the DISC, are other core parameters.In particular, c-Flip and procaspase 8 initial values play an important role in apoptosis signal propagation. At least, activation of C8 by C6 through C3 loop ($k7$) is a significative parameter because generates a lot of active C8 in a short period of time. To sum up, the essential parameters that lead to initiator caspases activation are those involved in DISC formation, inibition and amplification.

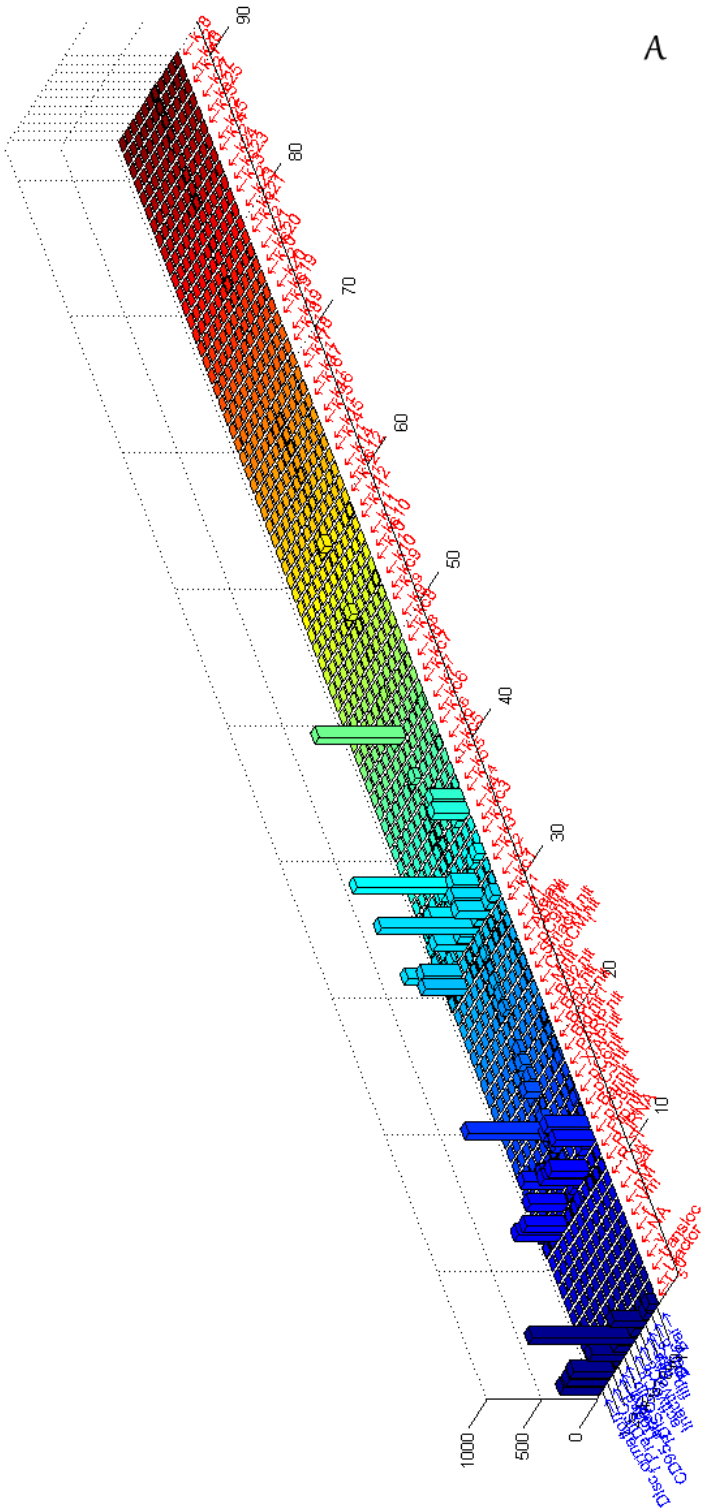
A
90
80
70
60
50
40
30
20
10
0
500
1000

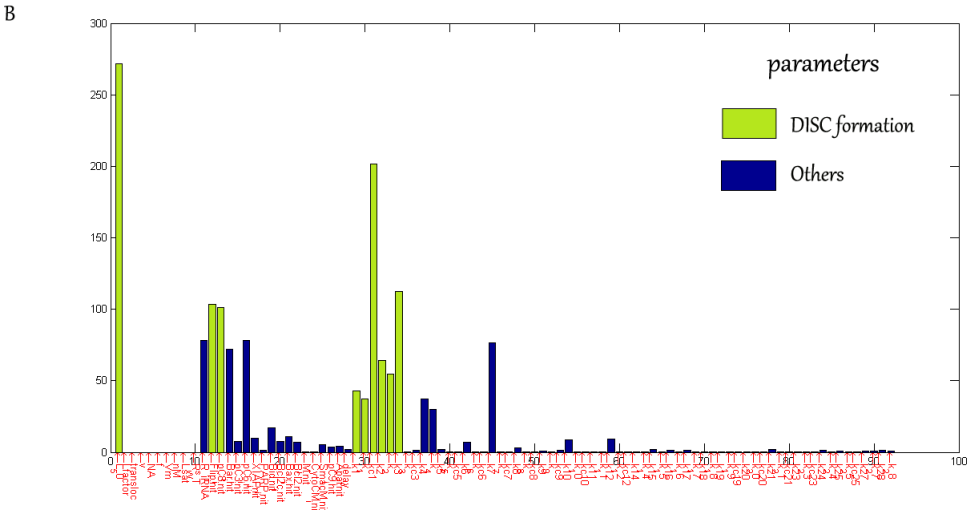

Figure 4.5: Figure A represents sensitivity analysis made in Albeck's model using like observabels: DISC reclutation, trail receptors, pro C8, its active form, Bar and Flip (axis y). In axes x there are the parameters of the model. Figure B represents a 2D bar diagram showing the sensitivity coefficent of active C8 like. In green color there are the parameters involved in DISC formation.

4.4.2 Merging using nonlinear least-squares method

The least squares method is a standard approach to the approximate solution of overdetermined systems, i.e., sets of equations in which there are more equations than unknowns. "Least squares" means that the overall solution minimizes the sum of the squares of the errors made in the results of every single equation. The most important application is in data fitting. The best fit in the least-squares sense minimizes the sum of squared residuals, a residual being the difference between an observed value and the fitted value provided by a model. Least squares problems fall into two categories: linear or ordinary least squares and non-linear least squares (NLLSQ), depending on whether or not the residuals are linear. The linear least-squares problem occurs in statistical regression analysis; it has a closed-form solution. A closed-form solution (or closed-form expression) is any formula that can be evaluated in a finite number of standard operations. The non-linear problem has no closed-form solution and is usually solved by iterative refinement; at each iteration the system is approximated by a linear one, and thus the core calculation is similar in both cases. A non linear least squares problem is an unconstrained minimization problem of the form:

$$minimize_x\, f(x) = \frac{1}{2}\sum_{i=1}^{m} f_i(x)^2 \equiv \frac{1}{2}F(x)^T F(x) \tag{4.6}$$

where F is the vector-valued function:

$$F(x) = (f_1(x)\, f_2(x)\, \ldots\, f_m(x))^T$$

F is composed by a series of function ($f_m(x)$) we want to minimize. Usually we want to fit a model to a concentration of samples of a particular molecule (e.g: insulin or oxigen evoltution). Hence, $f_1(x)$ represents the difference between the discrete-experiment concentration and that obtained with our parameter variation of the model. For a good data fitting is important to find a reasonable starting point. To perform parameters estimation in MatLab we used the lsqnonlin function:

```
options = optimset('TolFun',1e-3);
[x ,resnorm, residual, exitflag, output, lambda, jacobian] = lsqnonlin(ObjFun, x0,
lb, ub, options);
```

Where$ObjFun$ is the nonlinear vector function whose sum of squares you want to minimize; $x0$ is the initial point (vector) for the algorithm, lb and ub are the lower and upper bounds of the variables, specified as a vector, and *options* provides the function-specific details for the options values. If not specified, Gauss-Newton method was used to perform the algorithm. We specified $ObjFun$ as a function handle of the form @objfun, where objfun.m is an M-file that returns a vector function value. With 'TolFun' setted to $1e-3$ the algorith run until the difference between the current residual and those calculated in the previous step is minor of $1e-3$. x represent the vector of the new parameters, $x0$ the initial parameters, $x0lb$ the lower bounds and $x0ub$ the upper bounds.

Objective function

Choosing the correct function to minimize and the right initial parameters is essential for a positive ending of the algorithm. Therefore, we used, like objective function, the difference between Albeck's active C8 ($aC8_{old}(x,t)$) and that obtained from the new model ($aC8_{new}(x,t)$). Referring to the the eq.4.6 we obtain:

$$F(x) = objFunc = (f(x))^T = (aC8_{new}(x,t) - aC8_{old}(x,t))^T$$

We use active C8 because it has a central role in determine both Nf-kB and active C3 apoptotic pathways.

The active C8 concentrations were obtained without considering the contribution of caspase 6 positive feedback loop. For these reason, we simulated the model by not considering the initial value of procaspase 6 (pC6init=0). In his work, Neumann et. al. [3] asserted that NfkB was activated at the same time of active C8 and it was indipendent from caspase activity. This, further confirm that C8 was the right objective function to consider.

4.4.2.1 Parameters calibration

Before you perform NLLSQ method for data fitting , by calibrating a set of parameters, is important to ask some questions about the model such as: what bounds can we place on the values of the initial parameters? Does the model adeguately fit the data? How sensitive are the parameters to changes in the data? To answer these questions we previously performed sensitivity analisys of both models (fig. 4.4, 4.5). A sensitive value is a parameter that, with a little variation of itself, cause a big mutation of the dynamics of the system. Both Neumann's and Albeck's models sensitive parameters are, above all, the initial concentrations and kinetics of the reactions and species involved in DISC formation and amplification (par. 4.4.1.1, 4.4.1.2). DISC formation and its initial concentrations play a crucial role in controlling the downstream reactions. In particular, dynamic of caspase 8 formation regulates both cell death (through mithochondrial activation and C6 feedback loop) and survival (through Nf-kB activation). Understanding dynamics of these system is very important in order to create a new integrated model. Therefore, to obtain the best fittings, it is important to reasonably calibrate the entire system.

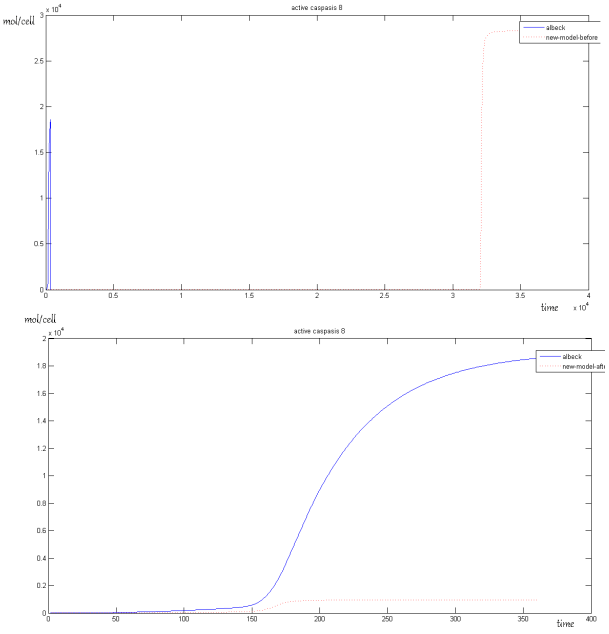

Figure 4.6: Figure on top showing the difference between original Albeck's caspase 8 concentration and those of the new model stymulated by TRAIL before parameter calibration. There is a marcable delay of caspase 8 activation of the new model. The second figure showing the concentrations after calibration. This has a difference in the number of molecules per cell activated.

We used, as most of the initial parameters, those of Albeck's model. We introduced two new molecules involved in DISC formation: FlipS and FlipL. Since procaspase 8 and 3 initial concentrations were present in both models, we set as initial value in the $x0$ vector the arithmetic mean of the two. E.g: Neumann's starting concentration of C3 molecules was 38000 while Albeck's was 20000. Therefore, we set procaspases 3 initial concentration with the mean: 29000. We decided to keep constant those parameters involved in mitochondrial pathway and Nf-kB formation and to give down and upper bounds at those implicated in DISC formation and C6 amplification loop. The bound values were set 100 times greater and smaller than the originals. After definition of starting initial parameters ($x0$), lower bounds ($x0lb$) and upper bounds ($x0ub$) we performed the NLLSQ method to obtain the new vector of parameters (x). It was difficult to fit concentration of active C8 like the original model because we introduced different dynamics in DISC formation. Therefore, we didn't obtain a perfect fit but we only reasonably reduced the distance between the two (fig. 4.6). The NLLSQ algorithm made the new model, as soon as possible, equal to the original.

In the bar diagram below (fig. 4.7) it is represented the ratio between the new estimated parameters and their starting values in a logarithmic scale. E.g: $k1$ represents affinity of Trail ligand in its receptor and it has a value of 9. So, the new obtained parameter is $e^9 = 8103.1$ times greater than its initial value.

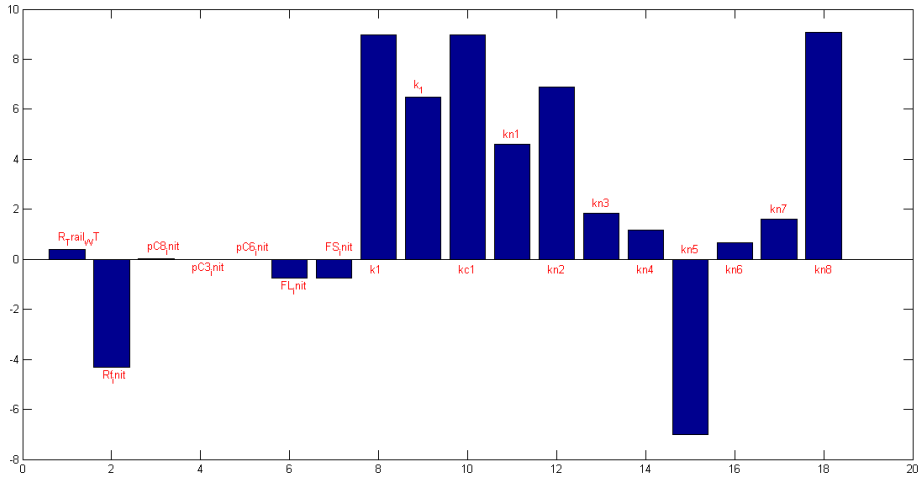

Figure 4.7: Bar diagram showing the ratio between the new parameters (obtained during the application of NLLSQ method) and the initial parameters in a logaritmic scale. E.g. the new kn3 parameter (flip that binds DISC) is $e^2 = 7,3$ times greater than its starting value.

For reasonably promote caspase 8 formation and activation, $kc1$ (invovled in DISC formation), $kn2$ (representing affinity of procaspasis 8 to DISC complex) and $kn8$ (that promoted active caspasis 8 formation by two molecules of p43p41) were enhanced. For the same reason, c-Flips molecules inhibit with a different mechanism. c-FlipL affinity to the DISC $kn6$ was enhanced while c-FlipS affinity $kn5$ was severely reduced. Thus, cFlipL molecule becomes more important in active C8 formation than cFlipS as confirmed in the next chapter by sensitivity analysis (par. 5.2.6). The initial DISC molecules concentration in Fas receptor (Rf_init) has a negative value, so it is $e^{-4} = 0.0183$ times smaller than its original value. In order to reproduce the lower concentration of DISC molecules, typical of type II cells, a new "Rf_init" value was setted. Procaspasi 8 and Trail receptors initial concentrations were increased while procaspasi 3, FlipS, FlipL and Fas receptors initial concentrations were decreased. These values remain consistent because they are between the initial values of both the models. To sum up, the NLLSQ algorithm calibrated the model by fastening all reactions involved in procaspase 8 activation and guarantee the number of molecules per cell predicted by Albeck's model.

Corrective factors

First of all, homogeneity in time units describing kinetics parameters must be guarantee. Neumann's models express the parameters in $[min^{-1}]$ whereas Albeck's model uses $[sec^{-1}]$. Hence, all the parameter expressed in $[sec^{-1}]$ should be multiplied for 60 to transform them in $[min^{-1}]$. It is worthy to discuss an essential aspect linked to BioNetGen implementation concerning the fact that concentrations should be expressed in units of copies per cell and thus bimolecular rate constants in per molecule per cell. This simply means that every time a quantity is expressed in M or in M^{-1} (unless time units) this has to be multiplied or divided by the product $(NA * V)$, where NA is the Avogadro's number and V indicates cellular volume. Since many biological systems involve ligands present in extracellular space, receptors spread out on the cell surface and molecules situated in the cytoplasm, the value of V changes depending on molecule location. For this reason it is important to identify where molecules are located, such as Trail that binds to his receptor on the plasma membrane and subsequently summon DISC mechanism in intracellular space. Therefore, the computed values of volume, expressed in (L), for the three most important cellular locations are:

- $V_o = 1.0 \cdot 10^{-10}$ for extracellular volume,
- $V_m = 3.0 \cdot 10^{-13}$ for plasmatic membrane volume, and
- $V = 3.0 \cdot 10^{-12}$ for cytoplasmic volume.

Albeck's model expresses its concentration both in #copies per cells and in M (Moles), so it's easy to pass from a unit to another. He had just trasformed all the units by multipling kinetics and concentrations by a corrective factor F that we can obtain form data. For example, k_1 is expressed in the two different units:

$$k_1 = 4 \cdot 10^{-7}\, in\, [(\frac{\#}{CC})^{-1} \cdot sec^{-1}]\, and\, k1 = 2.4 \cdot 10^{4}\, in\, [(nM)^{-1} sec^{-1}]$$

Therefore, passing from nM to $(\frac{\#}{CC})$ can be made by multipling the concentration expressed in $(\frac{\#}{CC})$ with the factor:

$$F = \frac{4 \cdot 10^{-7}}{2,4 \cdot 10^{4}} = 1,667 \cdot 10^{-3}$$

For the same reason we can pass from nM^{-1} to $(\frac{\#}{CC})^{-1}$by multiply the concentration expressed in $(\frac{\#}{CC})^{-1}$by $\frac{1}{F} = 5,9999 \cdot 10^{3}$. Once F is obtained we can transform all Neumann's kinetics and initial concentrations form nM to $(\frac{\#}{CC})$ in order to make congruent with Albeck's.

4.4.2.2 Conclusion

We finally obtained the new model. The complete scheme with all the graphic connection is represented in the next chapter, fig. 5.2 and the BioNetGen code of the model implementation is in the Appendix. The model has 101 parameters of which 23 are initial concentrations and 78 are reaction kinetics. It count 75 different molecule species controlled and generated with 61 reactions.

5 Model Analysis and validation

In this chapter, apoptosis model has been used to simulate the temporal series of the most significant chemical species in order to analyse the dynamic behavior of the system. We try to probe if apoptosis robustly occurs in all-or none manner and what is the "point-of-no-return" representing irreversibility in apoptosis. Concentrations time series permit to carry out a detailed analysis of dynamic behavior of the system. This could be used to develop a deeper understanding of network regulation processes and to characterize the main role played by each chemical species. Moreover, we can consider the dynamic behavior of each chemical species as a kind of fingerprint of the system working under physiological conditions. Network structure and type of interactions between different species determine characteristic response of the system upon stimulation. If some of these characteristic features are lost for different reasons, typical dynamics may change and then result in inappropriate actions of the system. System disregulations cause defects in signal transduction that can bring to apoptosis. Hence, characterize physiological working conditions of a signaling pathway may be a useful method to distinguish it from those in pathologic conditions, to investigate the origin of disregulations and, in future perspective, to find a drug or combination of drugs able to prevent or to induce apoptosis. In order to do this, a detailed and rational analysis of collected data from apoptosis model simulations have to be done. Since the main purpose is to characterize system response, we decide to classify the obtained time series according to their dynamic behavior. In other words, we distinguish them depending on their qualitative behavior, or pattern and for each of them we calculate Hill coefficent (par. 5.1.1.1). This help us to examine bistability[1] due to positive feedbacks, and sigmoidal responses arising from competitive inhibition. Such sigmoidal curves are frequently termed ultrasensitive (par. 3.3), as small alterations in the stimulus can elicit large changes in the response. It is known that bistability can emerge from ultrasensitivity in conjunction with positive feedback, whereas adaptation, oscillations, and, surprisingly, highly linear response can arise with negative feedback.

At last we perform a local sensitivity analysis of the system in order to find key parameters and core mechanisms in the pathway. Comparing these findings to those of the previous models helps us to validate the new integrated model. In next sections, we present details about classification of main patterns (section 5.1.1), results and analysis of apoptosis model simulations (section 5.1.2), and comparison with experimental data of previous models (section 5.2).

[1] A bistable system is a system that exhibits two stable steady states, separated by an unstable state. (par. 3.3.2)

5.1 Apoptosis model simulations: results and analysis

Simulations of apoptosis were realized using a step function of 5.1 nM = 50ng/ml of Trail as input. Trail stimulation started at 0 time and was held for 360 minutes. Using BioNetGen language:

```
#actions
generate_network({overwrite=>1});
# Kinetics
simulate_ode({t_end=>360,n_steps=>720});
```

where, as presented in Chapter 3, "generate_network" command permits to generate the complete reactions network according to an iterative method which terminates when no more new reactions are found. "simulate_ode command" indicates that simulation of dynamics is carried out implementing and numerically solving a set of ODEs. Simulation lasts for 360 minutes (t_end=>360) and shows in output 720 time samples for each observable species (n_steps=>720). Time series of all the observables species are reported in Appendix.

5.1.1 Pattern classification

Considering the remarkable importance of negative and positive feedback loops in transduction networks it could be helpful to distinguish the simulated concentrations according to those particular features. Hence, we can divide them in two sets, one for those concentrations characterized by overshoot, and one for those without overshoot. To classify dynamic behaviours according to their speed may also give useful information about how signaling system works and help in its characterization. Thus, we decide to classify predicted time series obtained from apoptosis model according to these two criteria, obtaining four main pattern sets, shown in Fig.5.1:

- slow (not-overshooting) response,
- rapid (not-overshooting) response,
- slow overshooting response, and
- rapid overshooting response.

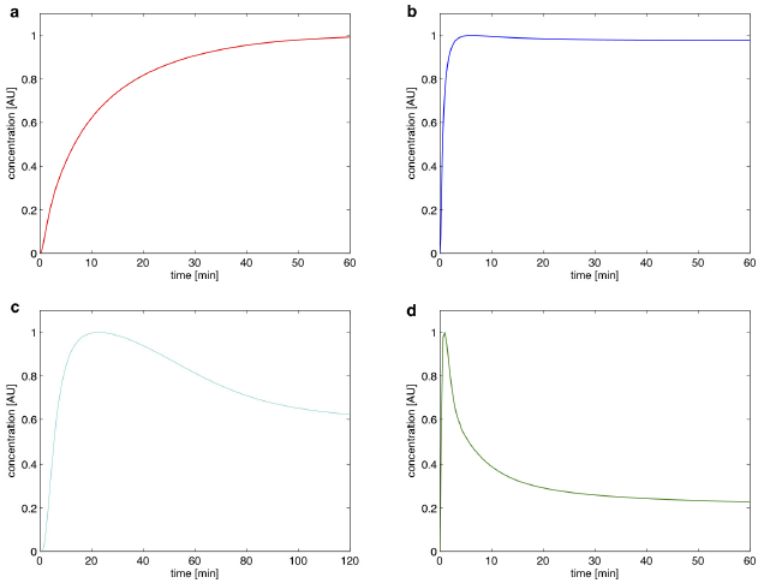

Figure 5.1: Representative dynamic behaviour for each pattern: slow (notovershooting) response (a), rapid (not-overshooting) response (b), slow overshooting response (c) and rapid overshooting repsonse (d).

Each pattern may be characterized by means of specific parameters.

5.1.1.1 Classification parameters

For pattern classification we define mainly four parameters that may help to further describe concentration dynamics:

1) $C_{0.9}$ [min] which indicates the time to reach the 90% of maximum level;

2) $C_{0.1}$ [min].

These two parameters may be particularly useful for characterization of increasing (notovershooting) responses. For concentrations characterized by overshooting response, we can easily obtain information about:

3)τ peak [min], which indicates the period of time the concentration takes to reach its peak value.

This parameter permits to distinguish concentration dynamics according to their speed. To better characterize not-overshooting response, in particular those showing sigmoidal curves, Hill coefficent was calculated:

4) Hill coefficent.

Hill coefficent

Hill coefficent could help to classify pattern definition. It quantifies the ultrasensitivity of a stimulus-response curve globally (see chapter 3.3). At the beginning it was the first

characterization of ultrasensitivity, introduced by Hill, as an empirical description of the cooperative binding[2] of oxygen to hemoglobin. Hill found that binding was well described by the following relationship, which is now known as the Hill equation:

$$y = \frac{x^h}{K_{0.5}^h + x^h}$$

where y is the bound fraction of oxygen, x is the oxygen pressure,$K_{0.5}$ is the oxygen pressure where half of the binding sites are occupied, and h is the Hill coefficient. Enzymes exhibiting positive cooperativity, such as hemoglobin, display ultrasensitivity; that is, their Hill coefficients exceed unity. For example, the Hill coefficient of hemoglobin equals 2.8, and in general, a Hill coefficient of 4 is often thought to be an upper limit for cooperative enzymes. The Hill coefficient is not commonly estimated by fitting the formula to the data, but it is often calculated from the cooperativity index, which is defined as $R_a = \frac{C_{0.9}}{C_{0.1}}$ where $C_{0.9}$ and $C_{0.1}$ are those defined in the previous section. To get the relationship between Ra and the Hill coefficient, h, the following equation need to be solved:

$$R_a = 81^{\frac{1}{h}} \rightarrow h = \frac{log81}{log(\frac{C_{0.9}}{C_{0.1}})} \tag{5.1}$$

If the Hill coefficient is 1, an 81-fold increase of the stimulus is needed to increase activation from 10% to 90%. For Hill coefficients higher than 1, the increase of the stimulus needed is smaller and the Hill curve gets sigmoidal. In some literature models of Apoptosome formation, Bax oligomerization and other species formation were described with cooperative interactions between molecules. As previous said, this can generate sigmoidal curves as molecules with ultrasensitivity behavior. Therefore, calculatin Hill coefficent can help to understand if a specific molecule has ultrasensitivity behavior and if a particular system is activated in a all-or none manner.

5.1.1.2 Classification rules

We decide to distinguish concentration dynamics according to their speed using the parameters introduced in section 5.1.1. τ peak was used to distinguish between overshooting and non-overshooting response. Among the species characterized by increasing (not-overshooting) response and (overshooting) response, we classify:

- as rapid those having $|C_{0.9} - C_{0.1}| < 1600$ sec=30 min, and
- as slow, all the others.

At last, we further classify the dynamics by calculating Hill coefficent (5.1) of each pattern. This can help to distinguish those concentration that may exhibit cooperativity, or ultrasensitivity. Since some reactions belong to a cascade of reactions and are enhanced

[2]Cooperative binding occurs if the number of binding sites of a macromolecule, that are occupied by a specific type of ligand, is a non-linear function of this ligand's concentration. This can be due, for instance, to an affinity for the ligand that depends on the amount of ligand bound. Usually a sigmidal curve occurs. (par. 3.3)

by feedback loops, the Hill coefficent may arise. Therefore, we decided to label the concentrations with an Hill coefficent more than 10 with an asterisk (*). All the detected concentrations classified according to their pattern are reported in Tab. 5.1.

5.1.2 Classification analysis and discussion

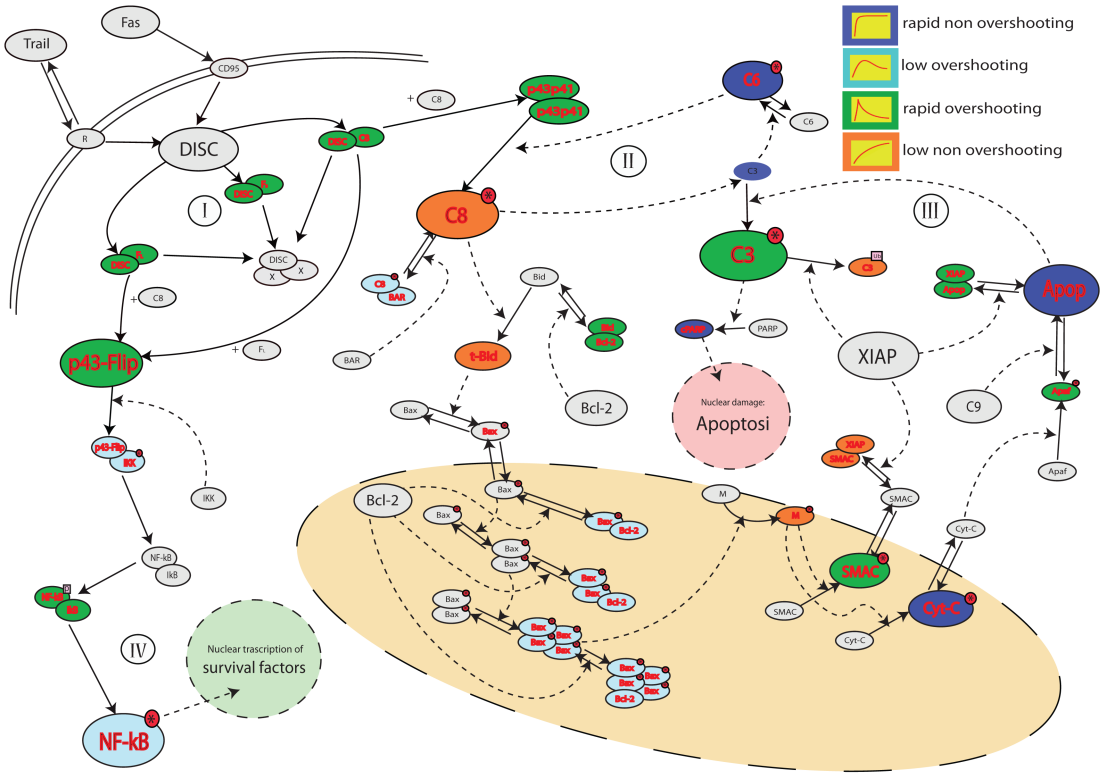

Figure 5.2: Complete apoptosis model. We integrated (red arrows and circles) Neumann's DISC dynamics in Albeck's model in order to introduce Nf-kB pathway. A pattern classification study was made to find network motif and to study molecule dynamics. The different dynamics response are represented by a yellow square sorrounded by a colored frame: blue for rapid non-overshooting, red for low non-overshooting , green for rapid overshooting and azure for low overshooting. We calculated the dynamics only of the species written in red bold color. We can recognise three major pathways involved in this model: I) p43-Flip and p43p41 activation by DISC formation II) C8-C3-C6-C8 positive feedback loop III) mitochondrial activation and C3 positive feedback loop (here is considered also the double-negative feedback loop of XIAP sequestred by SMAC) and IV) Nf-kB activation.

According to discussion in section 5.1.1, we decide to first distinguish the dynamic behavior of observable species according to the presence or not of overshooting response. Thus, chemical species characterized by overshoot response are: DISC complex, p43Flip and p43p41 molecules, Bar linked with C8, Bcl2 linked with Bid, active form of Bax, oligomerization of Bax in the mitochondrion, Bax linked with Bcl2 in the mitochondrion, active SMAC, active cytocrome-c, active Apaf, Apoptosome complex binded with XIAP molecules and active C3. In NfkB pathway we found: p43Flip bounded with IKK comlpex, NfkB phosphorilated with IkB and active Nf-kB. The remaining time series depict increasing concentrations, which reach the steady state level without any overshoot, and are: active C8 by processing of p43p41 and C3 loop, active C6, ubiquinated C3 by XIAP, truncation of Bid by active C8, active mitochondrion pores, SMAC sequestred by XIAP, apoptosome formation and finally PARP degradation.

We expect that all the species involved in apoptosome formation and C3 activation have an Hill coefficent greater than 1.

Resulting pattern classification is also presented in Fig. 5.2. It shows the most important chemical species involved in apoptosis model which are represented as distinct compartments. Compartments show also red asterisk indicating that the molecule is in an active form. Solid lines connecting different compartments indicate the transformation between a chemical species to another. Dotted lines joining two different species indicate interactions with complex formation. Dotted lines are also used to indicate chemical species controlling different reactions.

Rapid non-overshooting	Slow non-overshooting
Active cytocrome c (*)	active C8 (*)
Apoptosome formation (*)	tBid
Active C6 (*)	#MitochondrialPores (*)
PARP (*)	SMAC.XIAP (*)
	C3 ubiquinated (*)

Rapid overshooting	Slow overshooting
DISC.cFlipS (*)	activated p43Flip.IKK
DISC.cFlipL (*)	Nf-kB.IkB phosphorilated
DISC.C8 (*)	active C8.BAR (*)
p43Flip	active Bax
p43p41 (*)	Bax4 (*)
Bid.Bcl2 (*)	Bax.Bcl2 (*)
active C3 (*)	
Apaf (*)	
Apoptosome.XIAP (*)	

Table 5.1: Concentration classified according to their dynamics. Those with (*) indicate that Hill coefficent is higher than 10.

Detected quantities (observables) are indicated in red and, in their proximity, are present plots depicting their qualitative dynamic behaviours. Plots present colored frames which indicate under which pattern the detected concentration is classified, and are blue for rapid (notovershooting) response, red for slow (not-overshooting) response, green for rapid overshooting response, and cyan blue for slow overshooting response. The green species represented in the circles are inhibitors of apoptosis. cFlipL and cFlipS act in DISC formation preventing formation of p41p43 and p43Flip molecules. Free cytosolic Bcl-2 can inhibit Bid molecule before being truncated by active C8; instead, mitochodrial Bcl-2, inhibit Bax oligomerization. Bar sequestrates active C8 and XIAP inhibits both mitochondrial and direct active C3 pathways.

Reactions involved in DISC formation are characterizided by rapid overshooting dynamics and high Hill coefficents. Model calibration (par. 4.4.2.1) accelerate Neumann's DISC dynamics that were less rapid. As a conseguence, both activation of p43p41 and p43Flip occur in rapid manner. Once p43Flip was activated, all the molecules in NfkB pathway , but the phosphorilated complex NfkB, show a slow overshooting responce and lower Hill coefficent. Active C8 shows a slow non-overshootin responce like caspase 6 in the feedback loop. By analizing graph connection of species (fig. 5.2) involved in non-overshooting, overshooting and sigmoidal responce we concluded that:

- usually complexes, generated by molecule interactions (represented in fig. 5.2 with dotted lines joining two different species), show a non-overshooting responce because they do not be degradeted by anyone. A molecule that exhibit this behavior is active C8 that promotes Bid truncation and C3 activation and it is only sequestred by BAR molecule in the cytosol. This kind of seqestration/degradation is not sufficient to convert concentration responce from non-overshooting to overshooting. Another molecule is active C6, that is activated by C3, and promotes C8 activation without degrading itself. Apoptosome iteracts with C3 and makes it active, but does not link to any molecule so, its concentration reach a stable state. We can find the same dynamics in mitochondrion active pores concentration, active cytocrome-c formation, SMAC sequestrated by XIAP, ubiquinated C3 and degradated PARP.

- There are some molecules that, once formed, bind with other molecules forming new molecular complexes. Usually they exhibit overshooting responce. While their concentrations increase, the complexes formation increase at the same time but with different dynamics. This may cause an overshooting response that may reach a stable state if the startintig molecules concentrations are finite. For example (fig. 5.2 and table 5.1) , a molecule that show this behavior is the complex formed by Bax and Bcl2. Once Bax is beeing active, it is sequestred at the same time by Bcl2 generating an overshooting responce.

By means of pattern classification we were able to characterize dynamic behaviour of some of the most important elements constituting apoptosis signaling system. As already said, pattern classification may help us to better understand the behavior of the

system and to characterize those concentration that exibhit sigmoidal and an all-no one irreversibility dynamic. Activation of caspase 3 occur in a very rapid manner and its high Hill coefficent (about 31) suggest that, once activated, it is difficult to stop it. Furthermore, it initiate PARP degradation, that has a similar Hill coefficent and sigmoidal dynamic. This suggest that apoptosis, when started, occurs in a all-no one manner. If this does not happen the cell may reach an intermediate state (partial death) between life and death. During classification analysis we noticed that almost all the reactions involved in mitochondrial pathway have a high Hill coefficent and a rapid, non-overshooting, sigmoidal responce instead several molecules show overshooting responce. This fast and rapid dynamic behavior is due to mitochordrion that, once stymulated with molecular extrernal signals (like tBid) or internal (stress, X-ray,..), starts a cascade of reactions that brings to apoptosis.

It is important that cells, when adeguately stimulated by death receptors, undergo rapidly to apoptosis and the system exhibit ultrasensitivity. The latter can help to filter out noise or delay responses. Mechanisms that lead to ultrasensitive stimulus-response curves include cooperativity, multisite phosphorylation, feed-forward loops, and enzymes operating under saturation. Bistability (par. 3.3.2) can occur if such an ultrasensitive cascade is equipped with a positive feedback, like apoptosis pathway is. For this reasion we have studied below the influence of feedback loops in apoptosis death cascade.

Feedback loops analysis

Albeck et. al., as just described in chapter 4.2.1, found in his model three principal positive feedbacks that we also have in our new model:

1. a positive feedback loop in which pro-caspase-6 (pro-C6) is cleaved by C3* to form C6* , which then activates additional active C8;

2. a double negative feedback loop, that act as a positivie one, with XIAP, that inhibit active C3, that is inhibited by SMAC;

3. a positive active C3 feedback loop due to mitochondrial formation of Apoptosome (this includes also SMAC loop as part of mitochondrial reactions);

We simulated the model without considering the contribute of the loops and then we evaluated dynamic behavior of the system. Removing C6 feedback loop (by setting to zero the initial concentration of C6) do not cause sensible dynamic variation on the apoptotic dynamics. This means that cell undergo apoptosis whether with the loop or not. We noticed only a little delay on signal propagation. On the other hand, the removal of SMAC double-negative loop permits at XIAP molecule to inhibit more active C3. The cell undergo the same to apoptosis, but cause an important reduction of active C3 molecules that delay PARP degradation. By removing all the mitochondrial loop (both Apoptosome and SMAC contribute) we noticed a marcable delay on apoptosis signal propagation. After this long delay C3 starts to become active and the cell dies. This means that not even the removal of this amplification loop permits at the cell to survive. Between the feedback loops, the last is the most important in terms of how it affects apoptosis dynamic.

5.2 Model validation

Complete apoptosis model (fig. 5.2) of type II cells is the integration of two different models. Although the difficulties to deal with the overlapping parts of these networks, we were able to obtain a final model which is a counterfeit between state of art chemistry knowledge and simplicity in implementation procedure. Then, we run simulations and we compared them with those obtained from original models [3, 2] verifying a good agreement. Figures show the comparison between models are presented in Appendix. When we performed parameter calibrations some dynamics changed in order to fit Albeck's concentrations (chapter 4.4.2.1). For these reasons, the model simulate better TRAIL simulation rather than FAS.

5.2.1 DISC formation, p43Flip and p43p41 activation

We noticed very different dynamics in DISC formation. Nuemann at. al. and Albeck et. al. modeled it with a slow kinetic, while our new model considered it faster. By changing DISC parameters (see fig. 4.7) we have sped up reactions involved in ligand-receptor, DISC formation and DISC linked with cFlips or procaspase 8. The different kinetics introduced in DISC formation affect both p43Flip and p41p43. p43Flip was produced faster and so reached its peak value before those on Neumann's. Since the initial concentrations of cFlipL and cFlipS also changed, the peak values of p43Flip was affected. It was 400 molecules per cell in Neumann's model and about 140 molecules per cell in our new model. Therefore, we can assert that Nf-kB pathwat was less stimulated in TRAIL receptor.

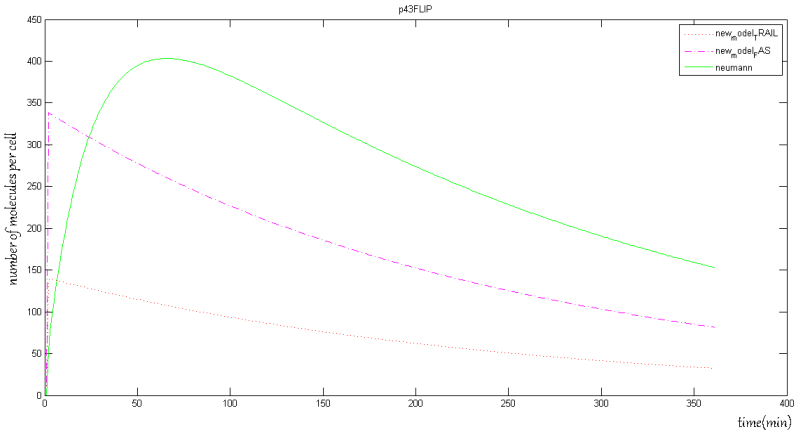

Figure 5.3: p43Flip molecule

Formation of p41p43 was modeled in a different way. Neumann et. al. modelled it with a low overshooting responce and with a peak value reached in 70 minutes while,

in our new model, it had an overshooting responce characterized by two peak values: one at the beginning (due to DISC activation) and the other at 160 minutes (due to C3 feedback loop).

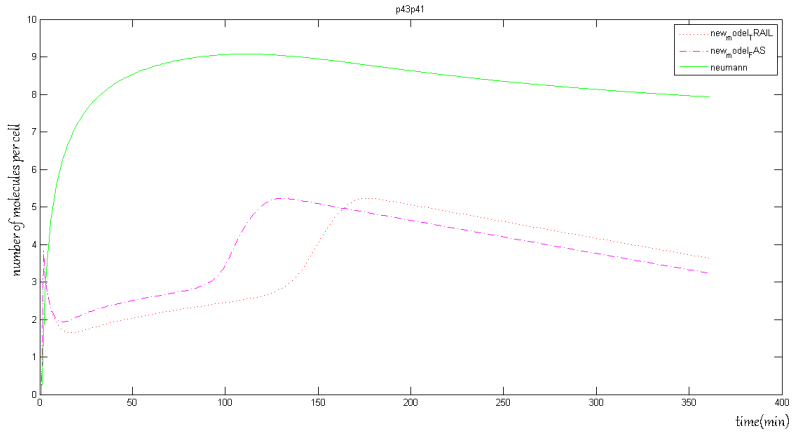

Figure 5.4: p43p41 in a logarithmic scale

Despite these differences in DISC formation and p41p43 activation, caspase 8 concentration became active in similar way as Albeck's model (Fig. 5.5). The inital concentration of procaspase 8 in our model was diminished and also the initial starting dynamic. It reaches a steady state value showing a low non-overshooting responce and mantained it until apoptosis was done.

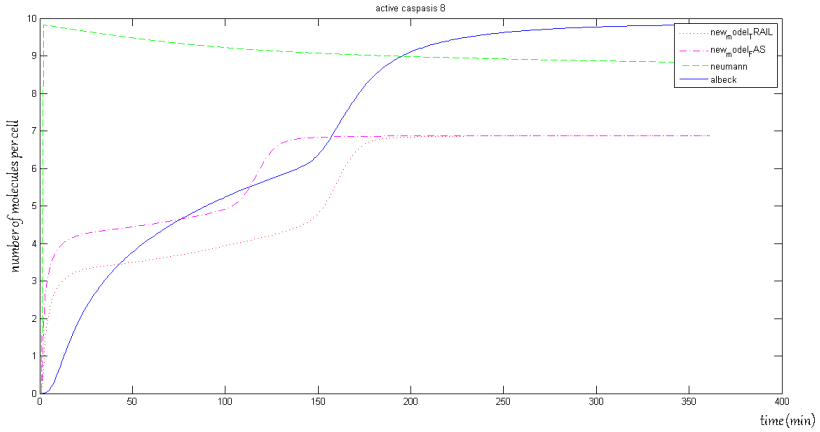

Figure 5.5: active caspase 8 in a logarithmic scale

5.2.2 mitochondrial amplification loop

When we performed model calibration, the initial concentrations and kinetics of the mitochondrial loop remained almost constant. Little modification on caspase 8 activation affects Bid truncation and Bax activation.

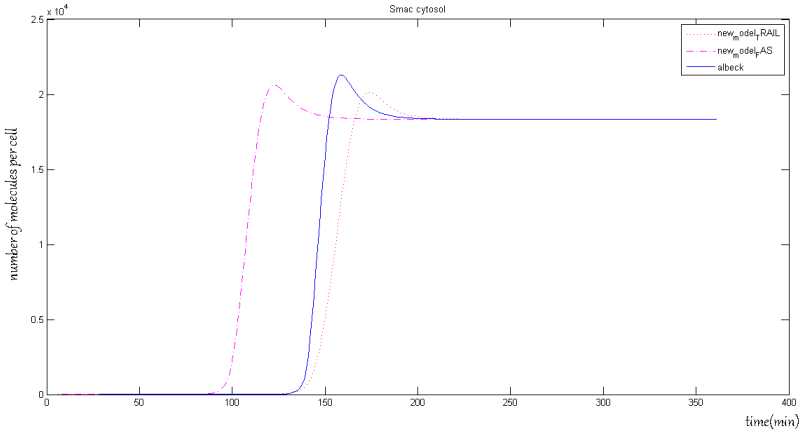

Figure 5.6: cytosolic SMAC

The last, reaches its peak value at the same time as the original (Fig. 5.9). It has a peak value of ∼9000 molecules per cell instead of ∼7000 molecules per cell.

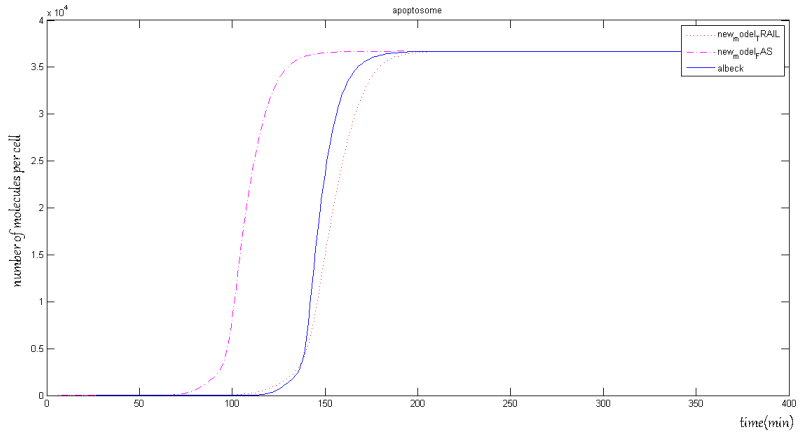

Figure 5.7: apoptosome formation

Despite of this findings, the dynamics of cytocrome-c release (Fig. 5.8), SMAC release (Fig. 5.6) and Apoptosome formation (Fig. 5.7) show a good fit.

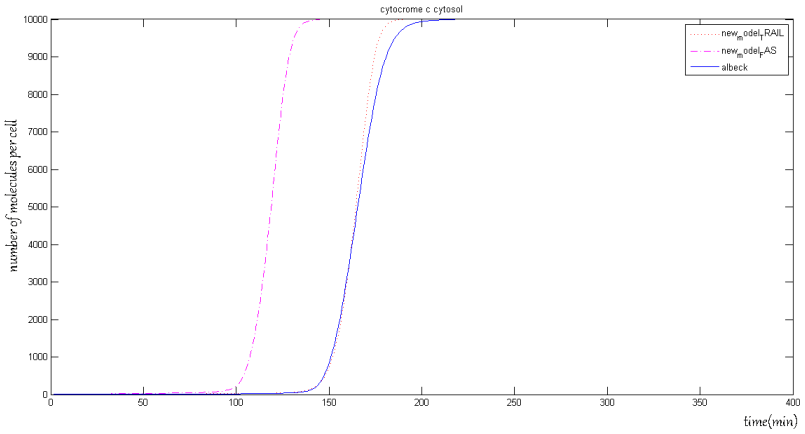

Figure 5.8: Cytosolic cytocrome-c

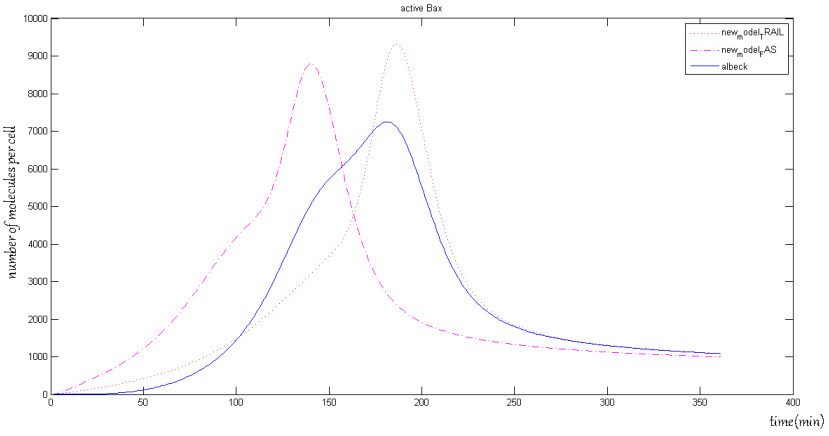

Figure 5.9: active Bax

5.2.3 C3 - C6 feedback loop

Active C3 dynamic was very similar to the original (Fig. 5.10). Since the initial concentration of procaspase 3 changed, its peak value changed too. We noticed a different

of ∼5000 molecules between Albeck's original value and those obtained with our model. Activation of C6 feedback loop occurs at the same time and with the same number of molecule as the original model (Fig. 5.11).

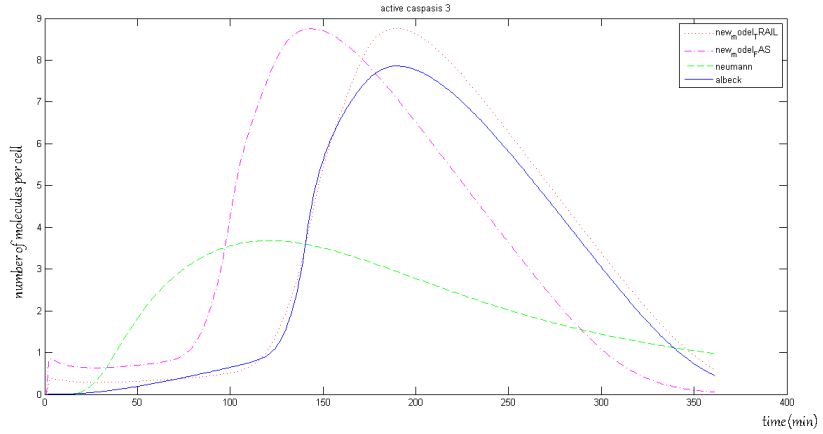

Figure 5.10: active caspases 3 in a logarithmic scale

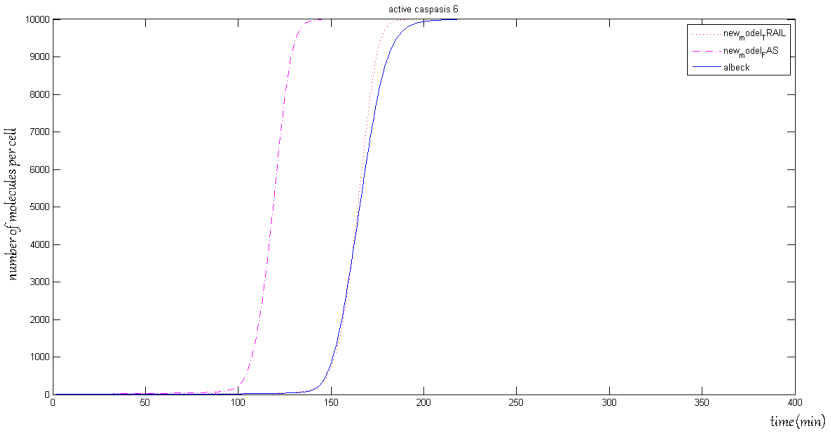

Figure 5.11: active caspase 6

5.2.4 NfkB activation

To validate NfkB pathway we compared concentrations obtained with our model with those of Neumann's.

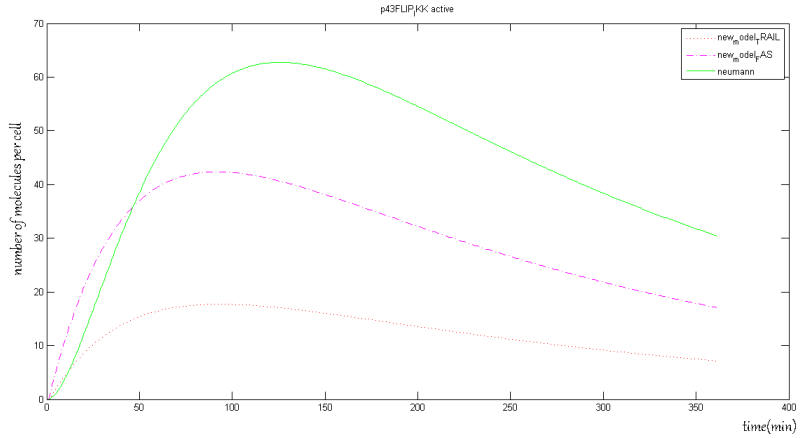

Figure 5.12: p43FLIP molecule bound with IKK

The peak of IKK activated by p43Flip (Fig. 5.12) was reached faster than the original. Its peak has a value of ∼15 molecules per cell instead of ∼62 molecules per cell. This low concentration of molecules stimulates only a little part of Nf-kB. This one, reaches its peak value ∼40 minutes later and with less than ∼400 molecules per cell than the original (Fig. 5.13).

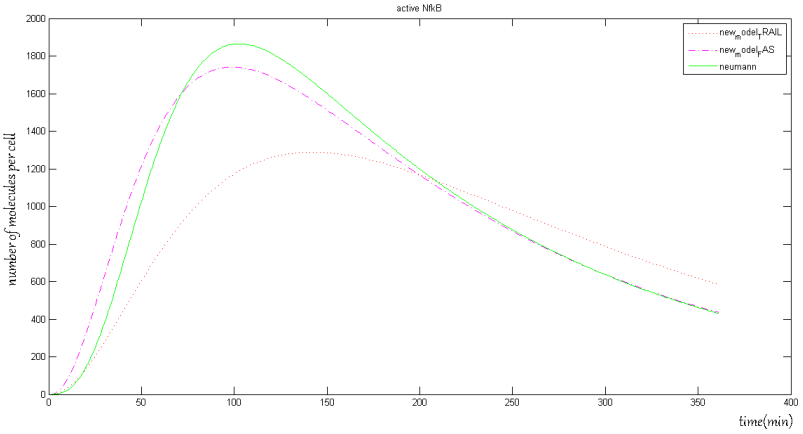

Figure 5.13: active NfkB

5.2.5 FAS pathway

The new model, stymolated by Fas receptors, was compared to Albeck's model concentrations stymolated by Trail because the original Neumann's model was of type I cells. In system biology we know that type I cells are characterized by greater DISC formation in order to generate an adeguate C8 stimolation without involving mitochondrial amplification. This implicates that DISC formation from Fas was less strong than the original (see chapter 4.4.2.1). The wew model concentrations have similar dynamics as those stymulated by Trail, and discussed in previous chapters, but in a different time scale. In fact, mitochondrial and active C8-C3 reactions seem to occur 50 minutes before those of Albeck's stymulated with Trail. Since Albeck et. al. conceived their model like a biological time switch, these results are a consequence.

In particulare, we simulated Nf-kB pathway generated by Fas and we compared it with those of Neumann's finding good agreement. Phosphorilated NfkB, linked with IKK, reaches its peak value just 10 minutes before Neumann's (Fig. 5.14). NfkB was activated in a similar time scale and reached its peak value of ∼1700 molecules per cell in ∼100 minutes. By comparing the different pathways stimulated with different receptors, we found that NfkB pathway seems more sensitive to Fas receptors rather than Trail.

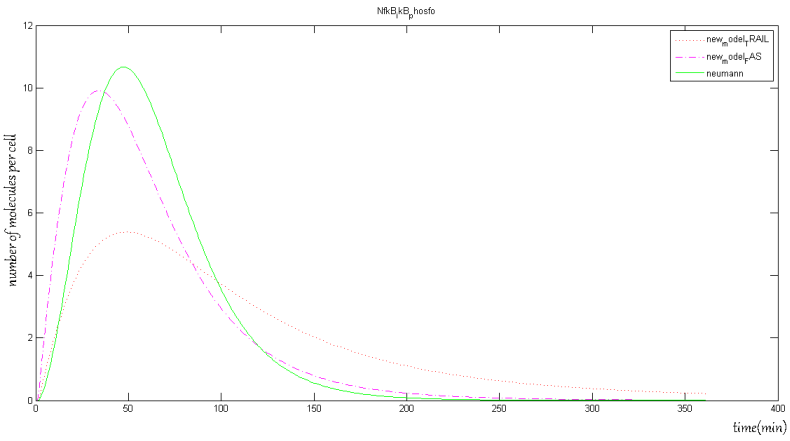

Figure 5.14: NfkB bonded with Ikb phosphorilated

To further validate the model we perform a sensitivity analisis using the robust PSA explained in chapter 4.4.1. In this way, we are able to compare our parameters with those in literature.

5.2.6 Sensitivity analysis

We decided to perform PSA of the main observables involved in apoptotic pathway like: active caspase 8, active caspase 3 and Apoptosome formation. The result is showed in

fig. 5.15. Parameters are labeled in red while observables in blue. Starting from the left (dark blue bars), it is represented the influence of initial concentrations of the species among all the 25 observables of the model. Since they show high values, they are the most sensitive parameters. A little variation of their values cause a big perturbation on the entire dynamics of the system. In particular, the most sensitive parameter is the initial concentration of *Bid* molecule. This is consistent with what found by Albeck et. al., that MOMP generation and stimulation plays an essential role in apoptosis. This further confirm the importance of the mitochondrial amplification pathway and prove that cell is of type I.

For these reasons, we found also that intial concentration of Bax, and the initial concentration of $Bcl2$ molecules present inside and outside the mitochondrion were key factors. The latter, controls Bax oligomerization in the mitochondrion and, as a consequence, inhibit pore opening and release of apoptotic factors. De facto, it inhibit the entire positive feedback mitochondrial loop. After that, we found that initial concentration of procaspase 8 ($proC8$) and TRAIL receptors were sensitive parameters. This is obvious, for the reason that active C8 controls both mitochondrial loop and caspase 3 direct activation pathway and TRAIL receptors control all the reactions of the model. Another important molecule was $cFlipL$. Neumann et. al. found the same result in his model (see 4.4.1.1). DISC molecules and kinetics (in particular cFlipL) are decisive in the determination of the downstream reactions. By adding Neumann's DISC complexity at Albeck's model we made the new model more sensitive to Flip molecules in particular, to c-FlipL (see chapter 4.4.1.2). Since $XIAP$ initial concentration was a powerful inhibitor of active caspase 3 activation and positive mitochondrial feedback loop, it is a key sensitivity parameter. After the initial concentrations, we found some kinetics that had an important role in the dynamic of the model: $kn2$ involved in the formation of DISC complex with proC8, $kn3$ that controls DISC and FlipL affinity, $k10$ that promotes truncation of Bid and activates mitochondrial reactions and $k12$ that encurage inibithion of Bid molecule by Bcl2.

If we select an horizontal row (among all the colors) we will obtain how parameters affect a single observable. Selecting a vertical column (a single color) we will get how a single parameter variation influences the different observables/species. Since we introduced different dynamics at DISC, it may be useful to understand what parameters affect more the different species. Therefore, we focused on p43Flip formation (that upregulates NfkB formation) and active C8 (that upregulates apoptosis).

Active caspases 8 formation

By watching the horiziontal row representing active C8 (fig. 5.15) we can see that, after procaspase 8 and Trail receptor, the most sensitivity parameter are $cFlipL$ and $XIAP$ concentrations. The first is due to the major affinity that cFlipL has in DISC formation (regulated by $kn3$ and $kn7$, also sensitive parameters) while the second is due to the C3-C6-C8 amplification loop that is strongly inhibited by XIAP molecule. In particular, XIAP binds active C3 and degrades it through ubiquination.

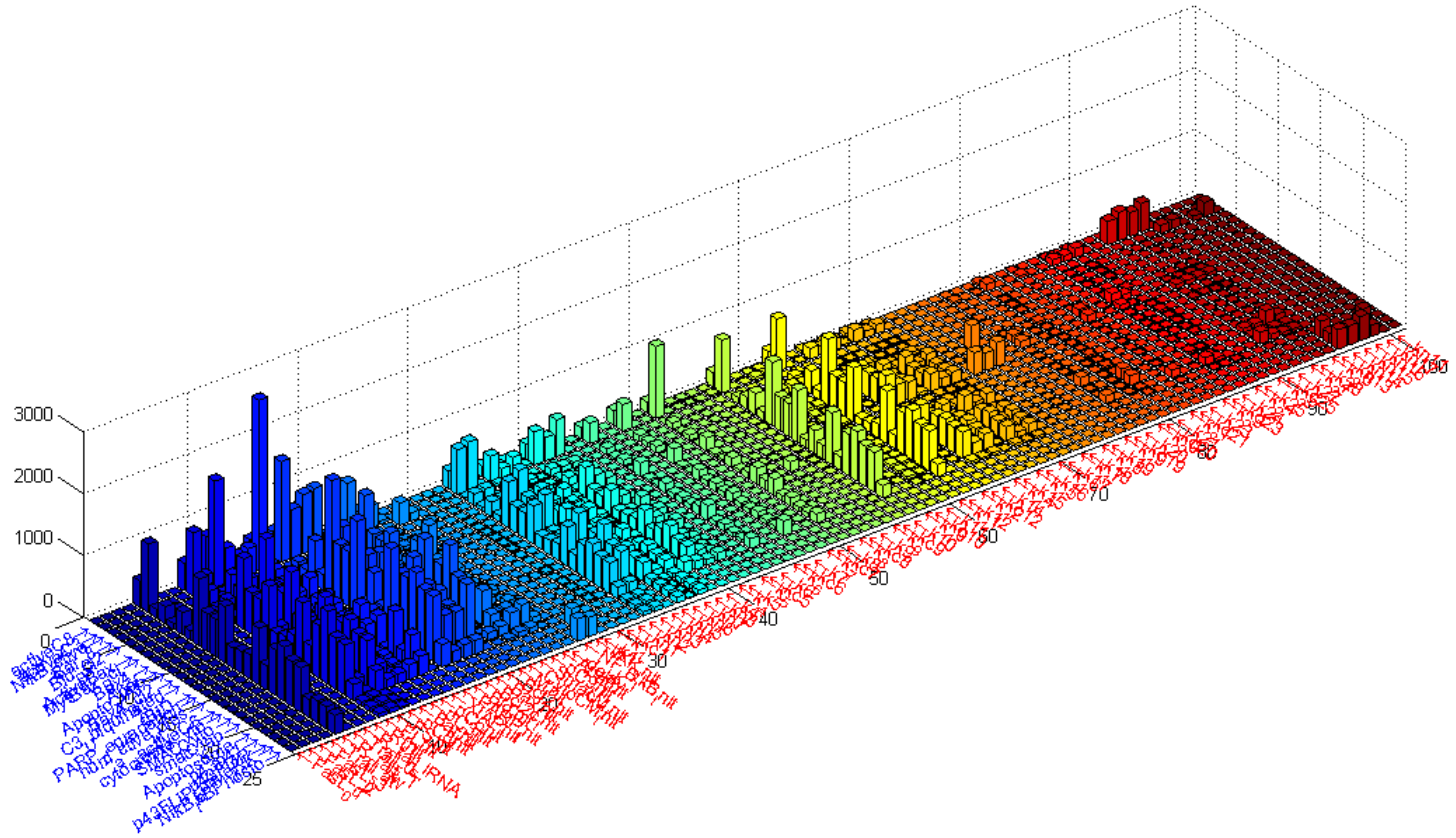

Figure 5.15: Robust PSA of the new model stimolated with TRAIL. The sensitivity analysis was calculated on 25 different observables (blue lables). In this 3D diagram the parameters (red labels) were organized starting from initial parameters concentration (the blue bars on the left) through DISC formation (azure bars), mitochondrial pathway (the green-yellow part in the middle) to C3 activation and PARP degradation (the red bars on the right). The initial parameters involved in DISC formation and C8 activation are the most sensitive: procaspase 8, cFlipS and cFlipL initial concentration.

.

cFlipS and cFlipL role on pathway activation

Overexpression of cFlipL and cFlipS molecules cause activation delay of both caspase 8 and Nf-kB activation. cFlipL has a stronger inhibition power than cFlipS. When we simulated the model, we found that these molecules only delay cell death and not prevent it. These findings argue with Albeck's study that apoptosis is like a biological switch delayed by Flips molecules. We found that DISC plays a central role in deciding divergence between Nf-kB and apoptosis pathway. By overexpressing cFlip molecules we found that Nf-kB became active before apoptosis pathway. This could permit to generate transcriptional factors, that interact with mitochondrial pathway and inhibit it. cFlipS and cFlipL inhibit apoptosis more than NfkB pathway. By varying cFlipS concentrations we noticed that Nf-kB peak was always reached in a short time and between a little range of values. Thus, apoptosis inhibition may be guaranteed by iteraction between delay on caspase activation and NfkB survival transcriptional factors. E.g: in system biology it is known that, when active, Nf-kB produces as transcriptional factors molecules like Bcl2 and XIAP. These may interact with Bax oligomerization, Apoptosome formation and active caspase 3 cascade. If apoptotic pathway was delayed by cFlips, it would give time to XIAP and Bcl2 to act as a negative feedback and to prevent apoptosis in a definitive manner.

p43Flip formation

In order to study parameters influencing p43Flip molecules we selected the horizontal row labelled as "p43Flip" in fig. 5.15. In particular, we found that parameters that influence more p43Flip dynamics are: Trail concentration, Ikk initial concentration and $kn13$ (representig p43Flip interaction with IKK complex). Other parameters are: $cFlipS$ concentration at DISC, $kn5$ and $kn7$. The last two are involved rispectively in DISC.C8 formation and DISC.cFlipS formation. Since p43Flip molecule generation is due to DISC complex linked with a combination of cFlipL and procaspase 8, sequestration of DISC by C8 and cFlipS influence its formation.

Role of XIAP in cascade propagation

XIAP molecule is a pontent inhibitor of apoptosis. It acts on both mitochondrial pathway (by blocking Apoptosome formation) and C3 formation (by degrading it). In order to undestand its dynamic better, we overexpessed the inital concentration of XIAP molecules. By only doubling its concetration, the peak of Apoptosome number of molecules was reduced from 37000 to 3400 and consequently C3 active's peak was drammatically reduced from 6500 to 150 active molecules.

6 Conclusions

In this thesis we implemented a computational model of apoptosis signaling pathway. We made use of two models already published in the literature that were integrated to realize the final and more complete apoptosis model. The first model considers apoptosis like a biological switch and involves TRAIL receptor, DISC formation and mitochondrial activation; while, the second considers both Nf-kB and caspase activation from DISC. The new model assumes that Nf-kB pathway was generated from DISC complex formed by both receptors. It was implemented using rule-based modelling approach which permitted a simple system description by a set of reaction rules. In particular, we used BioNetGen software and, by means of its tools, we generated predictions of chemical species populating apoptosis system. The final model has 101 parameters of which 23 are initial concentrations and 78 are reaction kinetics. It counts 75 different molecules species controlled and generated by 61 reactions. Simulated time series (describing the concentrations of molecules) were used to characterize dynamic behavior of the system. Sensitivity analisys was used to define core mechanisms of the system. We used these results to clear some fundamental regulation processes. First, we distinguished concentrations depending on overshoot presence. Then, we evaluate response time and we distinguished between rapid, slow and sigmoidal dynamics. To further characterize non-overshooting response, Hill coefficent was calculated. Hence, we classified dynamics according to four main pattern sets: rapid (non-overshooting), slow (not-overshooting), rapid overshooting, and slow overshooting responses. Through this analysis we realized that rapid (not-overshooting) response characterizes those process related to mitochondrial pathway and caspases 6 activation. They demonstrated sigmoidal curves and Hill's high coefficents that indicate cooperative and ultrasensitive behavior. This means that, a little variation of the input, produces rapid and fast growing of the output until it reaches a steady state. Three positve feedbacks were present in the model. They mainly ensure an all-or-none response but any of them is straight necessary to lead to apoptosis. The same sigmoidal curves was found in PARP degradation, that above all, indicates that a rapid all-or none responce occurs when the cell undergoes apoptosis. Slow overshooting response characterizes NfkB pathway: from IKK activation to NfkB translocation. Rapid overshooting response characterizes those molecules involved in DISC, p41Flip and active caspase 3 formation. At last, slow (not-overshooting) response characterizes those species that are not degraded or linked with anyone. This is the case of molecules as active caspase 8 and Apoptosome.

We found good agreement with most of our sensitive parameters and those of the previous models. We found that Bax activation, Bcl2 and procaspase 8 initial concentrations were essential for mitochondrial signal propagation and the feedback loop. Both cFlips and XIAP molecules play dominant roles in apoptosis inhibition. In particular, c-FlipL

and c-FlipS discriminate either apoptosis or survival pathway. We found that cFlipL had a stronger inhibition power than cFlipS. By varying cFlipS concentrations we noticed that the peak of Nf-kB was always reached in a short time and between a little range of values.

Through overexpressing concentrations of apoptotic inhibitor we were able to introduce significative delays on apoptosis pathway. In system biology it is known that active Nf-kB translocates into the nucleus and produce transcriptional factors like Bcl2 and XIAP. These delays, in particular those of cFlips, could be used to enhance activation of inhibitors that definitely interrupt apoptosis pathway.

Finally, we discussed model validation comparing our predictions with those of Albeck's and Neumann's. Since we introduced different mechanisms in DISC formation, we changed its dynamics. Anyway, we found a good agreement in caspase cascade, feedback loops, mitochondrial propagation and PARP degradation. From the other side, we found good agreement between Neumann's Nf-kB pathway and that generated by our model with FAS. Trail generation of NfkB and apoptosis induction by FAS were not trained against quantitative data but only evaluated with biological knowing of dead receptor pathways.

6.1 Future plans

There are some cytokines, such as those of the tumor necrosis factor (TNF) superfamily, that induce apoptosis in many cell types. Others, such as cytokines from the epidermal, insulin-like, and nerve growth factor (EGF, IGF, and NGF) families, act as survival cues that block or attenuate the action of TNF-family cytokines. Evaluating cross talks between them, can give new insigh in apoptosis mechanism. Numerous groups have reported that CD95 mediate activation of other pathways like ERK, and MAPK. The model could be integrated in studies that consider transcriptional factors of Nf-kB and could help to definitely understand the role of these molecules.

In ODE modeling it is assumed that the cell represents a well-stirred reactor, implying that diffusion effects do not matter. In apoptosis networks, these assumptions are likely to be fulfilled, as caspase and their regulators are typically expressed at the number of several hundred thousand molecules per cell. Furthermore, the time scale of apoptosis induction (hours) is slow relative to the time scale of protein diffusion within a cell (milliseconds to seconds); therefore, spatial gradients of apoptosis signaling molecules can be considered decisive in apoptosis initiation.

7 Appendix

Source code of the model of apoptosis implemented in BioNetGen language.

begin parameters

 # Initial amounts of cellular components (copies per cell)

*FasL_01 1.1322e2*5.9999e2*
*FasL_02 3.7740e1*5.9999e2*
*FasL_03 1.887e1*5.9999e2*
Trail_sat 6e4
R_Trail_WT 3e2 # TRAIL receptor (for experiments not involving siRNA)
Trail_50 3e3 # baseline level of ligand for most experiments (corresponding to 50 ng/ml SuperKiller TRAIL)
R_Trail_siRNA 1e5 # TRAIL receptor for experiments involving siRNA;
Rf_init 730 # concentration of CD95-FADD
FL_init 2.1064e3
FS_init 1.4473e3
pC8_init 3.04684e4
Bar_init 1e3 # Bifunctional apoptosis regulator
pC3_init 2.01871e4 # procaspase-3 (pro-C3)
pC6_init 1e4 # procaspase-6 (pro-C6)
XIAP_init 1e5 # X-linked inhibitor of apoptosis protein
PARP_init 1e6 # C3 substrate*
Bid_init 4e4 # Bid
Bcl2c_init 2e4 # cytosolic Bcl-2
Bax_init 1e5 # Bax
Bcl2_init 2e4 # mitochondrial Bcl-2
M_init 5e5 # mitochondrial binding sites for activated Bax
CytoCM_init 5e5 # mythocondrial cytochrome c
SmacM_init 1e5 # mitochondrial Smac
pC9_init 1e5 # procaspase-9 (pro-C9)
Apaf_init 1e5 # Apaf-1
delay .01 # translocate CC <-> MC
*NF_kB_IkB_init 4.7395*5.9999e2*
*iIKK_init 5.7728*5.9999e2*

 # model kinetics

k1 0.188241
k_1 39.7244
kc1 4.72700
*kn1 1*1.6667e-3*
*kn2 1.27772e-4*1.6667e-3 # proC8 to DISC*
kn3 0.0070538 # Flip long to DISC
kn4 5.382766e-8 # Flip short to DISC
kn5 8.987359e-4 # proC8 to DISC
kn6 0.00320177 # Fl to DISC
kn7 0.00748049 # Fs to DISC
*kn8 0.01164630 # p43/p41 to C8**

*k4 1e-6*60 k_4 1e-3*60 k5 1e-7*60*
*k_5 1e-3*60*
*kc5 1*60*
*k6 1e-6*60*
*k_6 1e-3*60*
*kc6 1*60*
*k7 3e-8*60*
*k_7 1e-3*60*
*kc7 1*60*
*k8 2e-6*60*
*k_8 1e-3*60*
*kc8 .1*60*
*k9 1e-6*60*
*k_9 1e-2*60*
*kc9 1*60*
*k10 1e-7*60*
*k_10 1e-3*60*
*kc10 1*60*
*k11 1e-6*60*
*k_11 1e-3*60*
*k12 1e-7*60*
*k_12 1e-3*60*
*kc12 1*60*
*k13 delay*60*
*k_13 delay*60*
*k14 1e-6*60*
*k_14 1e-3*60*
*k15 1e-6 *60*
*k_15 1e-3*60*
*k16 1e-6*60*
*k_16 1e-3*60*
*k17 1e-6*60*
*k_17 1e-3*60*
*k18 1e-6*60*
*k_18 1e-3*60*
*k19 1e-6*60*
*k_19 1e-3*60*
*kc19 1*60*
*k20 2e-6*60*
*k_20 1e-3*60*
*kc20 10*60*
*k21 2e-6*60*
*k_21 1e-3*60*
*kc21 10*60*
*k22 delay*60*
*k_22 delay*60*
*k23 5e-7*60*
*k_23 1e-3*60*
*kc23 1*60*
*k24 5e-8*60*
*k_24 1e-3*60*
*k25 5e-9*60*
*k_25 1e-3*60*
*kc25 1*60*

```
    k26 delay*60
    k_26 delay*60
    k27 2e-6*60
    k_27 1e-3*60
    k28 7e-6*60
    k_28 1e-3*60
    kn13 7.2043e-4*1.6667e-3
    kn14 3.5882e-1*1.6667e-3
    kn15 3.6842 # activation
    kn16 2.2299e-2 # degradation
    kn17 6.4182e-3 # degradation
end parameters
begin molecule types
    Trail(Rb)
    Rp(B)
    C3(B,S~a~i~u)
    C6(B,S~a~i)
    C8(B,S~a~i)
    C9(B,S~a~i)
    XIAP(B)
    PARP(B,S~a~d)
    Bax(B1,B2,B3,B4,S~i~a~m)
    Bax2(B)
    Bax4(B)
    Bid(B,S~t~i)
    cytC(B,P~m~a~c)
    SMAC(B,P~m~c~a)
    Mit(B,S~i~a)
    Apop(B)
    Bcl2(B,S~m~c)
    Apaf(B,S~a~i)
    BAR(B)
    Trash()
    I()
    FasL(Rb)
    Rf(B1) # CD95 + FADD, B1,B2,B3= trimerization of FADD
    FL(Bs)
    FS(Bs)
    p43p41(B)
    P(B)
    p43FLIP(B)
    IKK(B,S~i~a)
    NfkB(B,S~i~a)
    IkB(B1,B2)
    DISC(B1,B2)
    DISC_F(B1,B2)
    DISC_T(B1,B2)
end molecule types
begin species
    Trail(Rb) Trail_50
    Rp(B) R_Trail_siRNA
    C8(B,S~i) pC8_init
    BAR(B) Bar_init
```

```
    C3(B,S~i) pC3_init
    C6(B,S~i) pC6_init
    XIAP(B) XIAP_init
    PARP(B,S~a) PARP_init
    Bid(B,S~i) Bid_init
    Bcl2(B,S~c) Bcl2c_init
    Bax(B1,B2,B3,B4,S~i) Bax_init
    Bcl2(B,S~m) Bcl2_init
    Mit(B,S~i) M_init
    cytC(B,P~m) CytoCM_init
    SMAC(B,P~m) SmacM_init
    C9(B,S~i) pC9_init
    Apaf(B,S~i) Apaf_init
    FasL(Rb) FasL_02
    Rf(B1) Rf_init
    FL(Bs) FL_init
    FS(Bs) FS_init
    NfkB(B!1,S~i).IkB(B1!1,B2) NF_kB_IkB_init
    IKK(B,S~i) iIKK_init
end species

begin observables
    Molecules activeC8 C8(B,S~a)
    Molecules activeC3 C3(B,S~a)
    Molecules NfkB_active NfkB(B,S~a)
    Molecules proC8 C8(B,S~i)
    Molecules proC3 C3(B,S~i)
    Molecules Bar_C8 BAR(B!1).C8(B!1,S~a)
    Molecules Bid_Bcl2 Bid(B!1,S~i).Bcl2(B!1,S~c)
    Molecules ActiveBax Bax(B1,B2,B3,B4,S~a)
    Molecules MytBax_Bcl Bcl2(B!1,S~m).Bax(B1!1,B2,B3,B4,S~m)
    Molecules Bax2_Bcl2 Bax2(B!1).Bcl2(B!1,S~m)
    Molecules Bax4 Bax4(B) Molecules Apaf Apaf(B,S~a)
    Molecules Apopto_XIAP Apop(B!1).XIAP(B!1)
    Molecules Bax4_Bcl2 Bax4(B!1).Bcl2(B!1,S~m)
    Molecules C3_Ubiquinated C3(B,S~u)
    Molecules tBID Bid(B,S~t)
    Molecules PARP_degradation PARP(B,S~d)
    Molecules num_active_Holes Mit(B,S~a)
    Molecules activeC6 C6(B,S~a)
    Molecules Active_Myth_cyto cytC(B,P~a)
    Molecules cytocrome_Cyto cytC(B,P~c)
    Molecules Active_Myth_SMAC SMAC(B,P~a)
    Molecules SMAC_Cyto SMAC(B,P~c)
    Molecules smac_xiap SMAC(B!1,P~c).XIAP(B!1)
    Molecules Apoptosome Apop(B)
    Molecules DISC_TRail DISC_T(B1,B2)
    Molecules DISC_Fas DISC_F(B1,B2)
    Molecules DISC DISC(B1,B2)
    Molecules DISC_FS DISC(B1!1,B2).FS(Bs!1)
    Molecules DISC_C8 DISC(B1!1,B2).C8(B!1,S~i)
    Molecules DISC_FL DISC(B1!1,B2).FL(Bs!1)
    Molecules p43p41 p43p41(B)
    Molecules p43FLIP p43FLIP(B)
```

```
    Molecules p43FLIP_active_IKK p43FLIP(B!1).IKK(B!1,S~a)
    Molecules NfkB_IkBPhosfo NfkB(B!1,„S~i).IkB(B1!1,B2!2).P(B!2)
end observables

begin reaction rules
    # TRAIL receptor DISC formation
    1 Trail(Rb) + Rp(B) <-> Trail(Rb!1).Rp(B!1) k1, k_1
    2 Trail(Rb!1).Rp(B!1) -> DISC_T(B1,B2) kc1
    3 DISC_T(B1,B2) + C8(B,S~i) -> DISC(B1!1,B2).C8(B!1,S~i) kn2
    4 DISC_T(B1,B2) + FL(Bs) -> DISC(B1!1,B2).FL(Bs!1) kn3
    5 DISC_T(B1,B2) + FS(Bs) -> DISC(B1!1,B2).FS(Bs!1) kn4
    # FAS receptor DISC formation
    6 FasL(Rb) + Rf(B1) -> DISC_F(B1,B2) kn1
    7 DISC_F(B1,B2) + C8(B,S~i) -> DISC(B1!1,B2).C8(B!1,S~i) kn2
    8 DISC_F(B1,B2) + FL(Bs) -> DISC(B1!1,B2).FL(Bs!1) kn3
    9 DISC_F(B1,B2) + FS(Bs) -> DISC(B1!1,B2).FS(Bs!1) kn4
    10 DISC(B1!1,B2).C8(B!1,S~i) + FS(Bs) -> DISC(B1!1,B2!2).C8(B!1,S~i).FS(Bs!2) kn7
    11 DISC(B1!1,B2).FS(Bs!1) + FS(Bs) -> DISC(B1!1,B2!2).FS(Bs!1).FS(Bs!2) kn7
    12 DISC(B1!1,B2).FS(Bs!1) + C8(B,S~i) -> DISC(B1!1,B2!2).C8(B!1,S~i).FS(Bs!2) kn5
    13 DISC(B1!1,B2).FL(Bs!1) + FL(Bs) -> DISC(B1!1,B2!2).FL(Bs!1).FL(Bs!2) kn6
    14 DISC(B1!1,B2).FS(Bs!1) + FL(Bs) -> DISC(B1!1,B2!2).FS(Bs!1).FL(Bs!2) kn6
    15 DISC(B1!1,B2).FL(Bs!1) + FS(Bs) -> DISC(B1!1,B2!2).FS(Bs!1).FL(Bs!2) kn7
    16 DISC(B1!1,B2).FL(Bs!1) + C8(B,S~i) -> p43FLIP(B) kn5
    17 DISC(B1!1,B2).C8(B!1,S~i) + FL(Bs) -> p43FLIP(B) kn6
    18 DISC(B1!1,B2).C8(B!1,S~i) + C8(B,S~i) -> p43p41(B) + p43p41(B) kn5
    # C8 activation and apoptosis pathway
    19 p43p41(B) + p43p41(B) -> C8(B,S~a) 2*kn8
    20 C8(B,S~a) + BAR(B) <-> BAR(B!1).C8(B!1,S~a) k4, k_4
    21 C3(B,S~i) + C8(B,S~a) <-> C3(B!1,S~i).C8(B!1,S~a) k5, k_5
    22 C3(B!1,S~i).C8(B!1,S~a) -> C3(B,S~a) + C8(B,S~a) kc5
    23 C6(B,S~i) + C3(B,S~a) <-> C6(B!1,S~i).C3(B!1,S~a) k6, k_6
    24 C6(B!1,S~i).C3(B!1,S~a) -> C6(B,S~a) + C3(B,S~a) kc6
    25 C8(B,S~i) + C6(B,S~a) <-> C8(B!1,S~i).C6(B!1,S~a) k7, k_7
    26 C8(B!1,S~i).C6(B!1,S~a) -> p43p41(B) + p43p41(B) + C6(B,S~a) kc7
    27 XIAP(B) + C3(B,S~a) <-> XIAP(B!1).C3(B!1,S~a) k8, k_8
    28 XIAP(B!1).C3(B!1,S~a) -> XIAP(B) + C3(B,S~u) kc8
    29 C3(B,S~a) + PARP(B,S~a) <-> C3(B!1,S~a).PARP(B!1,S~a) k9, k_9
    30 C3(B!1,S~a).PARP(B!1,S~a) -> C3(B,S~a) + PARP(B,S~d) kc9
    # mitochondrial pathway
    31 Bid(B,S~i) + C8(B,S~a) <-> Bid(B!1,S~i).C8(B!1,S~a) k10, k_10
    32 Bid(B!1,S~i).C8(B!1,S~a) -> Bid(B,S~t) + C8(B,S~a) kc10
    33 Bid(B,S~i) + Bcl2(B,S~c) <-> Bid(B!1,S~i).Bcl2(B!1,S~c) k11, k_11
    34 Bax(B1,B2,B3,B4,S~i) + Bid(B,S~t) <-> Bax(B1!1,B2,B3,B4,S~i).Bid(B!1,S~t) k12, k_12
    35 Bax(B1!1,B2,B3,B4,S~i).Bid(B!1,S~t) -> Bax(B1,B2,B3,B4,S~a) + Bid(B,S~t) kc12
    36 Bax(B1,B2,B3,B4,S~a) <-> Bax(B1,B2,B3,B4,S~m) k13, k_13
    37 Bax(B1,B2,B3,B4,S~m) + Bcl2(B,S~m) <-> Bcl2(B!1,S~m).Bax(B1!1,B2,B3,B4,S~m) k14,
k_14
    38 Bax(B1,B2,B3,B4,S~m) + Bax(B1,B2,B3,B4,S~m) <-> Bax2(B) k15, k_15
    39 Bax2(B)+ Bcl2(B,S~m)<-> Bax2(B!1).Bcl2(B!1,S~m) k16, k_16
    40 Bax2(B) + Bax2(B) <-> Bax4(B) k17, k_17
    41 Bax4(B) + Bcl2(B,S~m) <-> Bax4(B!1).Bcl2(B!1,S~m) k18, k_18
    42 Bax4(B) + Mit(B,S~i) <-> Bax4(B!1).Mit(B!1,S~i) k19, k_19
```

```
    43 Bax4(B!1).Mit(B!1,S~i) -> Mit(B,S~a) kc19
    44 Mit(B,S~a) + cytC(B,P~m) <-> Mit(B!1,S~a).cytC(B!1,P~m) k20, k_20
    45 Mit(B!1,S~a).cytC(B!1,P~m) -> Mit(B,S~a) + cytC(B,P~a) kc20
    46 Mit(B,S~a) + SMAC(B,P~m) <-> Mit(B!1,S~a).SMAC(B!1,P~m) k21, k_21
    47 Mit(B!1,S~a).SMAC(B!1,P~m) -> Mit(B,S~a) + SMAC(B,P~a) kc21
    48 cytC(B,P~a) <-> cytC(B,P~c) k22, k_22
    49 cytC(B,P~c) + Apaf(B,S~i) <-> cytC(B!1,P~c).Apaf(B!1,S~i) k23, k_23
    50 cytC(B!1,P~c).Apaf(B!1,S~i) -> cytC(B,P~c) + Apaf(B,S~a) kc23
    51 Apaf(B,S~a) + C9(B,S~i) <-> Apop(B) k24, k_24
    52 Apop(B) + C3(B,S~i) <-> Apop(B!1).C3(B!1,S~i) k25, k_25
    53 Apop(B!1).C3(B!1,S~i) -> Apop(B) + C3(B,S~a) kc25
    54 SMAC(B,P~a) <-> SMAC(B,P~c) k26, k_26
    55 Apop(B) + XIAP(B) <-> Apop(B!1).XIAP(B!1) k27, k_27
    56 SMAC(B,P~c) + XIAP(B) <-> SMAC(B!1,P~c).XIAP(B!1) k28, k_28
    # NfkB pathway
    57 p43FLIP(B) + IKK(B,S~i) -> p43FLIP(B!1).IKK(B!1,S~a) kn13
    58 p43FLIP(B!1).IKK(B!1,S~a) ->Trash() kn16
    59 NfkB(B!1,S~i).IkB(B1!1,B2) + p43FLIP(B!1).IKK(B!1,S~a) -> NfkB(B!1,S~i).IkB(B1!1,B2!2).P(B!2)
+ p43FLIP(B!1).IKK(B!1,S~a) kn14
    60 NfkB(B!1,S~i).IkB(B1!1,B2!2).P(B!2) -> NfkB(B,S~a) kn15
    61 NfkB(B,S~a) -> Trash() kn17
end reaction rules
#ACTIONS
    generate_network({overwrite=>1});
    simulate_ode({t_end=>6*60,n_steps=>720});
```

Matlab source code of robust sensitivity analysis in par. 4.4.1.

```
function [S_int] = sensitivity(time, perc, step, pl , obs, fh, x, N)
% obs=1 -> sensitivity analisis of observable output
% pl=1 plot every step ov the sensitivity analisis
% step = time step for the trapezoidal integral method approximation
% perc = percentage of the parameter step
    [err, timepoints, species_out_old, observables_out_old, param_old ] = fh( time, [], x, 1);
    par_new=param_old; if(obs) species_out_old=observables_out_old; end
% seleziono solo gli indici che sono diversi da 0
    [ r ] = find(species_out_old~=0);
    S_int2=zeros(size(param_old,2),size(species_out_old,2));
    for j=1:size(param_old,2)
        % creo array N numeri casuali basati su probablita uniforme nell'
        % intervallo par*50 e par/50
        perc=15;
        casDiv= 1 - (random('unif',0,perc,1,round(N/2))./100);
        casPer=(random('unif',0,perc,1,round(N/2))./100) + 1;
        parCas=[param_old(j).*casDiv param_old(j).*casDiv];
        si2=zeros(1,size(S_int2,2));
        for i=1:length(parCas)
            par_new(j)=parCas(i);
            [err, timepoints, species_out, observables_out ] = fh( time, [], par_new, 1);
            if(obs)
                species_out=observables_out;
            end
```

```
                f=zeros(size(species_out_old,1),size(species_out_old,2));
                f(r)=abs( ( (species_out(r)-species_out_old(r)).*param_old(j) )./ ( species_out_old(r).*((param_old(j)
- parCas(i))) ) );
                si2 = si2 + ( step * ((sum(f,1)) - (f(1,:)/2) - (f(end,:)/2)));
            end
            S_int2(j,:)=si2./N;
            if(pl)
                pause(0.05);
                bar3(S_int');
            end
            par_new=param_old;
        end
        S_int2=S_int2';
    end
```

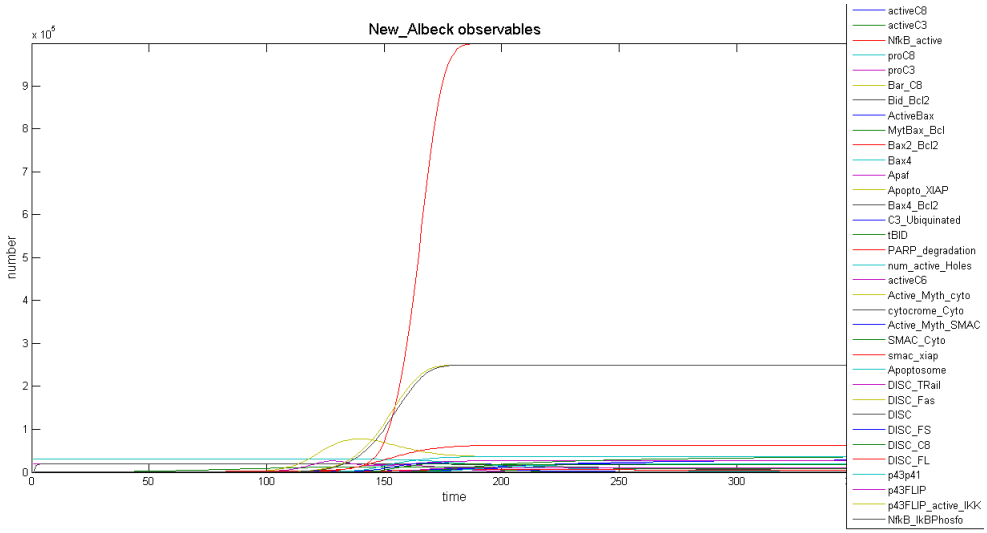

Figure 7.1: TRAIL apoptosis

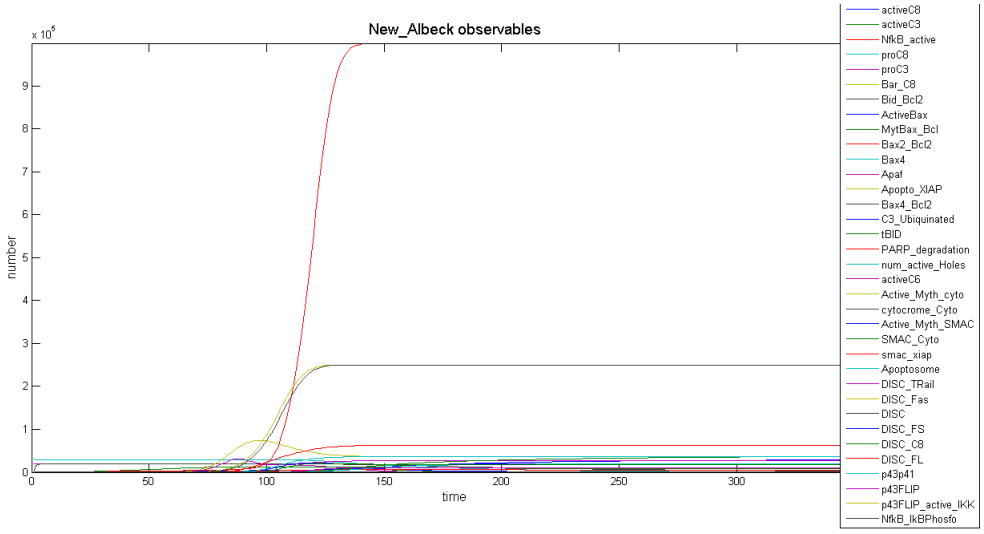

Figure 7.2: FAS apoptosis

Bibliography

[1] Inna N. Lavrik Editor, Springer (2013) Systems Biology of Apoptosis. DOI 10.1007/978-1-4614-4009-3

[2] Albeck JG, Burke JM, Aldridge BB, Zhang M, Lauffenburger DA, Sorger PK (2008) Quantitative analysis of pathways controlling extrinsic apoptosis in single cells. Mol Cell 30:11–25

[3] Neumann L, Pforr C, Beaudouin J, Pappa A, Fricker N, Krammer PH, Lavrik IN, Eils R (2010) Dynamics within the CD95 death-inducing signaling complex decide life and death of cells. Mol Syst Biol 6:352

[4] Ivan V. Maly. Methods in Molecular Biology, Systems Biology. Humana Press, vol. 500 edition, 2009.

[5] Albeck JG et al (2008b) Modeling a snap-action, variable-delay switch controlling extrinsic cell death. PLoS Biol 6(12):2831–2852.

[6] Kober AMM, Legewie S, Pforr C, Fricker N, Eils R, Krammer PH, Lavrik IN (2011) Caspase- 8 activity has an essential role in CD95/Fas-mediated MAPK activation. Cell Death Dis 2:e212

[7] Fricker N, Beaudouin J, Richter P, Eils R, Krammer PH, Lavrik IN (2010) Model-based dissection of CD95 signaling dynamics reveals both a pro- and antiapoptotic role of c-FLIPL. J Cell Biol 190:377–389

[8] Calzone L, Tournier L, Fourquet S, Thieffry D, Zhivotovsky B, Barillot E, Zinovyev A (2010) Mathematical modeling of cell-fate decision in response to death receptor engagement. PLoS Comput Biol 6:e1000702

[9] D. T. Gillespie. Stochastic simulation of chemical kinetics. Annu. Rev. Phys. Chem., 58:35–55, October 2007.

[10] T. Emonet. Efficient modeling, simulation and coarse-graining of biological complexity with NFsim. Nature Methods, 8(2):177–183, February 2011.

[11] Sangdun Choi, Introduction to System Biology. Humana Press (2007), chapter 15: Nils Blüthgen, Stefan Legewie, Hanspeter Herzel, and Boris Kholodenko. Mechanisms Generating Ultrasensitivity, Bistability, and Oscillations in Signal Transduction.

[12] Fussenegger M, Bailey JE, Varner J (2000) A m\athematical model of caspase function in apoptosis. Nat Biotechnol 18:768–774. doi:10.1038/77589

[13] Eissing T, Conzelmann H, Gilles ED et al (2004) Bistability analyses of a caspase activation model for receptor-induced apoptosis. J Biol Chem 279:36892–36897. doi:10.1074/jbc.M404893200

[14] Pace V, Bellizzi D, Giordano F et al (2010) Experimental testing of a mathematical model relevant to the extrinsic pathway of apoptosis. Cell Stress Chaperones 15:13–23. doi:10.1007/s12192-009-0118-9

[15] Bagci EZ, Vodovotz Y, Billiar TR et al (2006) Bistability in apoptosis: roles of bax, bcl-2, and mitochondrial permeability transition pores. Biophys J 90:1546–1559. doi:10.1529/ biophysj.105.068122

[16] Legewie S, Bluthgen N, Herzel H (2006) Mathematical modeling identifies inhibitors of apoptosis as mediators of positive feedback and bistability. PLoS Comput Biol 2:e120. doi:10.1371/ journal.pcbi.0020120

[17] Chen C, Cui J, Lu H et al (2007a) Modeling of the role of a Bax-activation switch in the mitochondrial apoptosis decision. Biophys J 92:4304–4315. doi:10.1529/biophysj.106.099606

[18] Cui J, Chen C, Lu H et al (2008) Two independent positive feedbacks and bistability in the Bcl-2 apoptotic switch. PLoS One 3:e1469. doi:10.1371/journal.pone.0001469

[19] Bentele M, Lavrik I, UlrichMet al (2004) Mathematical modeling reveals threshold mechanism in CD95-induced apoptosis. J Cell Biol 166:839–851. doi:10.1083/jcb.200404158

[20] Stucki JW, Simon H-U (2005) Mathematical modeling of the regulation of caspase-3 activation and degradation. J Theor Biol 234:123–131. doi:10.1016/j.jtbi.2004.11.011

[21] Rehm M, Huber HJ, Dussmann H, Prehn JHM (2006) Systems analysis of effector caspase activation and its control by X-linked inhibitor of apoptosis protein. EMBO J 25:4338–4349. doi:10.1038/sj.emboj.7601295

[22] Wikipedia. Ultrasensitivity. http://en.wikipedia.org/wiki/Ultrasensitivity. 2014.